AD

AD-E400 920

CONTRACTOR REPORT ARPAD-CR-82003

DETECTION OF CRITICAL DEFECTS IN THE M712 COPPERHEAD CONTROL SECTION HOUSING

W. R. RANDLE
B. D. WOODY
MARTIN MARIETTA CORP.
ORLANDO AEROSPACE DIV.
ORLANDO, FL 32855

GEORGE ZAMLOOT
PROJECT ENGINEER
ARRADCOM

OCTOBER 1982

US ARMY ARMAMENT RESEARCH AND DEVELOPMENT COMMAND
PRODUCT ASSURANCE DIRECTORATE
DOVER, NEW JERSEY

The views, opinions, and/or findings contained in this report are those of the author(s) and should not be construed as an official Department of the Army position, policy, or decision, unless so designated by other documentation.

The citation in this report of the names of commercial firms or commercially available products or services does not constitute official endorsement by or approval of the U.S. Government.

Destroy this report when no longer needed. Do not return to the originator.

UNCLASSIFIED

SECURITY CLASSIFICATION OF THIS PAGE *(When Data Entered)*

REPORT DOCUMENTATION PAGE

READ INSTRUCTIONS BEFORE COMPLETING FORM

1. REPORT NUMBER: Contractor Report ARPAD-CR-82003
2. GOVT ACCESSION NO.:
3. RECIPIENT'S CATALOG NUMBER:

4. TITLE *(and Subtitle)*: DETECTION OF CRITICAL DEFECTS IN THE M712 COPPERHEAD CONTROL SECTION HOUSING

5. TYPE OF REPORT & PERIOD COVERED: Final Report, 18 Nov 80 - Jan 82

6. PERFORMING ORG. REPORT NUMBER:

7. AUTHOR(s):
W. R. Randle and B. D. Woody
Martin Marietta Corp.
George Zamloot, Project Engineer, ARRADCOM

8. CONTRACT OR GRANT NUMBER(s): DAAK10-79-C-0332, MOD P00014

9. PERFORMING ORGANIZATION NAME AND ADDRESS:
Martin Marietta Corp
Orlando Aerospace Div
Orlando, FL 32855

10. PROGRAM ELEMENT, PROJECT, TASK AREA & WORK UNIT NUMBERS:
D/A Project: M6350
ACMS CODE: 53970M6350
MTT # 75

11. CONTROLLING OFFICE NAME AND ADDRESS:
ARRADCOM, TSD
STINFO Div (DRDAR-TSS)
Dover, NJ 07801

12. REPORT DATE: October 1982

13. NUMBER OF PAGES: 88

14. MONITORING AGENCY NAME & ADDRESS *(if different from Controlling Office)*:
ARRADCOM, PAD
Tech. & Auto., Info & Math Div (DRDAR-QAS)
Dover, NJ 07801

15. SECURITY CLASS. *(of this report)*: Unclassified

15a. DECLASSIFICATION/DOWNGRADING SCHEDULE:

16. DISTRIBUTION STATEMENT *(of this Report)*

Approved for public release; distribution unlimited.

17. DISTRIBUTION STATEMENT *(of the abstract entered in Block 20, if different from Report)*

18. SUPPLEMENTARY NOTES

This project has been accomplished as part of the U.S. Army's Materials Testing Technology Program, which has for its objective the timely establishment of testing techniques, procedures, or prototype equipment (in mechanical, chemical, (cont)

19. KEY WORDS *(Continue on reverse side if necessary and identify by block number)*

Nondestructive testing
Eddy current technique
Copperhead control housing inspectability
Copperhead control housing defects
MTT - nondestructive testing feasibility
M712 Copperhead NDT, eddy current
Feasibility study M712 Copperhead

20. ABSTRACT *(Continue on reverse side if necessary and identify by block number)*

This feasibility study was conducted to determine the inspectability of the M712 Copperhead control section housing for critical surface flaws and cracks which might occur as a result of heat treatment. Inspection is based on a crack inspection map which delineates the zones and associated crack size limits developed by a fracture mechanics analysis study. The allawable crack size within each zone is further categorized as an edge, corner, or surface crack. Any flaw or crack larger than the limit for a particular zone or type would, (cont)

DD FORM 1 JAN 73 1473 EDITION OF 1 NOV 65 IS OBSOLETE

UNCLASSIFIED

SECURITY CLASSIFICATION OF THIS PAGE *(When Data Entered)*

18. SUPPLEMENTARY NOTES (cont)

or nondestructive testing) to insure efficient inspection methods for material/ materiel procured or maintained by DARCOM.

20. ABSTRACT (cont)

theoretically, cause a catastropic failure of the control housing as the round was fired. Inspection studies have shown that the eddy current (E.C.) technique is quite sensitive to small flaws and cracks and it was agreed that E.C. offered the greatest success potential as a nondestructive inspection technique for evaluating and accepting cracks which occur in the control housing.

CONTENTS

	Page
Introduction	1
Purpose and Scope	1
Ground Rules	1
Equipment and Test Specimens	2
Eddy Current Equipment Selection	2
Probe Selection	2
Production Part Test Specimens	3
Ideal Test Specimens	4
Natural Crack Test Specimens	5
Test Program	5
General	5
Linearity of CRT Screen and X/R Controls	7
Two-Pole Probes	7
Magnetized Versus Demagnetized Material	7
Spatial Resolution	8
Relative Sensitivity	8
Response to Slot Depth	8
Response to Liftoff Change	8
Responsse to Slot Width	9
Response to Corner Slots and Edge Effects	9
Fatigue Cracks	9
Conclusions	11
Recommendations	12
References	13
Distribution List	73

TABLES

		Page
1	Equipment evaluation matrix	15
2	Actual dimensions of EDM slots (in.)	16
3	Probe, equipment, and frequency matrix	17
4	Range of output signals for given values of liftoff versus all slot depths	18
5	Fatigue crack dimensional and eddy current profiles	19
6	Fatigue crack F profiles	20

FIGURES

1	Copperhead control housing	21
2	Crack map	22
3	Crack geometry	23
4	Eddy current probes	24
5	Outside view, 1/2 control housing	25
6	Inside view, 1/2 control housing	26
7	EDM slots in control housing	27
8	EDM slots in control housing	28
9	Ideal test specimen	29
10	Corner slots	30
11	Edge slots	31
12	Varying width slots	32
13	Hole test setup	33
14	EDM generation of starter notch	34
15	Fatigue crack growth setup	35

16 Starter notch and fatigue crack 36

17 Fatigue crack A 36

18 Fatigue crack B 37

19 Fatigue crack C 37

20 Overall setup of test equipment 38

21 Micrometer stage probe holder 39

22 Equipment linearity 40

23 Two-pole probe response 41

24 Magnetized versus demagnetized material response 42

25 Spatial resolution response 43

26 Relative sensitivity of probes 44

27 Response to slot depths 45

28 Response to liftoff change 46

29 Response to slot widths 47

30 Response to corner slots and edges, Nortec 48

31 Response to corner slots and edges, Reluxtrol 49

32 Phase response to corner slots, Reluxtrol versus Nortec 50

33 Response to corner slots, phase rotation 51

34 Manual scanning of fatigue cracks 52

35 Dimensional profiles of A, B, and C 53

36 Profile of A, B, and C at 0.110-in. depth 54

37 Profile of A, B, and C at 0.100-in. depth 55

38 Profile of A, B, and C at 0.082-in. depth 56

39 Profile of A, B, and C at 0.063-in. depth 57

40 Profile of A, B, and C at 0.033-in. depth 58

41 Eddy current response, original centerlines of A, B, and C 59

42 Dimensional profile of F 60

43 Profile of F at 0.112-in. depth 61

44 Profile of F at 0.097-in. depth 62

45 Profile of F at 0.082-in. depth 63

46 Profile of F at 0.067-in. depth 64

47 Profile of F at 0.052-in. depth 65

48 Profile of F at 0.037-in. depth 66

49 Profile of F at 0.022-in. depth 67

50 Profile of F at 0.007-in. depth 68

51 Eddy current response, original centerline of F 69

52 Fracture through fatigue crack 70

53 EDM slot versus fatigue crack 300X 71

54 Slot irregularities, deburring 72

55 Slot irregularities, deburring and machining 72

INTRODUCTION

Purpose and Scope

This program was conducted to determine the inspectability of the Copperhead control housings (fig. 1) for critical surface flaws which might occur as a result of heat treatment. It is based on a crack inspection map and the associated crack size limits developed by a fracture analysis study (ref 1). The map (fig. 2) includes four types of crosshatching to delineate the zones in which certain sizes of cracks are allowable without impairment of the housing function. Within each zone the allowable size is further categorized as an edge, corner, or surface crack. The legend accompanying the maps provides specific values for all 12 acceptance limits (4 zones X 3 types). The geometry assumed for the three types is shown in figure 3. Any flaw larger than the limit for a particular zone or type would, theoretically, cause catastrophic failure of the control housing as the round was fired.

Ground Rules

Because inspection studies have shown that eddy current (E.C.) methods are quite sensitive to small fatigue cracks in plates (ref 2), it was agreed that such testing offered the greatest success potential as a nondestructive means for evaluating the acceptability of any cracks that might occur in control housings. An investigation was undertaken with the following principal concerns:

1. Evaluate available eddy current test equipment

2. Evaluate different types of eddy current probes from several sources

3. Fabricate test specimens and calibration standards including evaluation of the effects of variables and investigation of the existence of a correlation between machines slots and natural cracks

4. Develop special techniques for geometric peculiarities of control housings such as slots, keyways, and holes

5. Combine the results of the items above into a test concept for accepting or rejecting control housings in accordance with the criteria set forth in the crack maps at full production rates

The investigation showed the following conclusions:

1. Five types of equipment from three manufacturers were evaluated. Off-the-shelf equipment is available for automatic, multi-probe, multi-parameter, and high resolution evaluation of flaws.

2. Thirteen probes representing four genetric types and three manufacturers were evaluated with respect to a variety of simulated cracks. Probes present no problems in sensitivity, resolution, or availability.

3. Tool material and techniques can produce machined slots as narrow as 0.0035 inch in 4340 steel heat treated to Rockwell C55. Fatigue cracks of accurately controllable length and highly repeatable aspect ratio can be grown in the same type of steel plate. Specimens, including machined slots to simulate flaws of sequentially sized edge lengths, surface lengths, depths, and widths, were fabricated.

The equipment and probes were found to be capable of detecting simulated flaws that were smaller than the smallest described by the crack maps and were found capable of indicating the relative size of the machined slots. The fatigue cracks could not be characterized so that an accept or reject decision could be reached, and no correlation was found between machined slots and natural cracks.

Because of these uncertainties and the geometric variability that results from allowable tolerances and from fabrication processes such as deburring (figs. 54 and 55), the eddy current techniques must be considered unfeasible for accepting or rejecting control housings in accordance with the crack map criteria even though it demonstrated a capability of detecting the critical size flaws.

EQUIPMENT AND TEST SPECIMENS

Eddy Current Equipment Selection

The following five models of eddy current test equipment were evaluated during the program:

1. Magnaflux ED 800
2. Automation Industries EM 3300
3. Automation Industries EM 4300
4. Nortec NDT 16
5. Nortec NDT 25L

A matrix of the significant operating and performance characteristics for each is shown in table 1.

Only the EM 3300 and the nondestructive testing 16 (NDT 16) were used for probe evaluation and performance comparisons. The NDT 16 has an oscilloscope sweep mode with high-pass filtering that offers significant advantages in presenting the response to variables, while the EM 3300 offers continuously variable frequencies from 1.0 kHz to 2.5 mHz against the NDT 16's three fixed frequencies of 0.5, 1.0, and 2.0 mHz.

The Nortec NDT 25L was the choice for production testing of the control housing because it is completely programmable and could be readily multiplexed to a number of probes or test stations. The NDT 25 L was not available for use in this program; it was evaluated as a prototype unit at the Nortec plant.

Reluxtrol test equipment was not available for either evaluation or use in the program.

Probe Selection

The probes were selected to provide a cross-section of operating frequencies, configurations, and generic types. More sources were considered, but to avoid redundancy only the following three manufacturers were selected:

1. The Nortec probes were selected to represent commercial, off-the-shelf, general purpose units.

2. The Reluxtrol probes were selected to represent commercial, but very specialized types. The 3-152 was particularly chosen for its spatial resolution, on the order of several thousandths of an inch.

3. Pratt & Whitney is not a commercial supplier of probes for industry but has invested heavily in developing and fabricating high-precision probes for thier own jet engine applications.

The probes used in this program are shown in figure 4. Because the Reluxtrol 3-151 and 3-152 probes do not have self-contained balancing coils, the other two Reluxtrol probes were used for balance pruposes not subjected to evaluation.

Production Part Test Specimens

Because it is generally accepted in eddy current studies, the process of electric discharge machining (EDM) was selected to cut very narrow slots of known dimensions in a control housing to simulate cracks. The crack maps were analyzed and the dimensions and locations of slots were established so that all possible combinations of crack type (edge, corner, surface), crack size (from smaller than the smallest to larger than the largest allowable), and surrounding geometry (slot, hole, recess) for both ID and OD were included. Two control housings were required to accommodate all the slots. To facilitate EDM electrode access, the control housings were cut in half longitudinally as shown by figures 5 and 6. Although these particular housings were neither machined nor heat treated using precisely the same equipment or processes planned for production, they were sufficiently similar to production parts to serve the purposes of this investigation. Close-ups of some typical EDM slots are shown in figures 7 and 8.

Early in the program it became apparent that handheld probe scanning of the EDM slotted control housings would be unsatisfactory. The use of special shoes to control liftoff and orientation did not resolve the problem. Mechanical scanning was not possible because of part geometry irregularities which were a normal result of manufacturing tolera known dimensions in a control housing to simulate cracks. The crack maps were analyzed and the dimensions and locations of slots were established so that all possible combinations of crack type (edge, corner, surface), crack size (from smaller than the smallest to larger than the largest allowable), and surrounding geometry (slot, hole, recess) for both ID and OD were included. Two control housings were required to accommodate all the slots. To facilitate EDM electrode access, the control housings were cut in half longitudinally as shown by figures 5 and 6. Although these particular housings were neither machined nor heat treated using precisely the same equipment or processes planned for production, they were sufficiently simil## to production parts to serve the purposes of this investigation. Close-ups of some typical EDM slots are shown in figures 7 and 8.

Early in the program it became apparent that handheld probe scanning of the EDM slotted control housings would be unsatisfactory. The use of special shoes to control liftoff and orientation did not resolve the problem. Mechanical scanning was not possible because of part geometry irregularities which were a normal result of manufacturing tolerances and machine operations. There were too many unknown and/or uncontrollable variables in the control housing specimens for the effects to be separated in the eddy current responses, i.e., the responses of interest were suffering from a noise-to-signal ratio problem. The only recourse was the design of a geometrically ideal test specimen with the use of the slotted control housings to be at least temporarily sidetracked.

Ideal Test Specimens

A geometrically ideal test specimen was fabricated from 3/8-inch thick 4340 steel plate that had been heat treated by the same process as the production control housings. Special attention was given to smoothly ground parallel surfaces and to sharply formed 90° corners. This ideal specimen allowed better accessibility for more precise EDM slotting, as well as more simplified test positioning and holding than the control housing parts. The specimen is shown in figure 9 and the dimensions of the slots listed in table 2. The finished edge slots are shown in figures 10, 11, and 12. The specimen contains additional constant depth and varying width slots not called for by the crack map. The effects of these slots proved to be interesting.

To evaluate the many holes and recesses of the control housing without geometry induced noise, a special set of disc shaped ideal specimens were fabricated. The object was to minimize the difficulty and number of probes required to compensate for varying (but within tolerance) diameters. The technique would rotate the hole about an accurately and simply positionable probe rather than rotating a probe within the hole. One of the plates mounted on its matching mandrel and variable speed drive motor is shown in figure 13.

Natural Crack Test Specimens

One objective of the program was to investigate the existence of correlation between EDM slots and natural cracks so that calibration standards could be produced by controllable machining methods. While the ideal specimens were being tested, fatigue cracks were being grown in 3/8 x 6 x 18-inch 4340 plates that had been heat treated using the production process for control housings.

EDM starter notches were introduced into the plate stock as shown in figure 14. The depth of the starter notch was monitored by a dial indicator and controlled by a mechanical stop on the electrode drive mechanism.

The cracks were initiated and grown in a rotating mass fatigue machine (bending fatigue) shown in figure 15. This machine has options for pre-loading the specimen for fatigue in the tension-tension mode or for loading in pure tension. Cracks were grown in tension-tension. Crack initiation and growth were monitored with a microscope and stroboscope lighting. Crack length was measured using a calibrated reticle in the eyepiece. After a crack was grown to the desired length, the panel was repositioned in the fatigue machine to grow cracks in other areas. A 10X magnification of a starter notch and its fatigue crack is shown in figure 16. The required EDM electrode shape, size, depth, pre-load, and fatigue load were determined by fracture and examination of trial cracks. Once these parameters were established, consistency of crack growth was assured by monitoring length during growth.

Three straight, transverse cracks approximately 0.400-inch long were grown in a plate. It was estimated that the process produced cracks 0.200-inch deep. The plate was cut into three pieces, each containing a centered crack. The pieces were ground on the back side to produce a flat surface, then on the front side to produce a flat surface and to remove the starter notch. The result was three small plates with flat, parallel faces, each containing a natural crack approximately 0.400-inch long. Photomicrographs of the cracks, designated A, B, and C are shown in figures 17, 18, and 19.

TEST PROGRAM

General

The performance tests were designed to provide the best results that could be expected of any given equipment and probe combination. With the ideal geometry specimen minimizing response noise due to part variables, the setup shown in figure 20 minimized positioning and motion variables. The photo shows the granite surface plate, granite straight edge, NDT 16 with oscilloscope camera, EM 3300, probe holding micrometer stage, ideal specimen drawn via a string connected to a variable speed motor, and dial indicator used to set zero liftoff.

Using this arrangement, the probe was not moved above the surface of the part; the part was moved beneath the tip of the probe. A close-up view of the

probe-holding micrometer stage is shown in figure 21. It provided a stable, repeatable 0.0001-inch resolution adjustment of liftoff (Y axis) and edge distance (X axis). The combination of surface plate, straight edge, and parallelism of the ideal specimen assured that liftoff and edge distance would not deviate more tha 0.0002 inch during passes of the specimen beneath the probe. Motion of the specimen was either a continuous, synchronized (note microswitch) operation using the oscilloscope sweep, or a selective hand motion to evaluate one EDM slot at a time.

The oscilloscope camera attached to the NDT 16 in the photo was used to provide a permanent record of responses. Multiple exposures were often made for direct comparisons of signals. Since signal amplitude units are arbitrary, a vernier caliper or optical comparator was used to accurately measure signals (in inches).

To avoid the need for changing gain during any given test, the equipment was always adjusted so that the maximum signal to be seen (the deepest slot of the variable depth series) would not exceed the limits of the CRT graticule. Signal phase rotation was always adjusted so that the principal signal of interest would appear exactly on the X or Y axis of the CRT. To provide proportional graph presentation of responses, signal amplitude data were reduced for any given test by using the maximum indication as 100% regardless of its absolute amplitude. When required by direct comparison of different probes, the gain setting required to produce the full screen maximum signal from the largest slot is noted to provide relative sensitivity of each probe.

Because probes typically include wear faces or other material that extends beyond the tip of the coil or core, zero liftoff based on mechanical contact is not likely to be the same as electrical zero liftoff. To standardize probe liftoff, tips were ground down until the first winding of the coil was contacted. Zero liftoff for each test was then established by:

1. Placing the dial indicator horizontally against the side of the probe

2. Monitoring the dial indicator for deflection while moving the specimen back and forth beneath the probe

3. Adjusting the liftoff micrometer until the specimen and probe just cleared one another

Zero liftoff could be mechanically repeated to within 0.0001 inch. Unless otherwise specified, liftoff for all tests was 0.006 inch.

The effect of probe speed past the slots was evaluated at the outset of the test program. The speed necessary to produce degradation of the response data was found to be well beyond the practical limit for the test setup.

Except for one special test, specimens were demagnetized to evaluate the effects of part magnetization.

The laboratory environment was controlled at 68 ± 3°F and 50 ± 10% relative humidity, and the equipment was maintained in a power-on condition for the duration of the program.

Probes were not always run at their design frequencies. Any frequency at which null could be achieved was considered suitable, if not necessarily optimum.

The probe, equipment, and design frequency and operating frequency combinations used in tests of the ideal geometry specimen are listed in table 3.

Linearity of CRT Screen and X/R Controls

An oscilloscope camera photo of the response of the 3-152 Reluxtrol probe to the W-1 slot, positoned at various places on the CRT by using the X and R controls is shown in figure 22. Linearity of the NDT 16 is excellent. The traces correspond to the W-1 slot positioned immediately to the left of the probe tip, being drawn to the right beneath the probe tip, and stopping immediately to the right of the probe tip. This is typical of single slot evaluations which follow.

Two-Pole Probes

The Pratt & Whitney probes and the Nortec SPO-1515 probe are examples of two-pole units, both differential and absolute. They are completely unsuited to the Copperhead application because of their great sensitivity to crack orientation. The type of cracks considered in the control housing can have any orientation or even multiple orientations. The various responses as the probe and slot axis orientation was changed in 15° steps beginning with the probe poles straddling the slot are shown in figure 23. All responses are from the same probe over the same slot at the same liftoff. NDT 16 controls were untouched during the tests except to move the origin of the traces vertically over the CRT face for a multiple exposure photograph.

Magnetized Versus Demagnetized Material

Two CRT displays that were drawn beneath Nortec 3551 probe operating at 1.0 Mhz using the sweep synchronized mode are shown in figure 24 as an ideal specimen. The vertical spikes are responses to the various slots. The difference between the two lies in the flattened versus upturned baseline and magnetized versus demagnetized material. The smoothing effect could have been produced simpler and to a greater degree by using the internal high pass filters of the NDT 16.

Spatial Resolution

Two photographs of the CRT display as the two deepest slots, D-1 and D-2, were drawn beneath the probes in the sweep synchronized mode are shown in figure 25. With the distance between the slots known to be 0.400 inch, the 20% amplitude points on the Nortec responses are 0.053 and 0.051 inches wide. Subtracting the 0.006 and 0.005 slot widths and dividing the result by two gives resolution of ± 0.023 inch. The higher resolution Reluxtrol probe yields a signal with two widths: one corresponds to the positive-going signal and the other corresponds to the negtive which is a potential problem in an application where a wide variety of cracks must be evaluated as described in the crack map.

Relative Sensitivity

The deflection resulting from passing the same slot at the same liftoff with the same frequency, and the same equipment gain is shown in figure 26. Resolution is not free; it costs in relative sensitivity.

Response to Slot Depth

Data obtained when slots of all depths were drawn beneath a Nortec 3551 probe designed for 1 MHz, but operated at 0.5, 1.0, and 2.0 MHz, is plotted in figure 27. Liftoff was fixed at 0.006 inch. The greatest response from the 0.123 deep slot is the 100% reference level. The correlation is excellent.

Response to Liftoff Change

Data derived from passing slots of all depths below the probes at different liftoff spacings and at three different frequencies (Nortec probe) are plotted in figure 28. Zero liftoff is not practical; therefore, the baseline for determining the 100% response level is 0.002 inch.

The maximum and minimum signals were plotted for each liftoff value, and a smooth curve drawn connecting them. The results of any delta change about any liftoff value can be easily determined. For example, the dotted lines show the inherent output variation that could be expected from the Reluxtrol probe if the liftoff were held constant at 0.004 inch (62% to 70%) and if the liftoff varied ±0.001 inch (51% to 84%).

The curves have been reduced to data listed in table 4. Gain settings are included as an indication of relative sensitivity.

Response to Slot Width

The patterns that resulted when the Reluxtrol 3-152 and the Nortec 3551 probes were used to evaluate the varying width and constant depth series of slots is shown in figure 29. In each case the horizontal trace corresponds to the narrowest (0.0045 inch) slot, and the counterclockwise phase progression covers widths of 0.0100, 0.0136, 0.0156, 0.0180, and 0.0220 inch. It would be interesting to plot widths between 0.0002 and 0.0020 inch, but no technique is available for producing a controlled sequence of such narrow slots. From this test, it appears that an important parameter to be considered when crack width could vary significantly would be phase change of the output signal.

Response to Corner Slots and Edge Effects

A different procedure was followed to assess the measurement of corner slots. The probe liftoff was set at 0.006 inch with the Y axis micrometer, and the tip of the probe moved away from the edge of the ideal specimen using the X axis micrometer until there was no response to any of the corner slots as the specimen was drawn past the probe. The probe was then moved inboard over the ideal specimen in 0.010-inch steps and recordings made of the probe's response to all eight corner slots with each step. End view plots of the probe responses to the C-1, C-2, C-3, C-5, and C-7 slots are shown in figures 30 and 31. The Reluxtrol probe has a significantly steeper rise as the edge of the specimen is crossed which is a result of the fine spatial resolution and immunity to nearby discontinuities. Note the irregularity of the curves. There is nothing wrong with the probe. It is apparently reading the differences in slot width and the Nortec probe is not. To verify the point, the probes were placed over the corner slots at an inboard position that gave a high signal output, the scope presentation mode changed to provide phase information, and the photographs in figure 32 were taken. Note the almost constant phase of the Nortec signals and the widely divergent patterns of the Reluxtrol.

How the phase change could effect evaluation of the corner slots in a sweep mode of operation is shown in figure 33. The lower half of the photo is the response of the probe to the eight corner slots with the equipment's phase rotation control set for optimum output from the largest corner slot. Without any adjustment to the equipment other than a slight change in the phase rotation control, the pattern was rerun on the upper half of the CRT. In one instance slots C-1 and C-2 are indicated as being significantly larger than the other six slots. In the other they are smaller, nearly equal to C-7.

Fatigue Cracks

In an attempt to establish a correlation between EDM slots and natural cracks, a series of tests were designed in which fatigue cracks would be analyzed to produce response and dimension profiles. The plan called for the following steps:

1. Remove starter notch

2. Polish and etch the cracked surface

3. Assure absence of metal smear

4. Demagnetize sample

5. Measure the distance from the left end of the crack to the left end of the test specimen

6. Measure the length of the crack

7. Move along the crack length from left to right manually passing a probe back and forth over the crack every 0.050 inch and recording the amplitude of the response

8. Regrind the specimen to remove a prescribed amount of material to reduce crack depth (care to avoid disturbing surface condition includes full coolant flow and slow cutting not to exceed 0.0015-inch depth)

9. Return to step 2 and repeat until crack disappears

The arrangement used for manual scanning is shown in figure 34. The probe is mounted in a nylon shoe that holds it vertical, maintains a constant 0.006-inch liftoff, provides a rotational reference in the form of the set screw, and provides a surface to be held against the vernier caliper. The vernier caliper provides accurate repeatability of the probe paths over the crack that is set 0.050-inch larger for each successive pass.

The numerical data developed from the tests is listed in table 5. The depth was not known at the onset of the measurements. It was determined when the crack disappeared following the last grind, and the depth at the time of each measurement figured backward from the bottom of the crack.

The tests were performed using the NDT 16 and a Nortec 3551 probe operated at 2.0 MHz and 0.006-inch liftoff. Eddy current signals are in percent relative to the maximum signal obtained during all the measurements of all three cracks (i.e., crack A, 0.082 inch deep at position 0.150).

The dimensional data gathered during the successive grindings is plotted on figure 35. The scale factor is linear and is the same in both X and Y axes so that the aspect ratio of the cracks is presented directly. The three curves used to join the data points are identical. They prove the controllable nature of the crack growth process and of the profiling technique.

The eddy current signal amplitude versus crack cross section at each depth is plotted in figures 36 through 40. Although the three cracks have identical cross sections, they do not produce identical eddy current profiles, nor do the eddy current signals diminish in amplitude in proportion to the diminishing crack depth.

A set of plots for the signals produced at the center of each crack as the depth changed versus the response of another Nortec 3551 probe to increasing EDM slot depth (fig. 27) is shown in figure 41.

For the set of three cracks, the crack depth could not have been determined from instrument indications.

Because the results were so contrary to published information on eddy current and crack measurement applications, the entire test program for fatigue cracks was repeated using a newly fabricated specimen. Every step of the operation was subjected to the most critical scrutiny so that procedural errors might be uncovered, but none were found. In addition, the new fatigue crack was evaluated using Nortec 3551 probes at 0.50 and 0.10 MHz. Liftoff remained at 0.006 inch.

The numerical data developed from the test of fatigue crack F are provided in table 6, and the dimensional data plotted in figure 42. The points that had to be "fudged" are indicated by circles instead of dots. In all cases, the alteration was a simple bias shift to the right. The eddy current signal amplitude versus crack cross section at each depth is plotted in figures 43 to 50. The lack of correlation still exists, the frequency makes little difference in response. A set of plots for the signals at the center of the cracks versus eddy current response to EDM slot depth is shown in figure 51. The nonlinearity of response to crack F is unlike the response to cracks A, B, and C, worsening the prospect of determining the crack depth on the basis of signal amplitude.

During the fabrication of crack specimen F, another fatigue crack specimen was fractured, and the fracture zone photographed. Further evidence that the dimensional profiles were correct is provided in figure 52.

As a possible explanation for some of the differences between natural cracks and EDM slots, figure 53 shows the glaring difference between the two under 300X magnification. This photograph also indicates that the violent responses of some of the Reluxtrol 3-152 probe tests are probably invalid for natural cracks.

CONCLUSIONS

The project sucessfully solved the original problem of detecting small flaws in the Copperhead control housing through existing technology, but it also identified other problems that had not been anticipated.

Reliable detection of fatigue cracks and EDM slots of the sizes suggested to be critical to the control housing was demonstrated. However, characterization of the cracks or correlation of the response of cracks versus EDM slots was not established. Such correlation is required for the design of an eddy current calibration standard, because without it inspection for acceptance or rejection of the control housing per the crack map criteria is not possible.

RECOMMENDATIONS

The current requirements for liquid penetrant inspection, which is capable of detecting the critical flaw sizes per the crack map on over 90% of the surface area, should be continued. The remaining uninspectable areas of the control housing were judged for probability of thermal shock cracking based on the assumption that areas of the most abrupt change in material thickness were most susceptible. This judgement revealed the following three areas remaining of primary concern: 1. the key slot, 2. the support shelf for the wing extension housing, and 3. the fin slots. The fin slots cannot be inspected due to machining irregularities as shown in figures 54 and 55. An authoritative evaluation of these judgements is suggested.

An additional investigation should be conducted on the correlation between cracks and simulated cracks and also on the characterization of cracks in 4340 material. To support this effort it is further recommended that eddy current inspection be performed on the key slot and wing extension housing support shelf of production control housings using an arbitrary high sensitivity rejection level, and further, that all indications be destructively analyzed. The remaining critical areas of the fin slots could be included in this investigation if there was consistency in the part geometry. A study is recommended to determine the feasibility of replacing the hand deburring operation of the fin slots with a controlled machining operation in order to render this area inspectable by eddy current.

The basis for this project was the crack map which was constructed with some necessarily assumed data. Concern was expressed during the course of this project for actual stress data to be collected from instrumented projectile test firings. When that data are available it is recommended that the fracture analysis study be reviewed with added consideration for:

1. The degree of effect of crack orientation (which was not included in the original study) since that would help to identify the areas of greatest concern.

2. The effect of a chamfered corner versus a sharp corner.

3. Clarification of the size of critical edge cracks in areas where the inside surface map indicates a different crack size than the outside surface map or an edge crack that would connect the two surfaces.

REFERENCES

1. J. I. Bluhm and C. E. Freese, "Crack Inspection Maps - An Application To Copperhead," paper prepared for presentation to the Army Symposium on Solid Mechanics, 1978.

2. W. D. Rummel, et al, "Detection of Tightly Closed Flaws by Nondestructive Testing (NDT) Methods in Titanium and Steel," Final Report NAS 9-14653, NASA Cr-15098, September 1976.

Table 1. Equipment evaluation matrix

PARAMETERS EVALUATED	INSTRUMENTS				
	ED – 800	EM – 3300	EM – 4300	NDT – 16	NDT – 25L
PRICE, APPROXIMATE ($K)	5	7	8	9	18
PROGRAMMABLE/COMPUTER INTERFACE					A
CONTINUOUSLY VARIABLE FREQUENCY	X	X	X	B	X
CRYSTAL CONTROLLED OSCILLATOR		X	X	B	X
HORIZONTAL SENSITIVITY CONTROL (STEPS)	1	5	5	3	C
VERTICAL SENSITIVITY CONTROL (STEPS)	2	5	5	3	C
FLAW GATES	2	0	1	0	1
VISUAL ALARM	X		X		X
AUDIBLE ALARM			X		X
BATTERY OPERATION			X		D

NOTES: A – ALL TEST PARAMETERS MAY BE PROGRAMMED FOR AS MANY AS 16 TESTS

B – DEPENDS ON PLUG-IN UNIT SELECTION

C – CONTINUOUSLY VARIABLE

D – NDT-25 (SMALL CRT UNIT) CONTAINS RECHARGEABLE BATTERIES

Table 2. Actual dimensions of EDM slots (in.)

C-1 0.0056 x 0.242	D-1 0.0058 x 0.123	W-1 0.0220 x 0.059	S-1a 0.0060 x 0.404 x 0.020*
C-2 0.0088 x 0.152	D-2 0.0050 x 0.081	W-2 0.0180 x 0.060	S-1b 0.0040 x 0.392 x 0.010*
C-3 0.0040 x 0.104	D-3 0.0047 x 0.053	W-3 0.0156 x 0.060	S-2a 0.0040 x 0.218 x 0.020*
C-4 0.0043 x 0.071	D-4 0.0040 x 0.037	W-4 0.0136 x 0.061	S-2b 0.0045 x 0.197 x 0.010*
C-5 0.0040 x 0.051	D-5 0.0037 x 0.027	W-5 0.0100 x 0.062	S-3a 0.0040 x 0.103 x 0.020*
C-6 0.0040 x 0.037	D-6 0.0036 x 0.015	W-6 0.0094 x 0.062**	S-3b 0.0040 x 0.103 x 0.010*
C-7 0.0040 x 0.028	D-7 0.0047 x 0.011	W-7 0.0045 x 0.063	S-4a 0.0050 x 0.056 x 0.010*
C-8 0.0045 x 0.018			S-4b 0.0040 x 0.054 x 0.005*
			S-5 0.0030 x 0.025 x 0.005*
			S-6a 0.0035 x 0.195 x 0.010*
			S-6b 0.0065 x 0.208 x 0.022*

*BASED ON EDM MACHINE DEPTH INDICATION; NOT ACTUAL MEASUREMENT OF FINISHED PART (FIG. 9)

**MACHINING ERROR. TOO CLOSE TO WIDTH OF W-5. NOT USED FOR DATA.

Table 3. Probe, equipment, and frequency matrix

Probe	Design Freq (MHz)	Use Freq (MHz)	Equipment	
Nortec 3551F	0.100	0.020	EM 3300	
Nortec 3551F	0.100	0.100	EM 3300	
Nortec 3551F	0.100	0.100	EM 3300	
Nortec 3511F	0.100	0.100	EM 3300	
Nortec 3551F	0.100	0.250	EM 3300	
Nortec 3551F	0.100	0.250	EM 3300	
Nortec 3551F	0.500	0.500	EM 3300	
Nortec 3551F	0.500	0.500	NDT 16	
Nortec 3551F	0.500	0.500	NDT 16	
Nortec 3551	1.000	0.500	NDT 16	
Nortec 3551	1.000	1.000	EM 3300	
Nortec 3551	1.000	1.000	NDT 16	
Nortec 3551	1.000	1.000	NDT 16	
Nortec 3551	1.000	2.000	NDT 16	
Reluxtrol 3-151		1.000	NDT 16	
Reluxtrol 3-152		1.000	NDT 16	
Reluxtrol 3-152		1.000	NDT 16	
Nortec SPO-1515	1.000	1.000	NDT 16	Longitudinal
Nortec SPO-1515	1.000	1.000	NDT 16	Transverse
P&W GKF-7894		1.000	NDT 16	Longitudinal
P&W GKF-7894		1.000	NDT 16	Transverse
P&W GKF-7895		1.000	NDT 16	Longitudinal
P&W GKF-7895		1.000	NDT 26	Transverse
P&W HKF-0174		1.000	NDT 16	Longitudinal
P&W HKF-0174		1.000	NDT 16	Transverse

Table 4. Range of output signals for given values of liftoff versus all slot depths

RELUXTROL 3-152 PROBE OPERATED AT 1.0 MHz

LIFTOFF (IN.)	SIGNAL RANGE (%)	MAX/MIN RATIO
0.004 ± 0.0000	61.6 TO 70.2	1.14/1
0.004 ± 0.0010	50.5 TO 83.5	1.65/1
0.006 ± 0.0000	42.5 TO 51.5	1.21/1
0.006 ± 0.0010	36.0 TO 59.6	1.66/1
0.006 ± 0.0015	33.5 TO 64.6	1.93/1

NORTEC 3551 1 MHz PROBE OPERATED AT 0.5, 1.0, AND 2.0 MHz (ALL RESULTS COMBINED)

LIFTOFF (IN.)	SIGNAL RANGE (%)	MAX/MIN RATIO
0.004 ± 0.0000	81.7 TO 83.7	1.02/1
0.004 ± 0.0010	74.3 TO 91.6	1.23/1
0.006 ± 0.0000	67.5 TO 71.3	1.06/1
0.006 ± 0.0010	61.7 TO 77.3	1.25/1
0.006 ± 0.0015	59.0 TO 77.9	1.32/1
0.018 ± 0.0000	25.7 TO 32.0	1.25/1
0.018 ± 0.0010	23.5 TO 34.0	1.45/1
0.018 ± 0.0015	22.5 TO 35.0	1.56/1

Table 5. Fatigue crack dimensional and eddy current profiles

FATIGUE CRACK "A"

DIMENSIONAL PROFILE

DEPTH	LENGTH	LEFT END	RIGHT END
0.110	0.408	0.000	0.408
0.100	--	--	--
0.082	0.397	0.003	0.400
0.063	0.373	0.018	0.391
0.033	0.322	0.045	0.367
0.013	0.249	0.113	0.362
0.000	0.000	0.204*	0.204*

*ESTIMATED

EDDY CURRENT PROFILE

POSITION	0	0.050	0.100	0.150	0.200	0.250	0.300	0.350	0.400	0.450
DEPTH										
0.110	3	5	6	46	55	86	59	15	5	2
0.100	3	14	39	46	85	66	62	34	6	2
0.082	11	13	80	100	100	80	39	16	9	
0.063		7	13	21	25	24	19	14	4	
0.033		6	9	12	17	22	22	13	5	
0.013			5	13	10	9	6			

FATIGUE CRACK "B"

DIMENSIONAL PROFILE

DEPTH	LENGTH	LEFT END	RIGHT END
0.110	0.407	0.000	0.407
0.100	--	--	--
0.082	0.390	0.009	0.399
0.063	0.373	0.025	0.398
0.033	0.307	0.059	0.366
0.013	0.220	0.099	0.319
0.000	0.000	0.203*	0.203*

EDDY CURRENT PROFILE

POSITION	0.050	0.100	0.150	0.200	0.250	0.300	0.350	0.400
DEPTH								
0.110	2	4	5	16	24	14	5	3
0.100	5	42	52	83	80	83	79	30
0.082		36	80	88	81	51	36	14
0.063		10	19	24	53	36	31	12
0.033		5	16	21	36	45	33	19
0.013				6	4	8	4	

FATIGUE CRACK "C"

DIMENSIONAL PROFILE

DEPTH	LENGTH	LEFT END	RIGHT END
0.110	0.406	0.000	0.406
0.100	--	--	--
0.082	0.393	0.010	0.403
0.063	0.376	0.021	0.397
0.033	0.310	0.048	0.358
0.013	0.245	0.094	0.339
0.000	0.000	0.203*	0.203*

EDDY CURRENT PROFILE

POSITION	0	0.050	0.100	0.150	0.200	0.250	0.300	0.350	0.400	0.450
DEPTH										
0.110		3	4	5	11	11	6	4	3	1
0.100		10	13	40	48	55	38	20	6	2
0.082		53	90	86	78	49	36	58	51	
0.063		6	15	20	21	15	10			
0.033				8	12	10	13	6		

Table 6. Fatigue crack F profiles

DIMENSIONAL PROFILE

DEPTH	LENGTH	LEFT END	RIGHT END
0.112	0.478	0.000	0.478
0.097	0.465	0.007	0.472
0.082	0.449	0.014	0.463
0.067	0.408	0.035	0.443
0.052	0.393	0.034	0.427
0.037	0.372	0.009	0.381
0.022	0.294	0.009	0.303
0.007	0.117	0.076	0.193
0.000	0.000	0.239*	0.239*

EDDY CURRENT PROFILE (100 KHz)

POSITION	0	0.050	0.100	0.150	0.200	0.250	0.300	0.350	0.400	0.450
DEPTH										
0.112	6	14	30	56	100	96	93	50	30	6
0.097	11	20	20	26	34	31	26	26	20	6
0.082	7	20	39	49	49	53	49	39	26	10
0.067	7	19	21	39	57	49	54	37	23	7
0.052	3	10	24	34	39	33	33	27	16	6
0.037	3	6	19	26	26	21	20	17	11	3
0.022	1	6	16	33	41	41	40	20	11	3
0.007			1	16	27	31	19	6		

EDDY CURRENT PROFILE (500 KHz)

POSITION	0	0.050	0.100	0.150	0.200	0.250	0.300	0.350	0.400	0.450
DEPTH										
0.112	3	9	10	19	76	100	36	11	14	4
0.097	6	16	19	23	30	36	21	23	22	11
0.082	4	18	34	43	49	51	50	50	25	25
0.067	10	14	30	39	44	40	44	36	20	9
0.052	3	10	29	39	40	40	36	24	6	3
0.037		4	14	21	29	30	22	29	20	
0.022	1	1	14	33	34	40	31	20	16	3
0.007			1	16	40	44	22	14	3	

Figure 1. Copperhead control housing

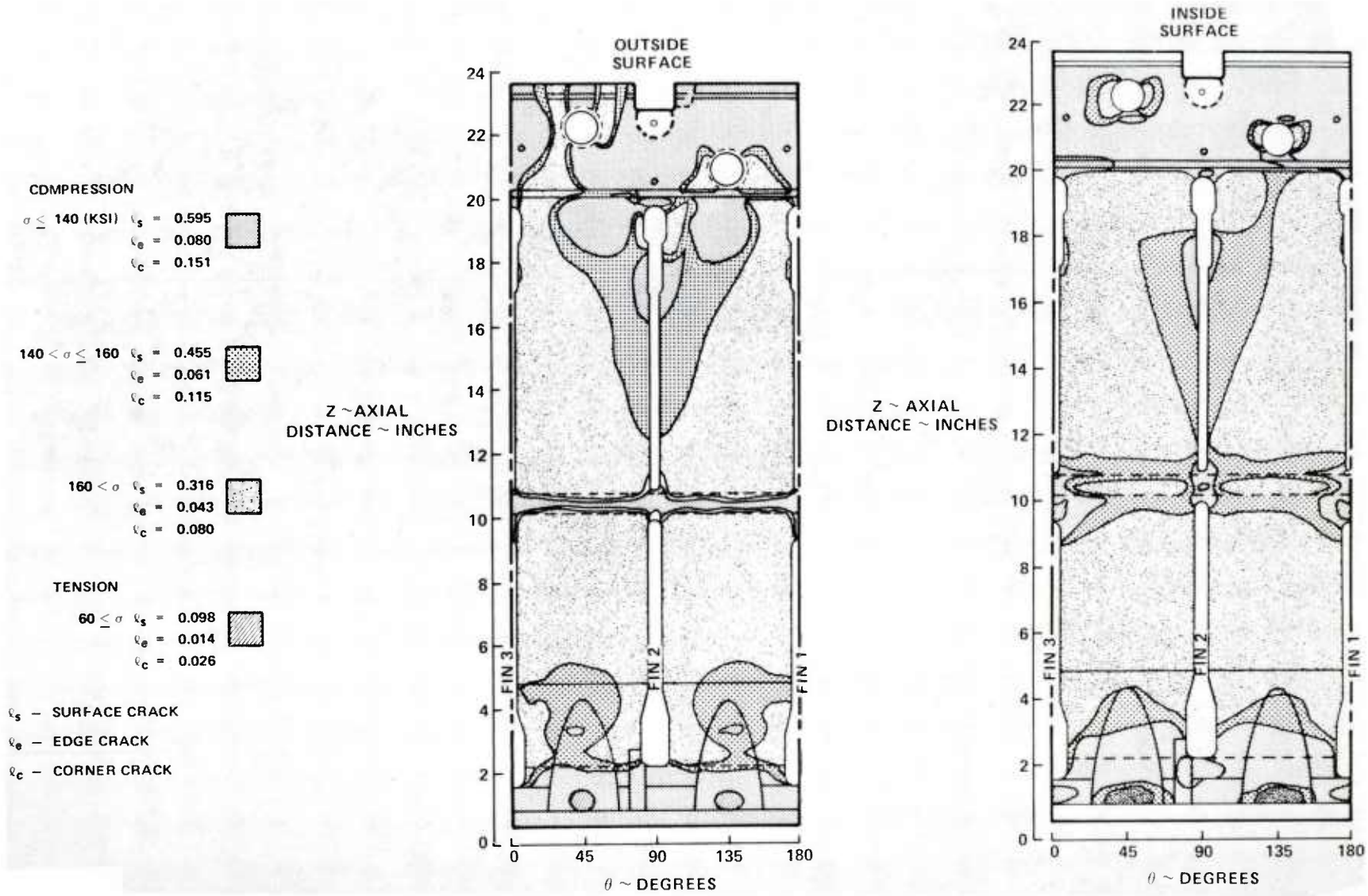

Figure 2. Crack map

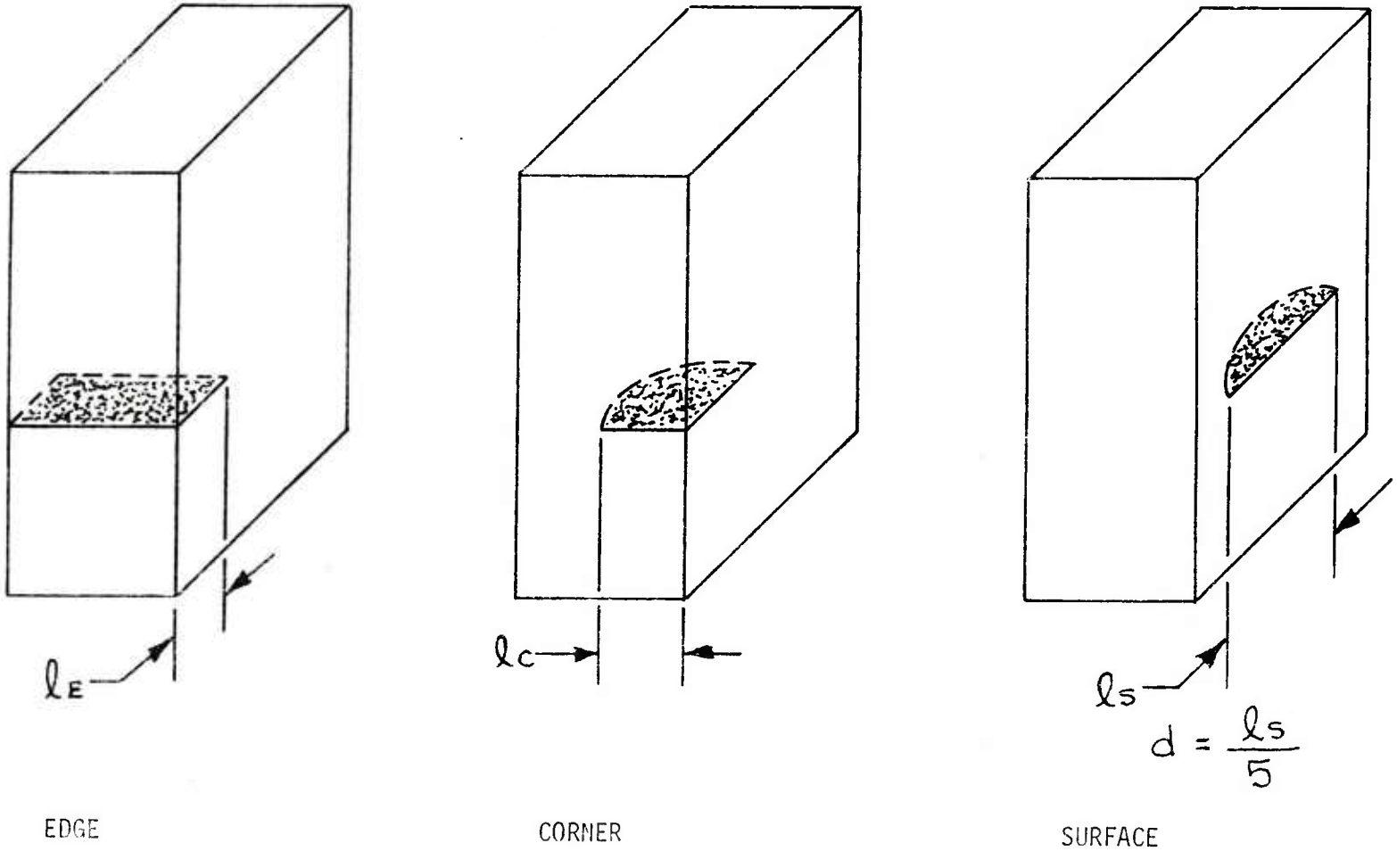

Figure 3. Crack geometry

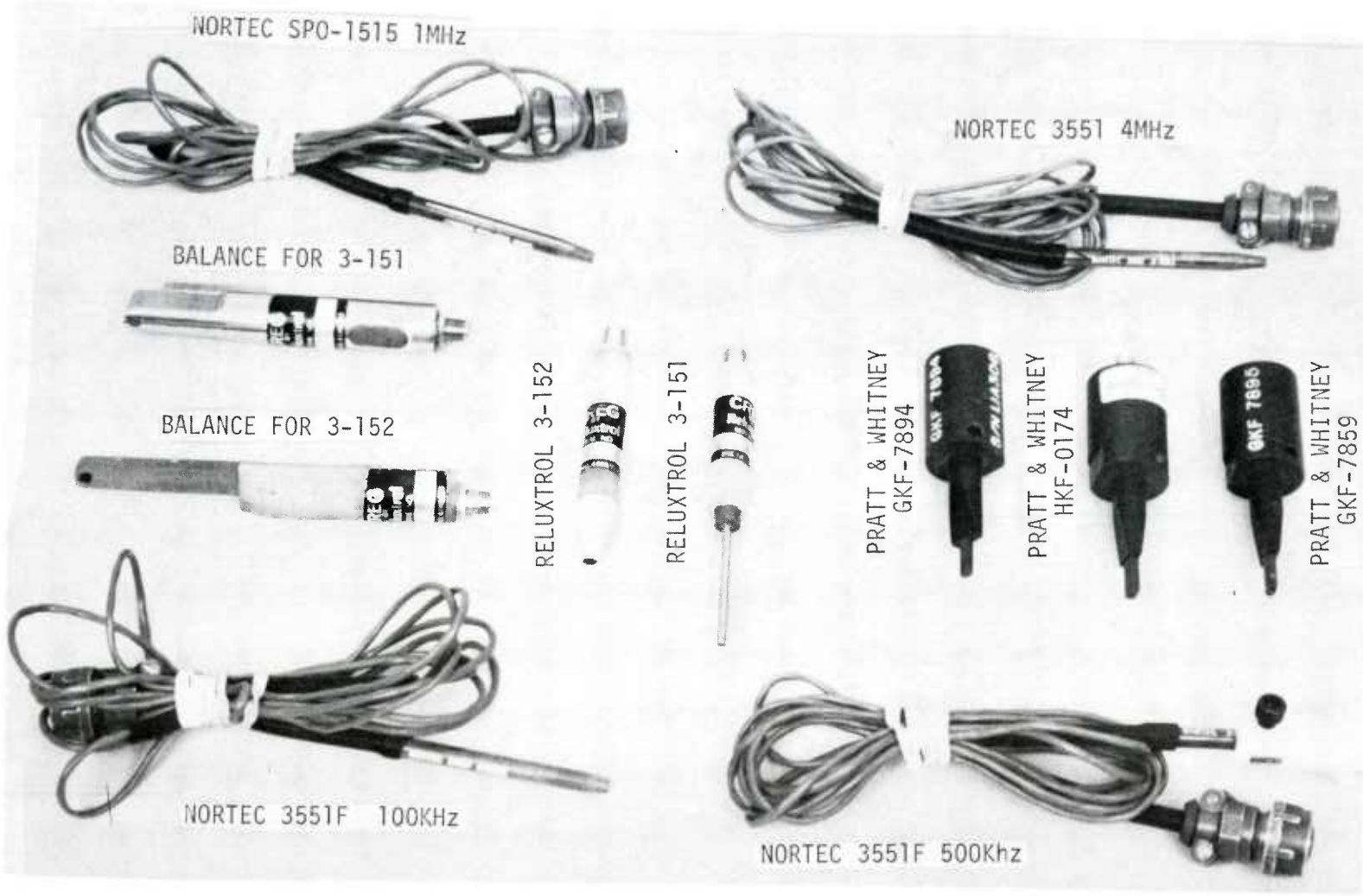

Figure 4. Eddy current probes

Figure 5. Outside view, 1/2 control housing

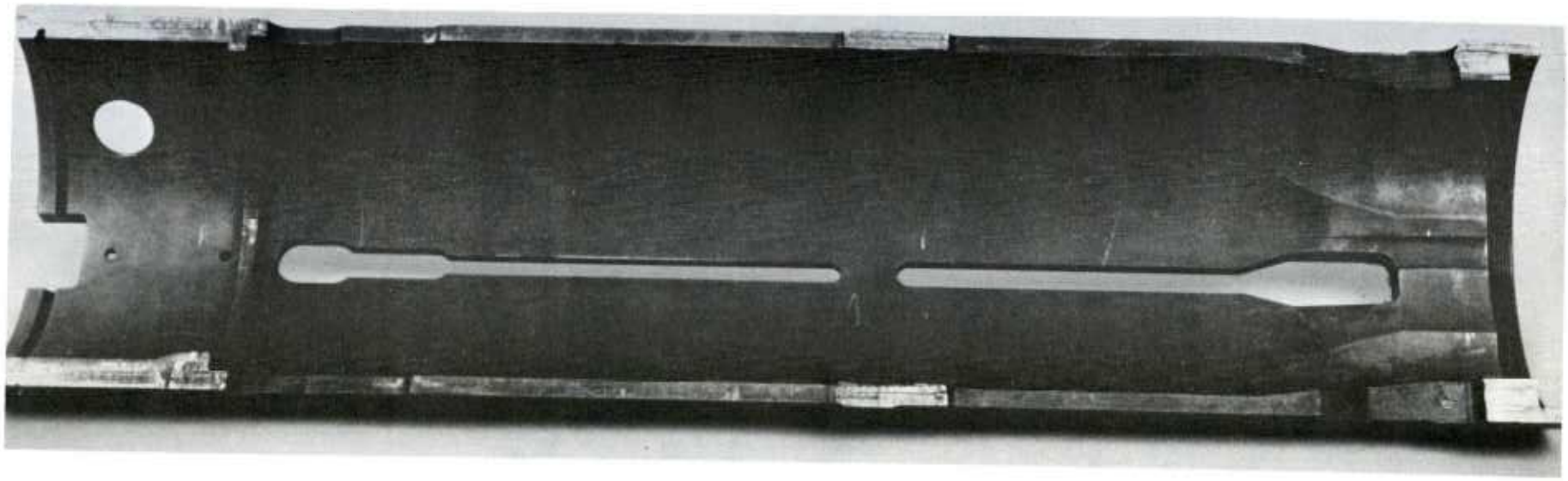

Figure 6. Inside view, 1/2 control housing

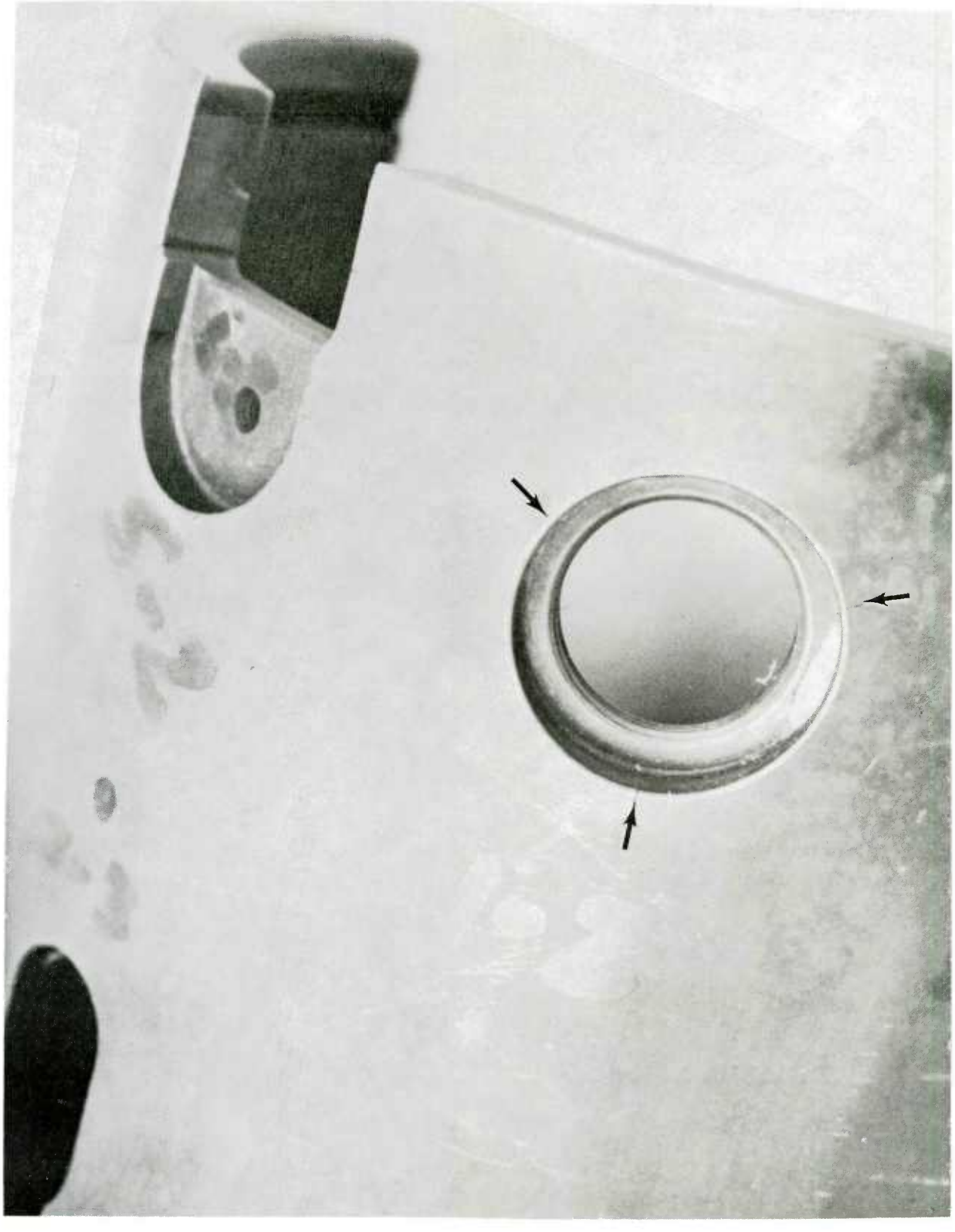

Figure 7. EDM slots in control housing

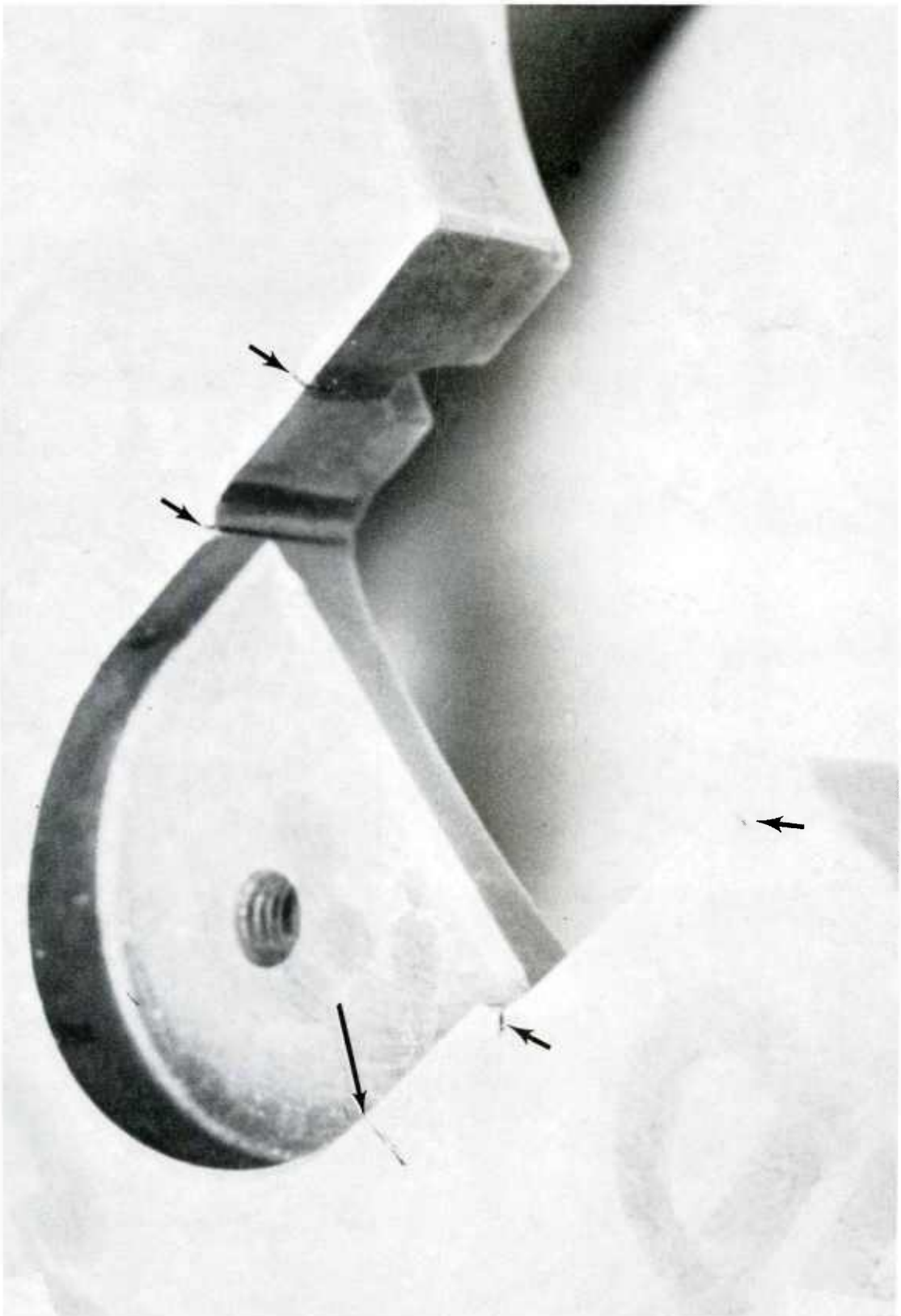

Figure 8. EDM slots in control housing

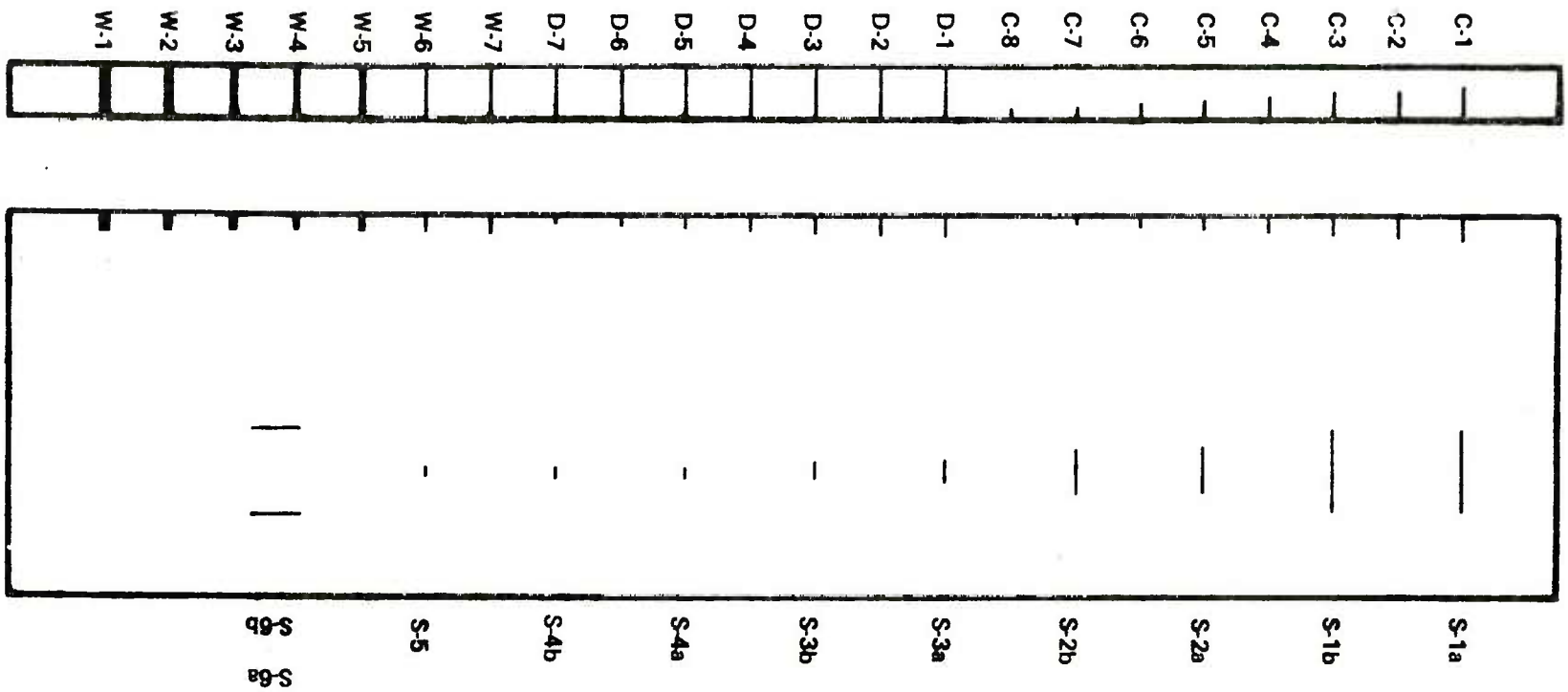

MAKE FROM 4340 STEEL HEAT TREATED PER COPPERHEAD CONTROL HOUSING PROCESS
GRIND TWO FACES FLAT AND PARALLEL WITHIN 0.0005 INCH
GRIND TWO LONG EDGES FLAT AND PARALLEL WITHIN 0.0005 INCH
EDGE-TO-FACE ANGLES 90 ± 0.1 DEG
DO NOT BREAK SHARP CORNERS
GRIND FINISH BETTER THAN 32 RMS
MAINTAIN HEAT TREAT CONDITION THROUGH GRINDING

Figure 9. Ideal test specimen

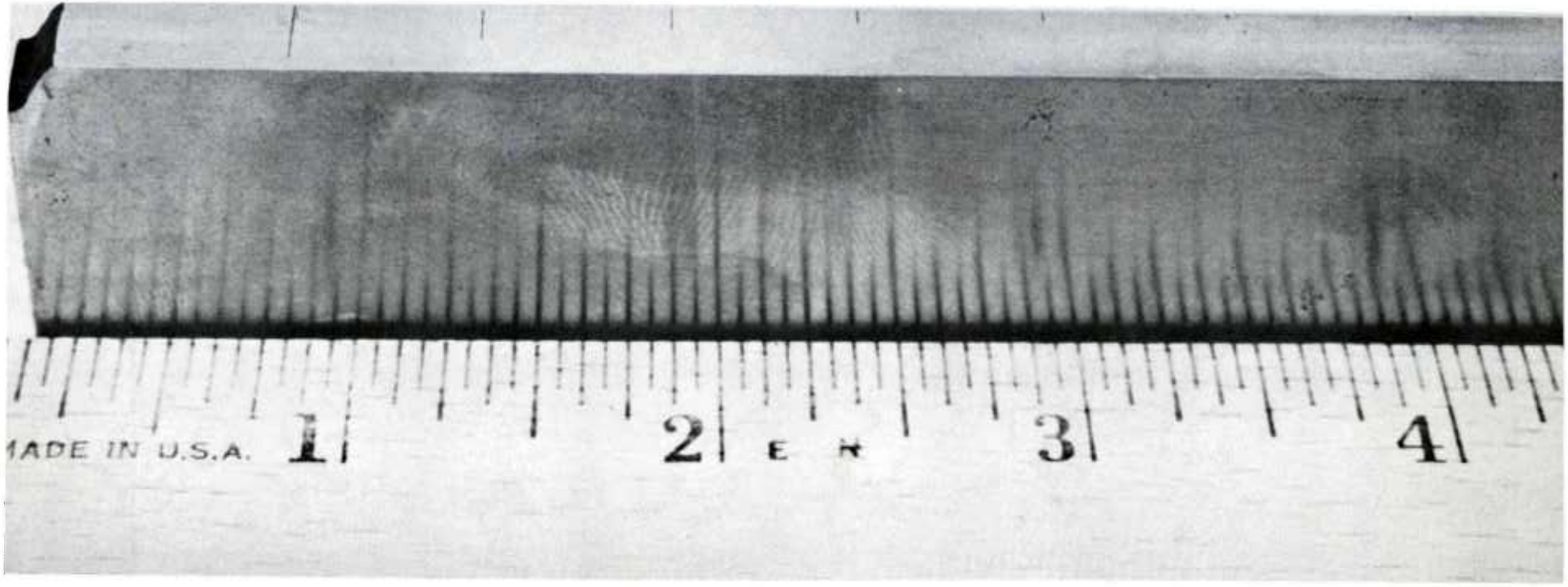

Figure 10. Corner slots

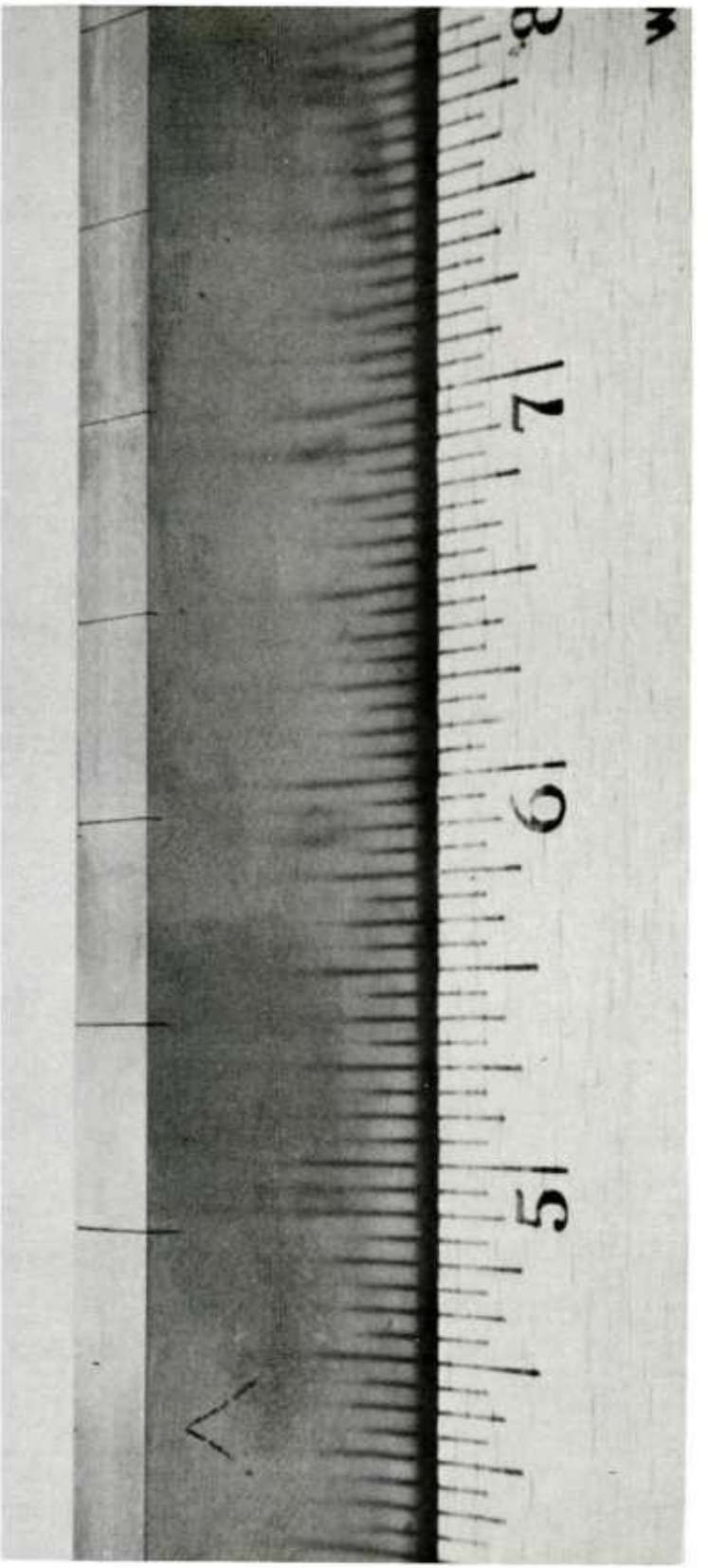

Figure 11. Edge slots

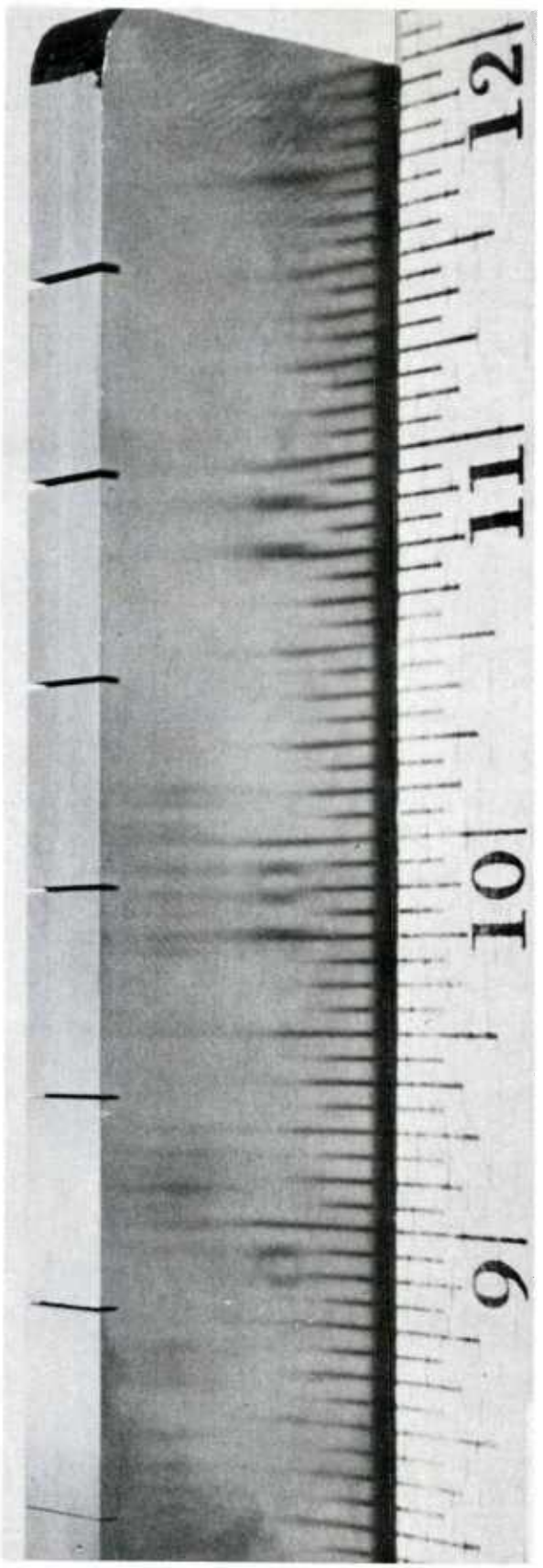

Figure 12. Varying width slots

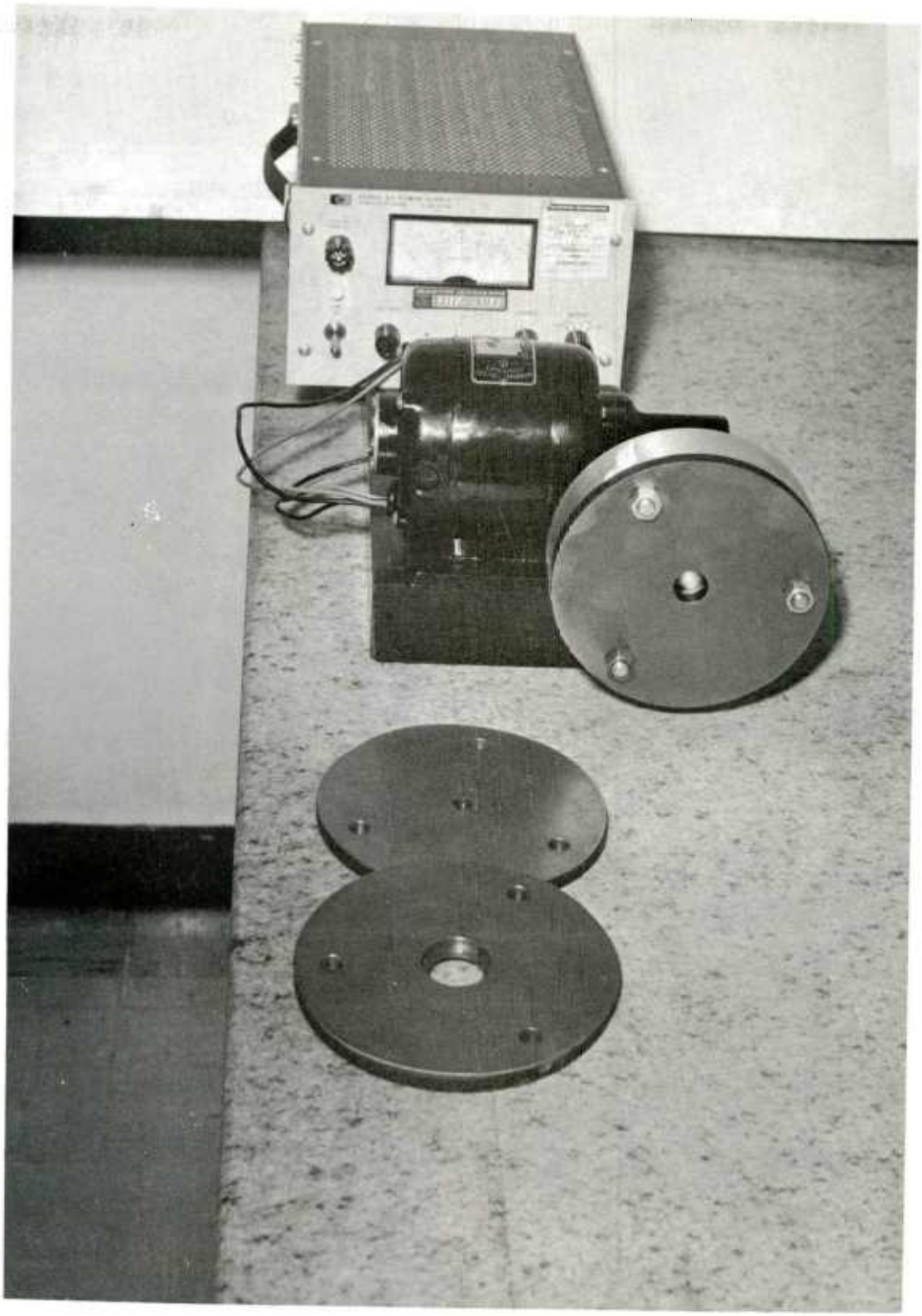

Figure 13. Hole test setup

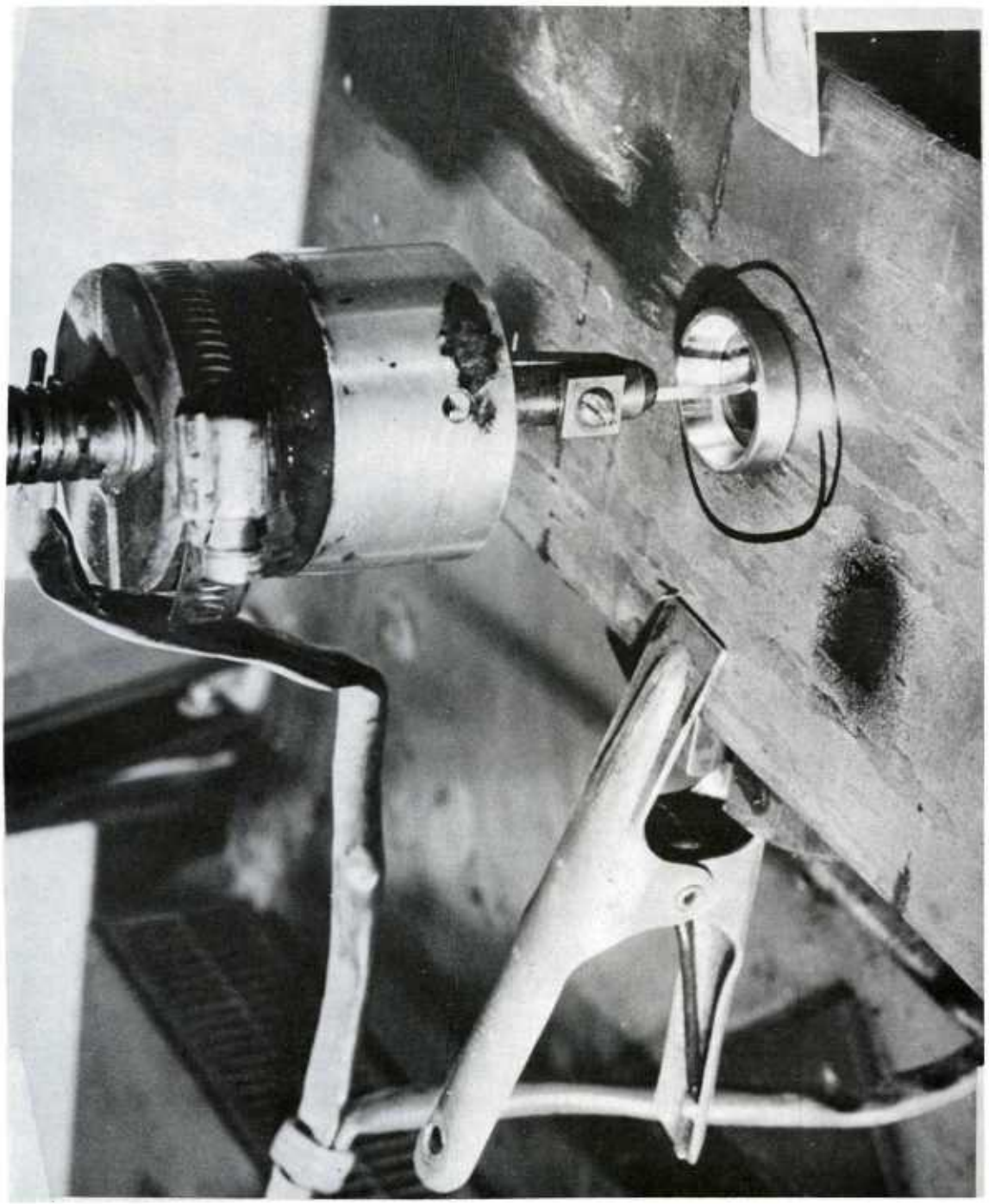

Figure 14. EDM generation of starter notch

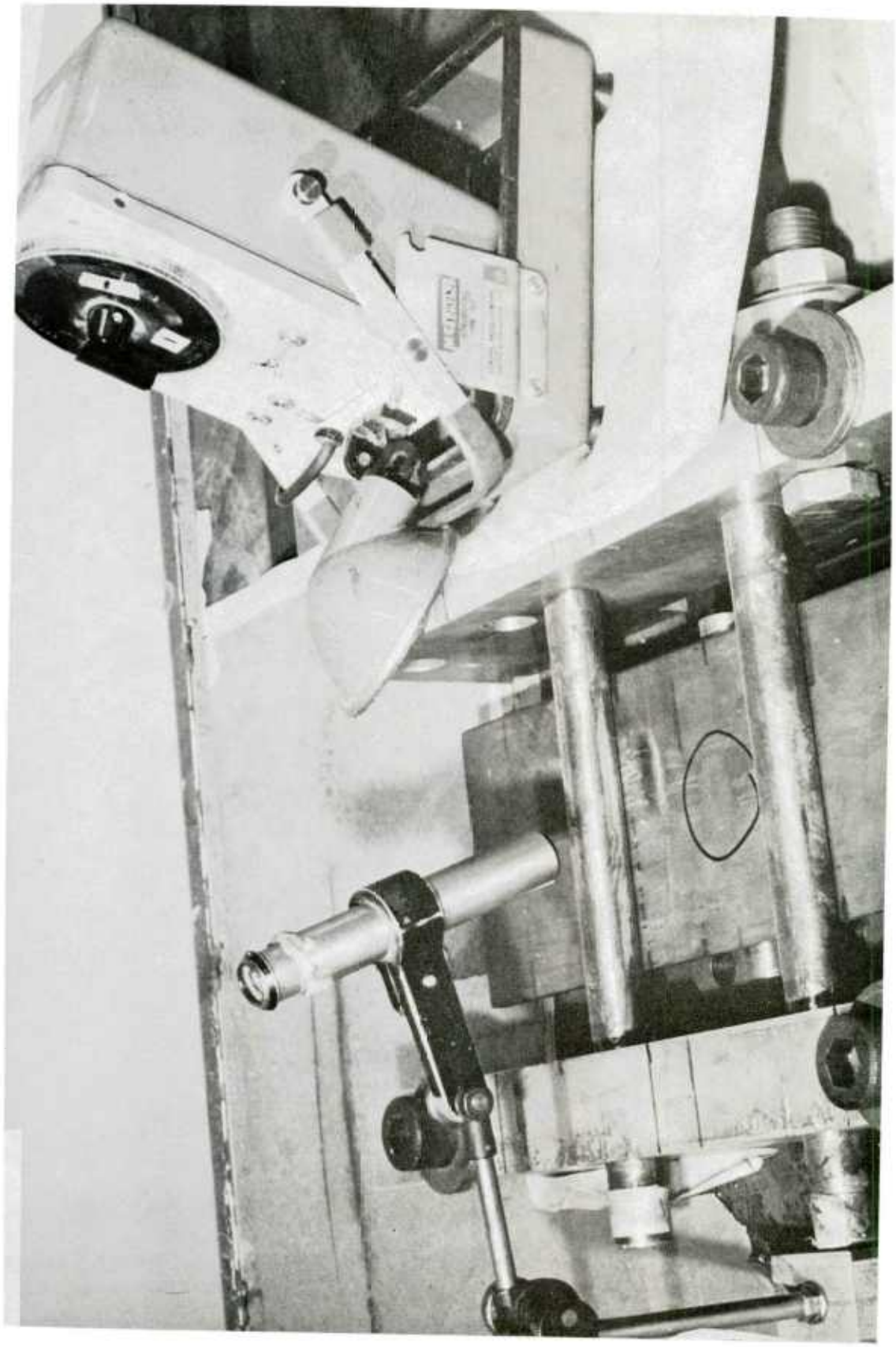

Figure 15. Fatigue crack growth setup

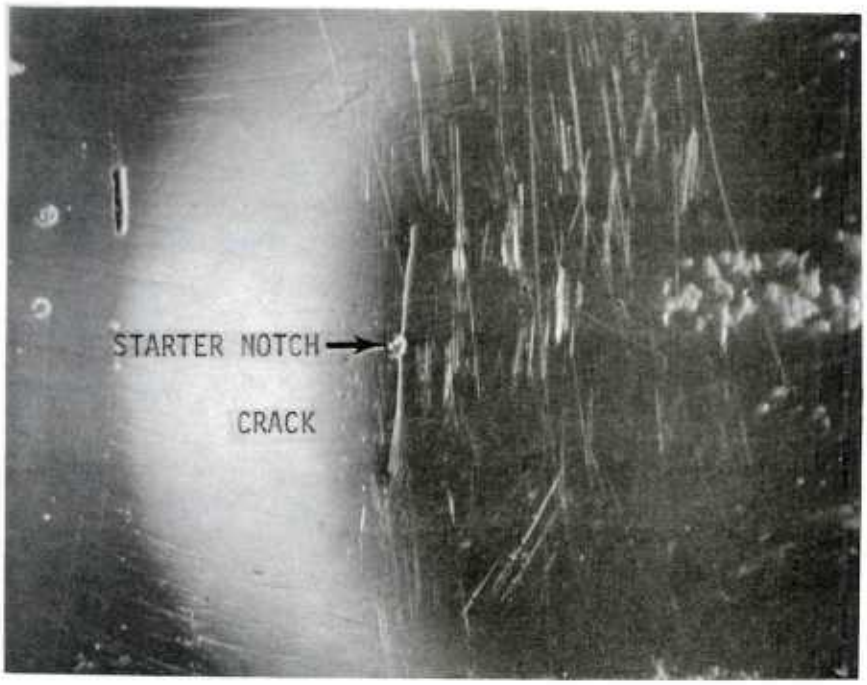

Figure 16. Starter notch and fatigue crack

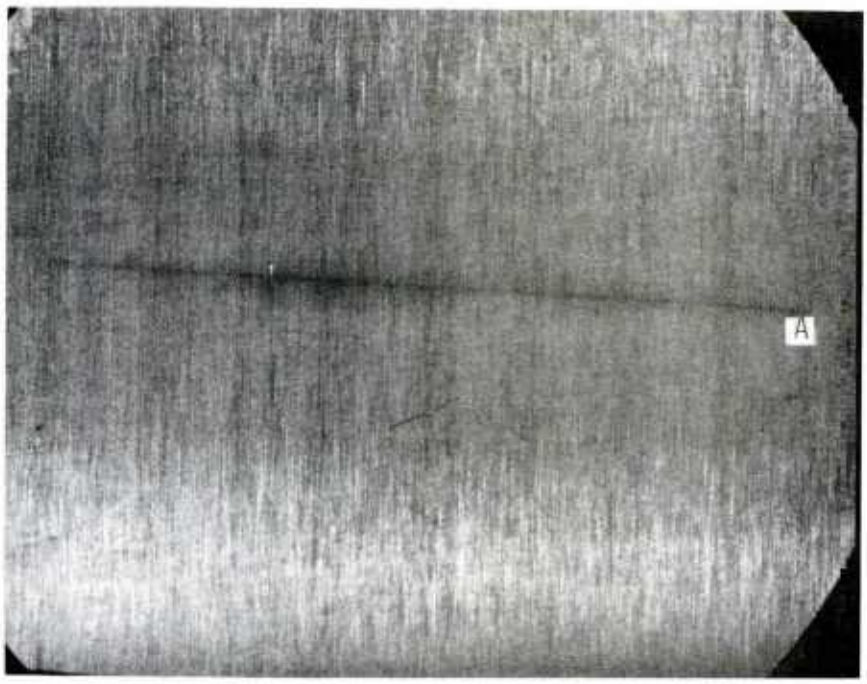

Figure 17. Fatigue crack A

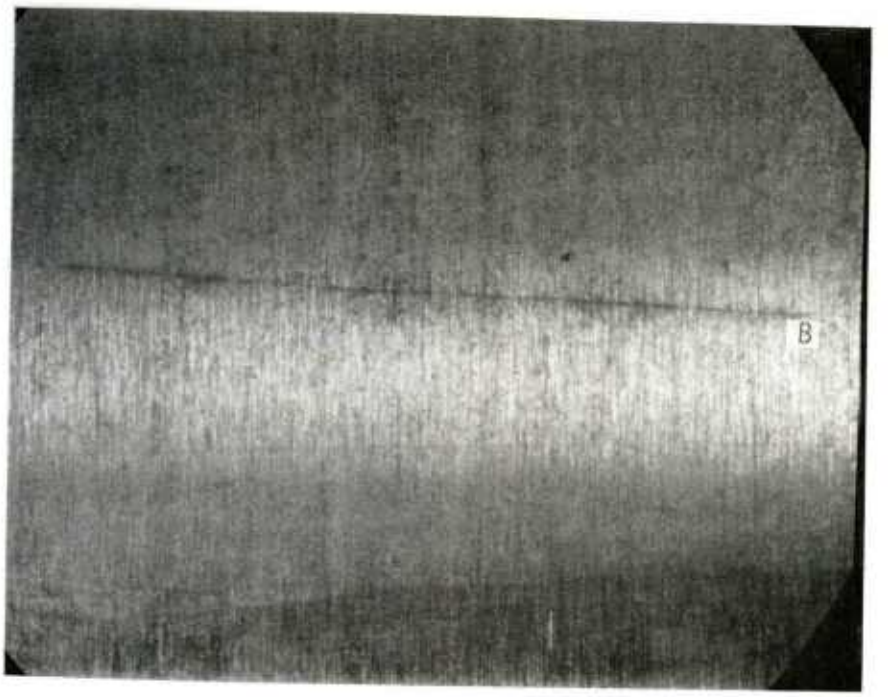

Figure 18. Fatigue crack B

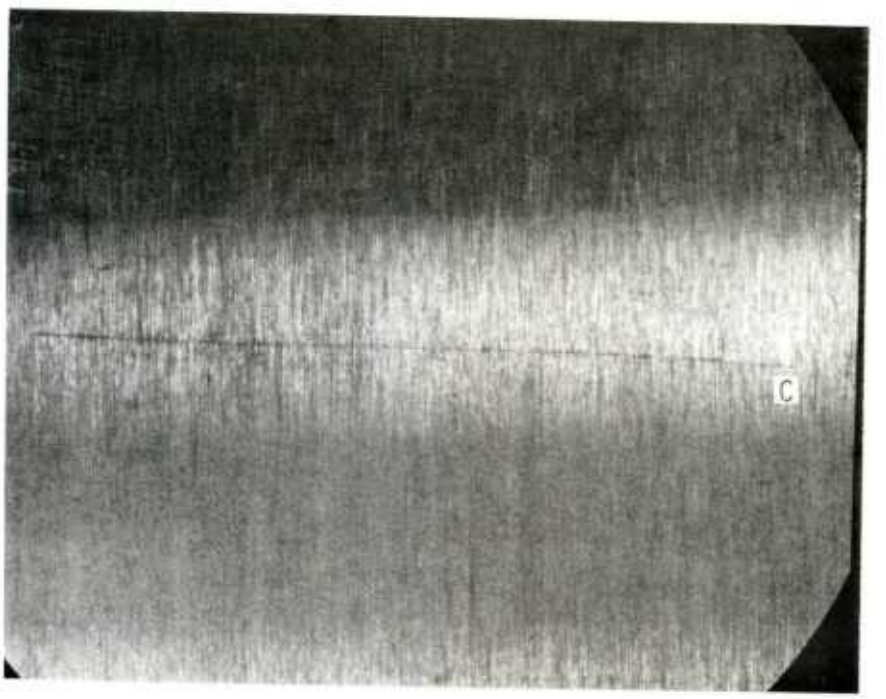

Figure 19. Fatigue crack C

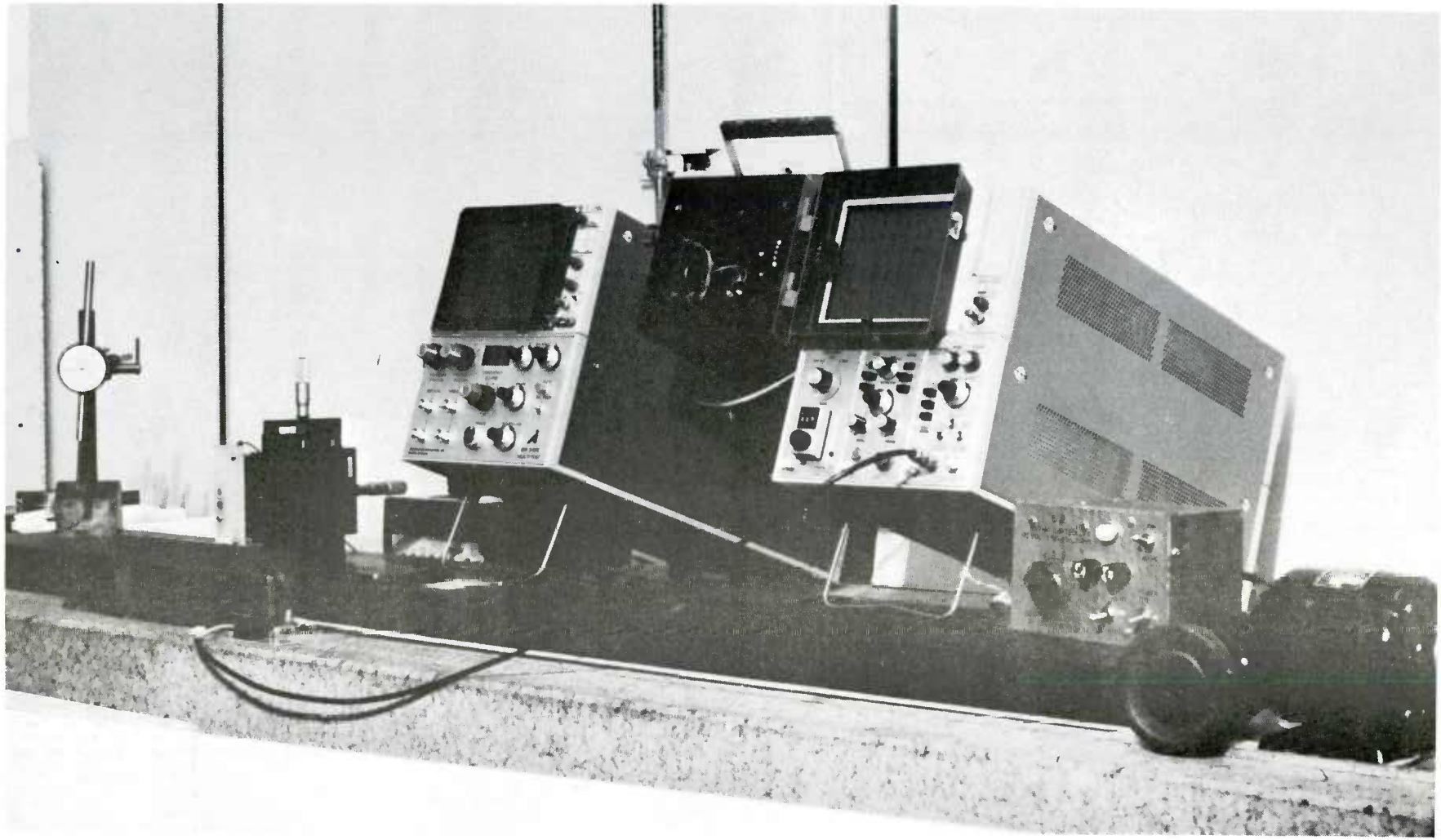

Figure 20. Overall setup of test equipment

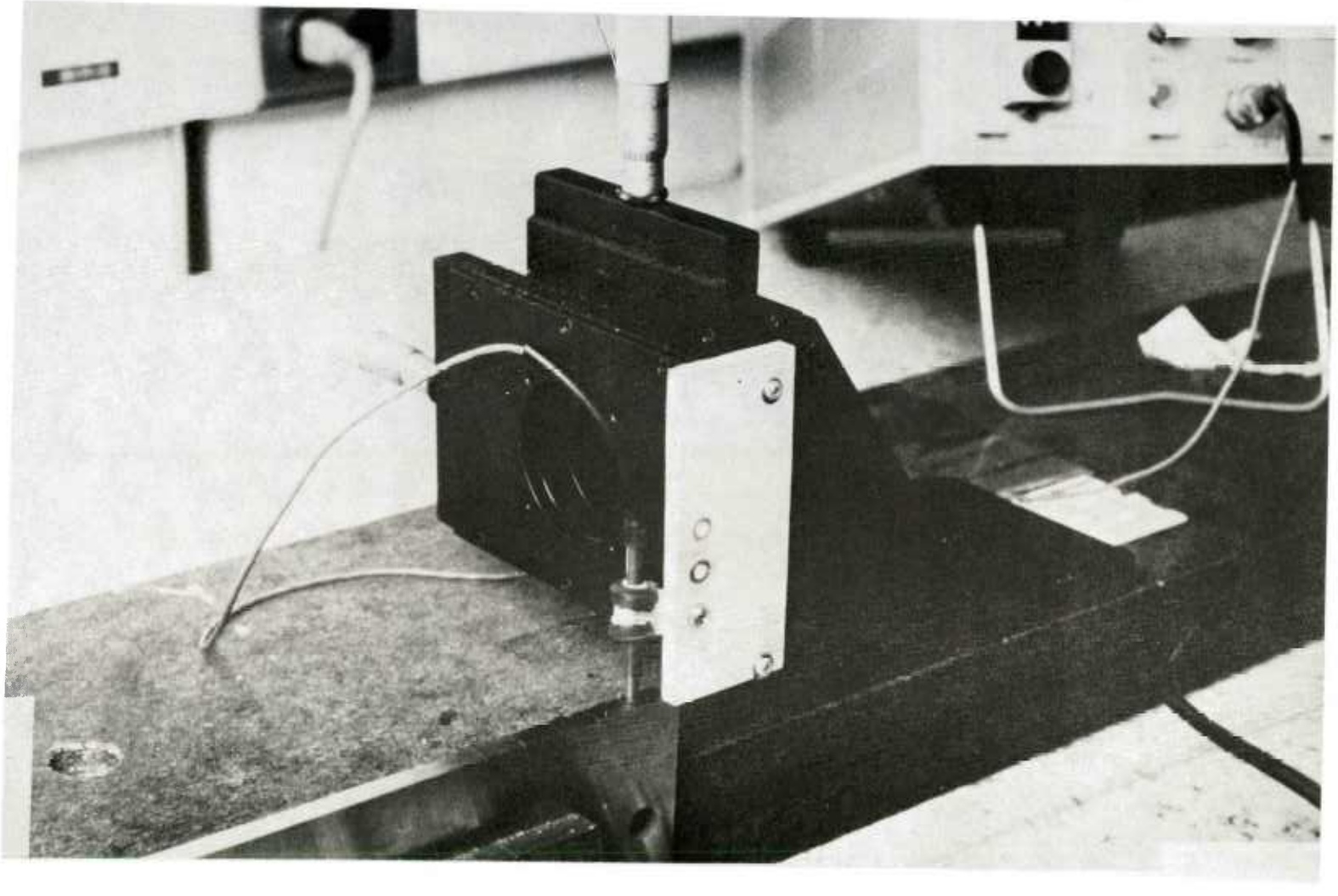

Figure 21. Micrometer stage probe holder

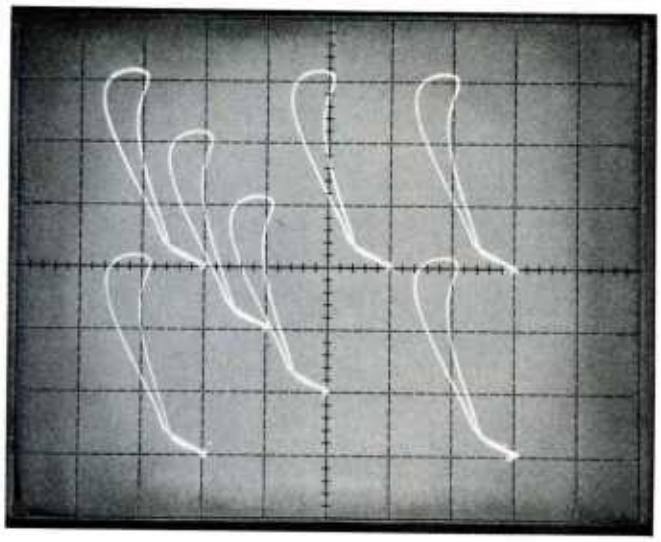

Figure 22. Equipment linearity

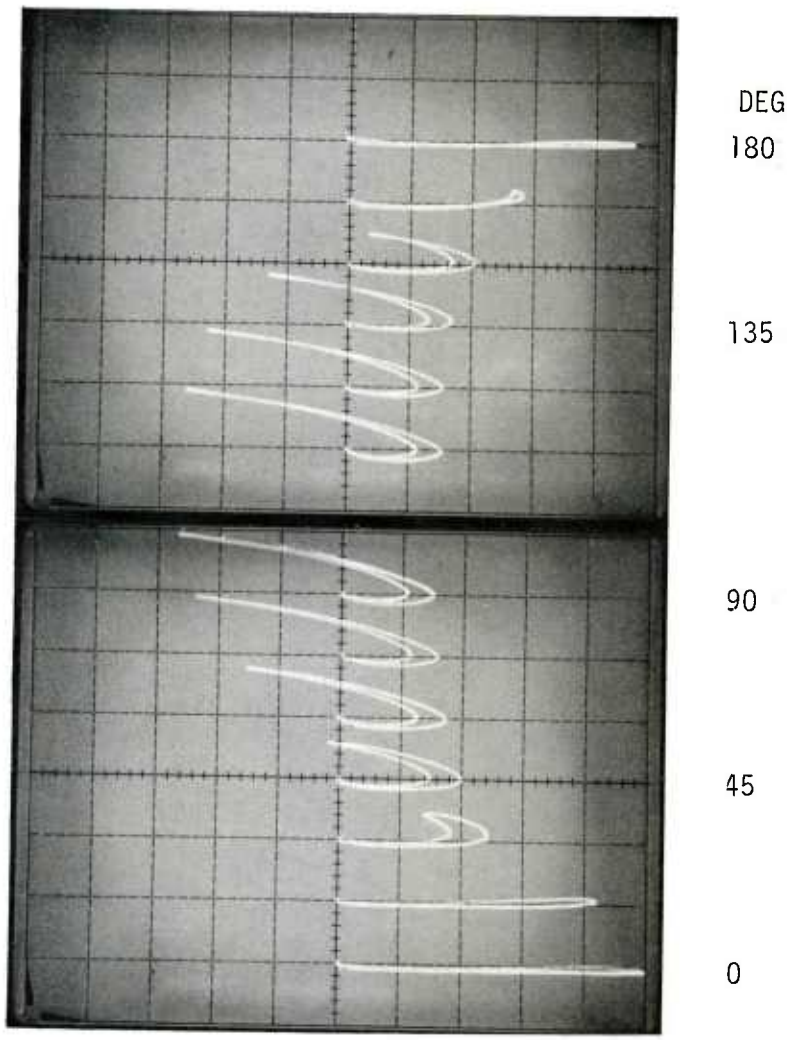

Figure 23. Two-pole probe response

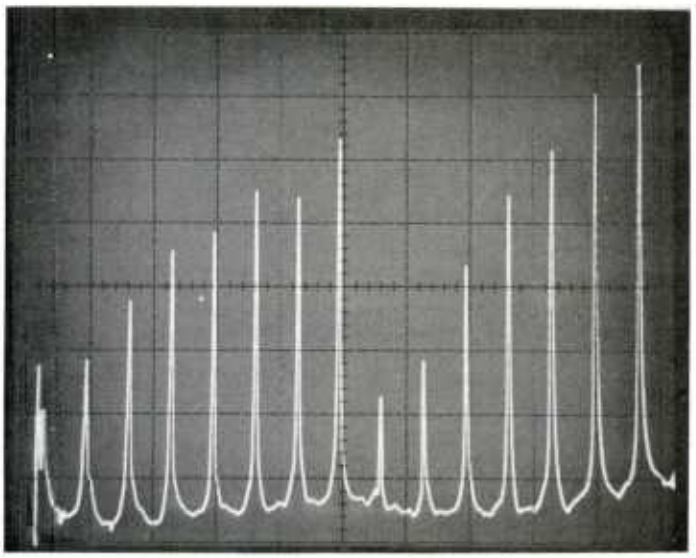

MAGNETIZED

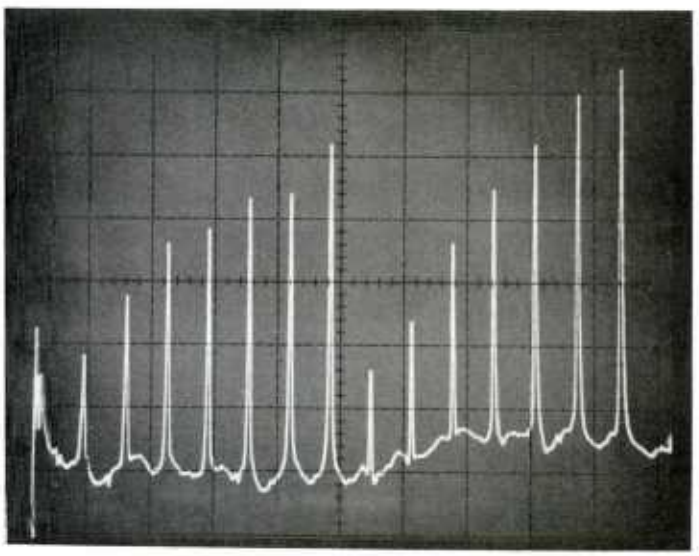

DEMAGNETIZED

Figure 24. Magnetized versus demagnetized material response

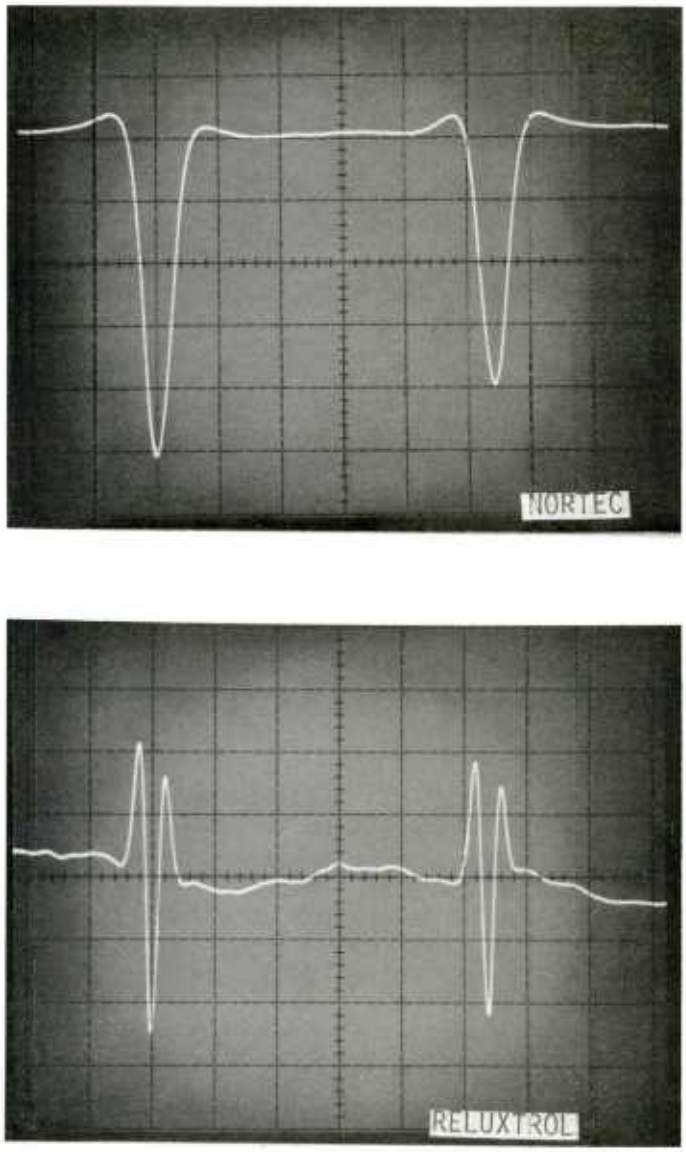

Figure 25. Spatial resolution response

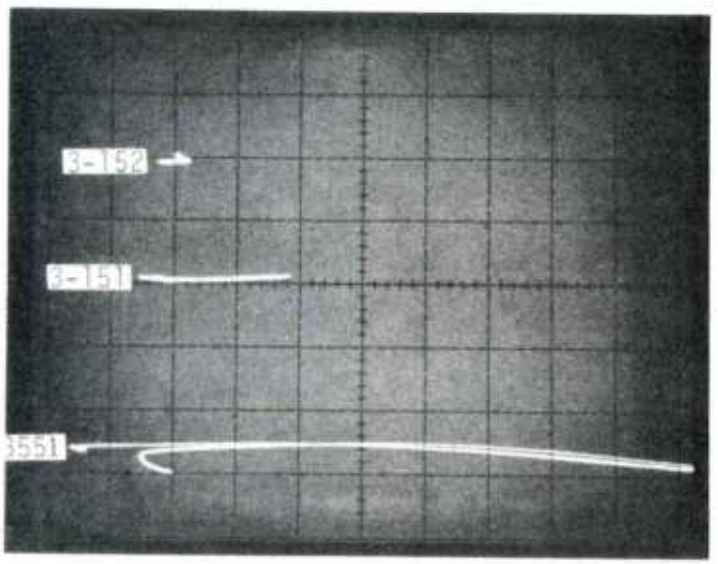

Figure 26. Relative sensitivity of probes

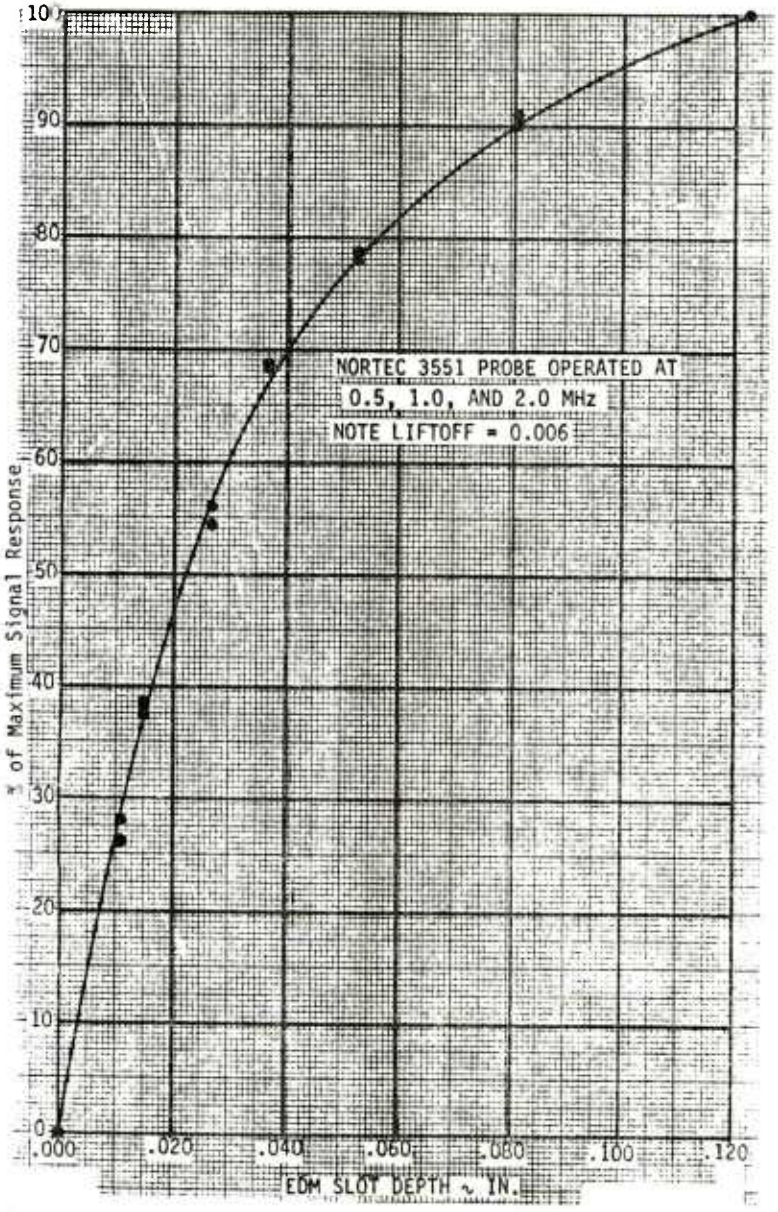

Figure 27. Response to slot depths

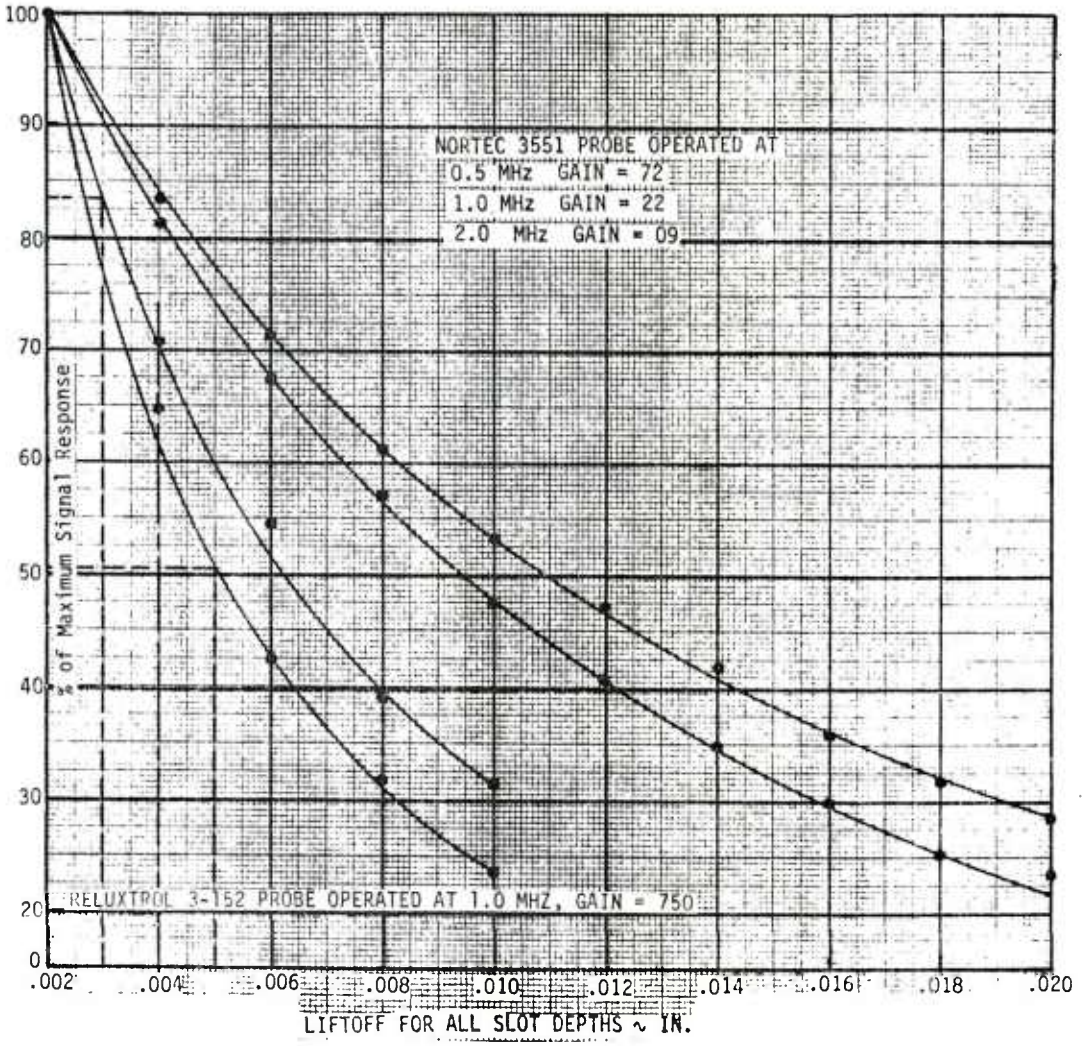

Figure 28. Response to liftoff change

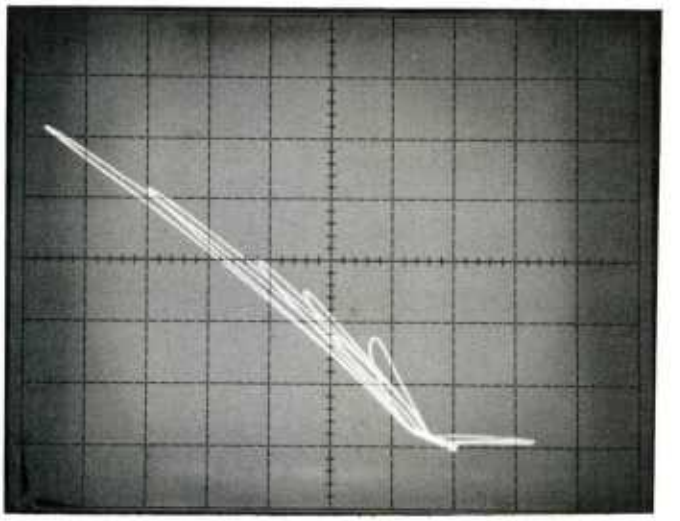

RELUXTROL 3-152

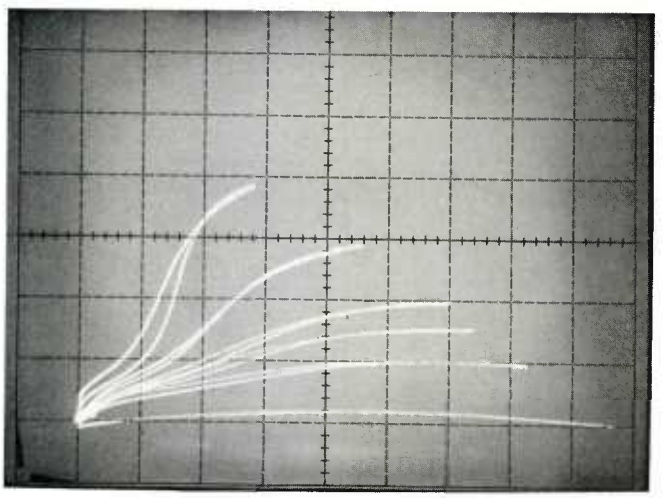

NORTEC 3551

Figure 29. Response to slot widths

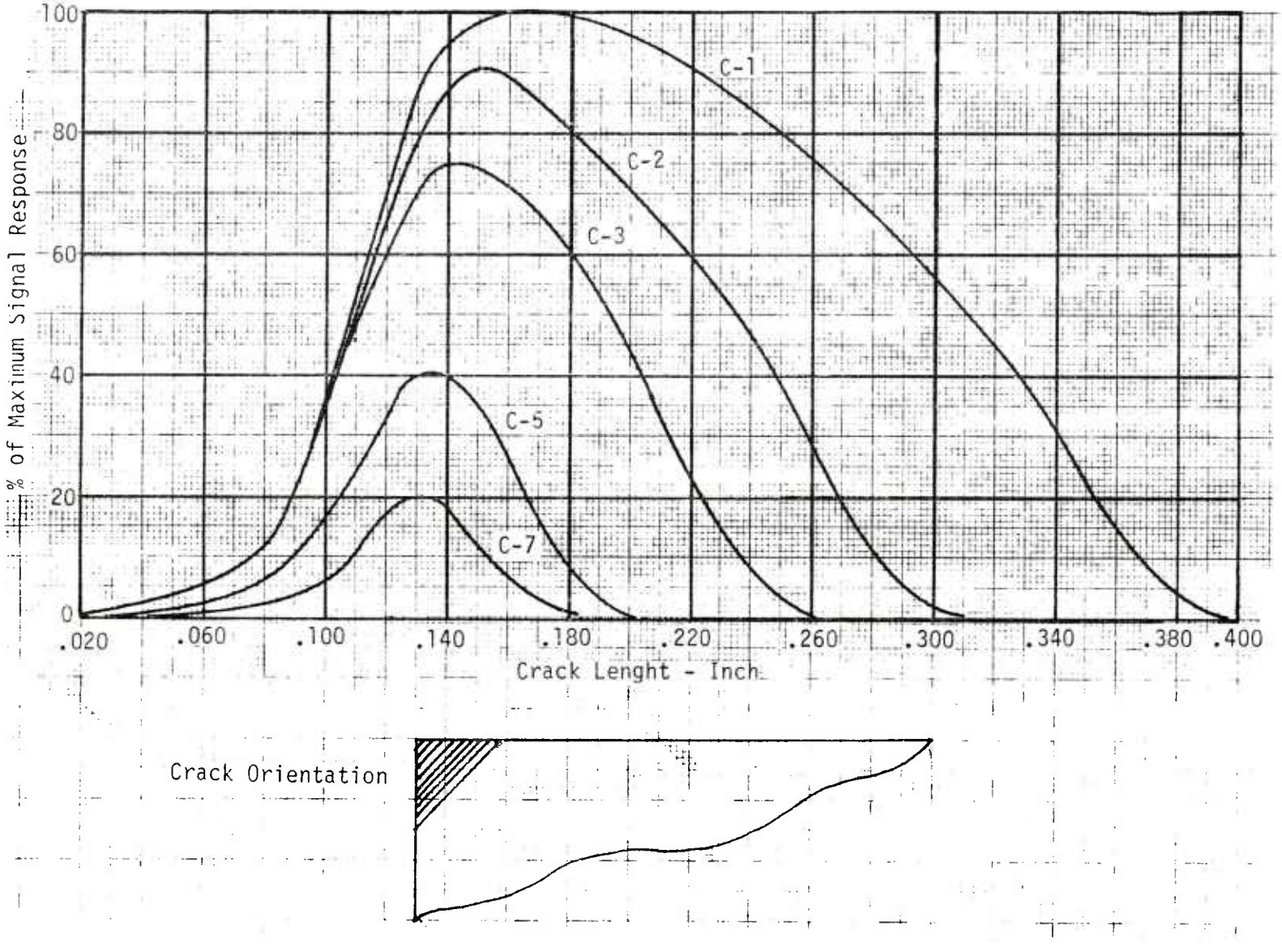

Figure 30. Response to corner slots and edges, Nortec

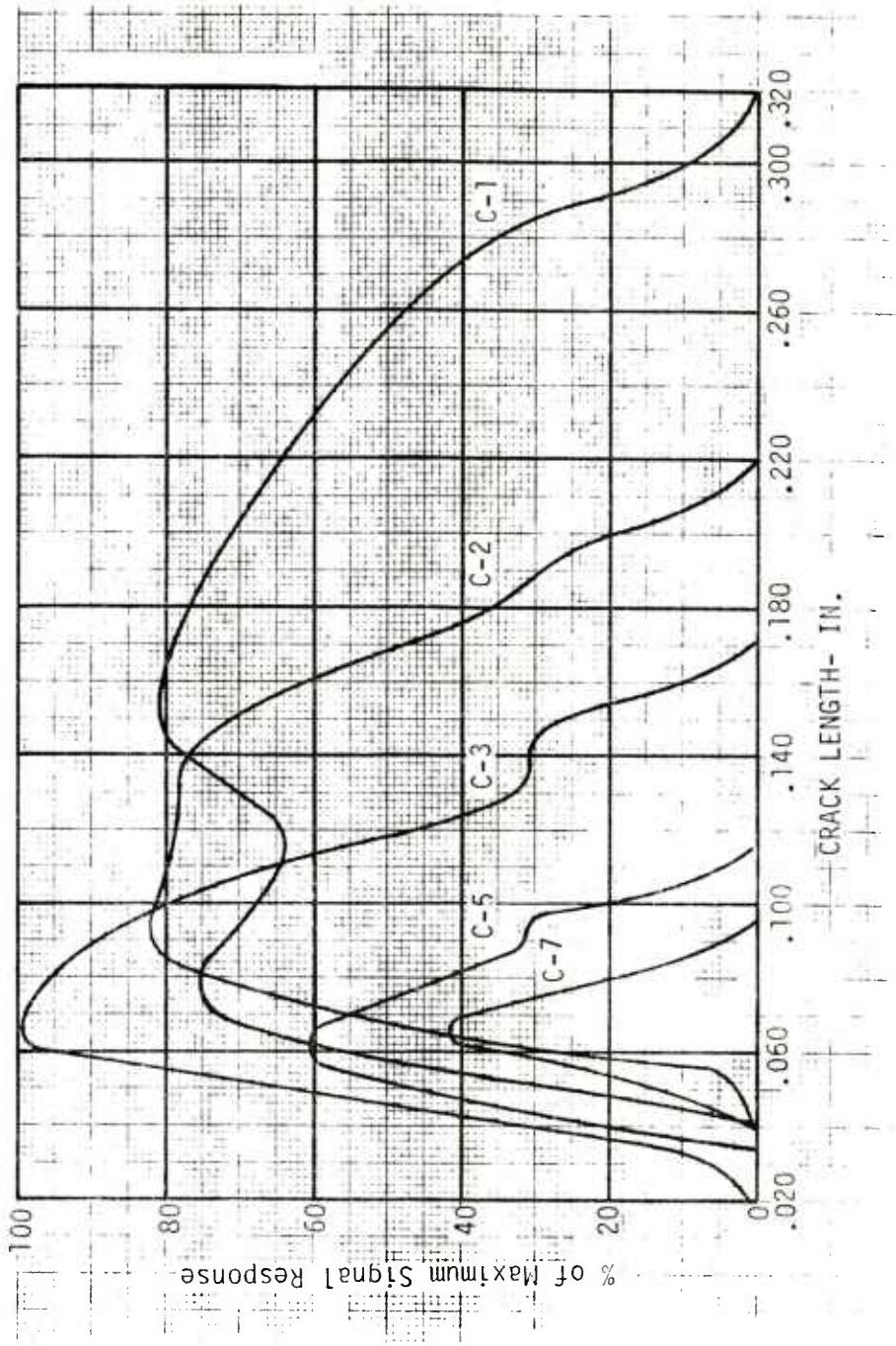

Figure 31. Response to corner slots and edges, Reluxtrol

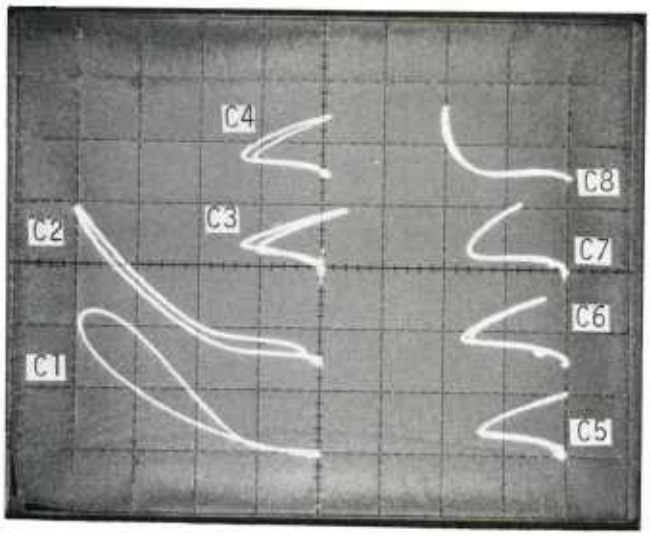

RELUXTROL 3-152

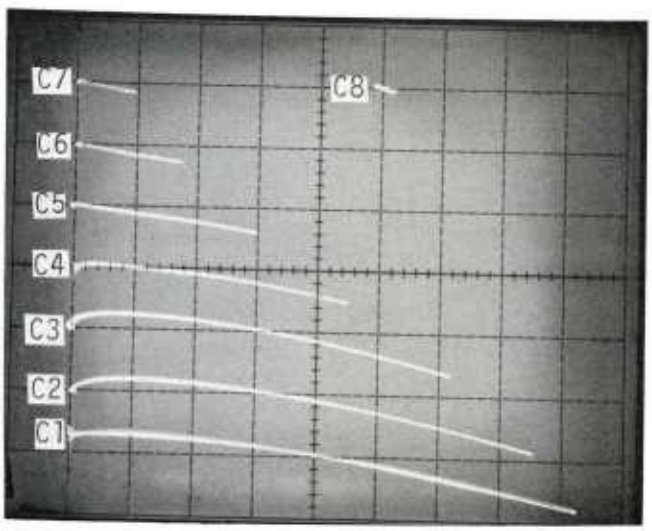

NORTEC 3551

Figure 32. Phase response to corner slots, Reluxtrol versus Nortec

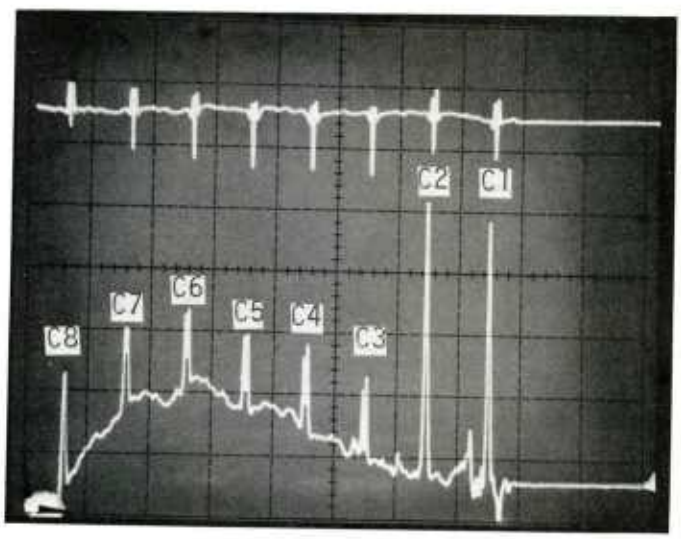

Figure 33. Response to corner slots, phase rotation

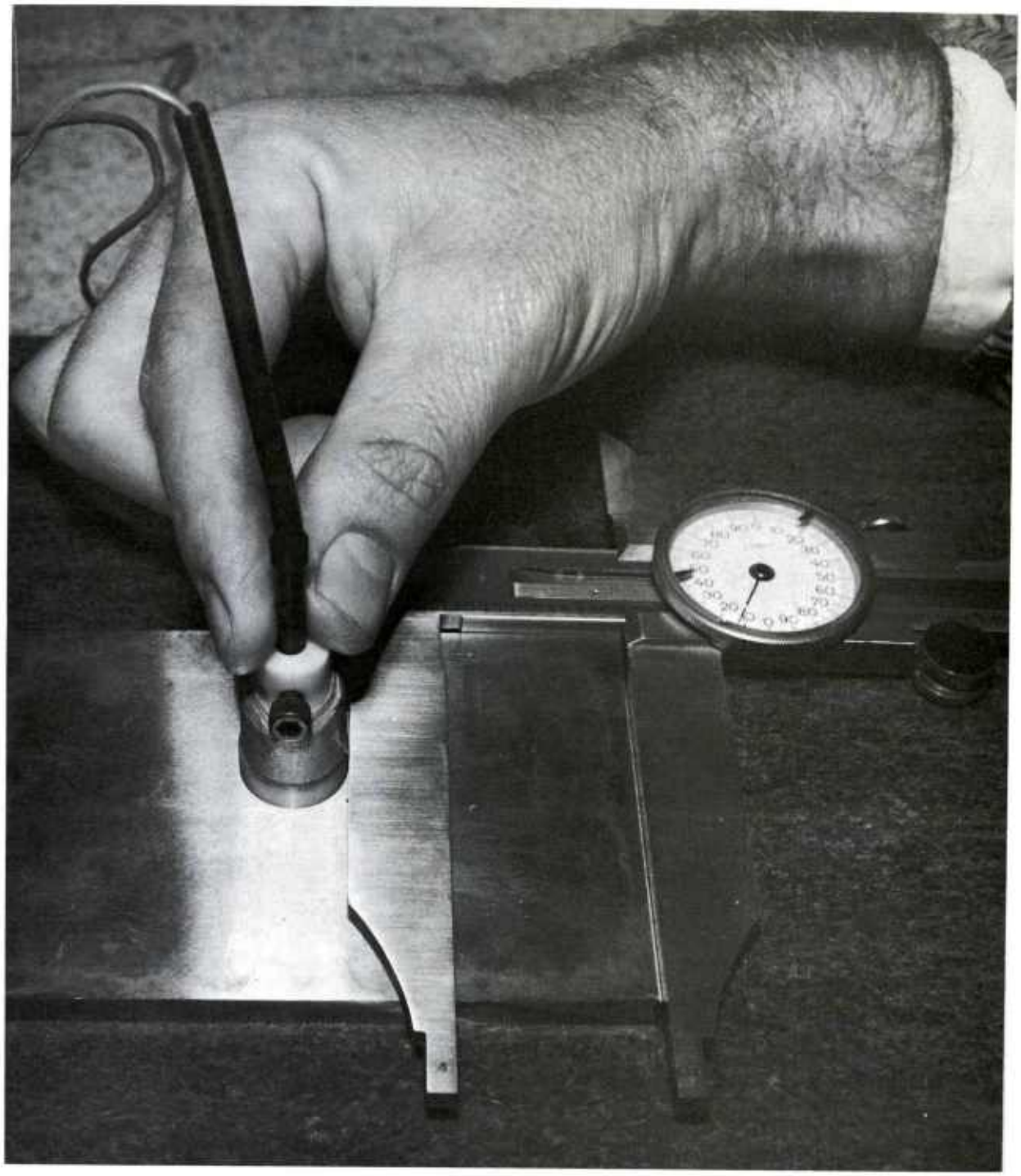

Figure 34. Manual scanning of fatigue cracks

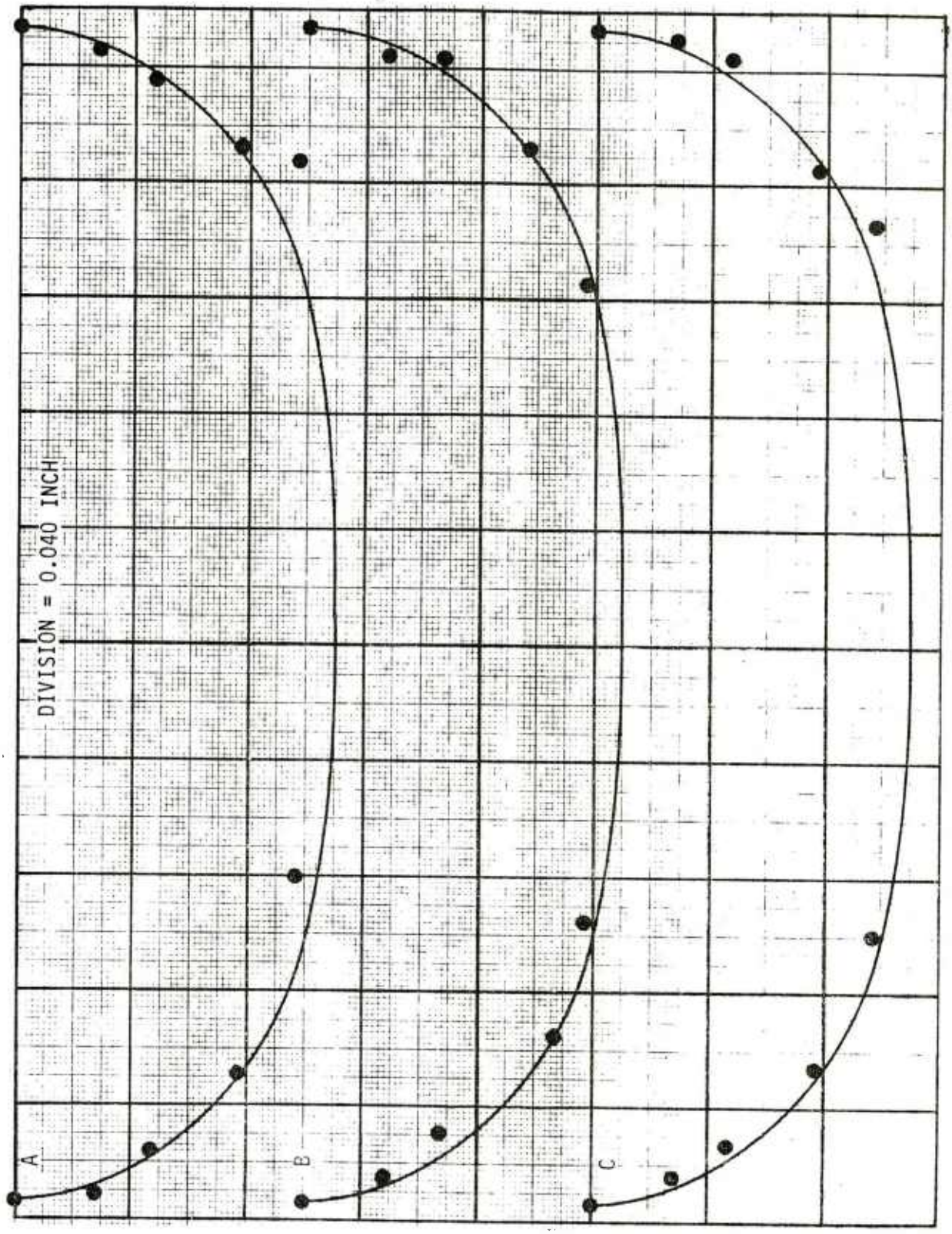

Figure 35. Dimensional profiles of A, B, and C

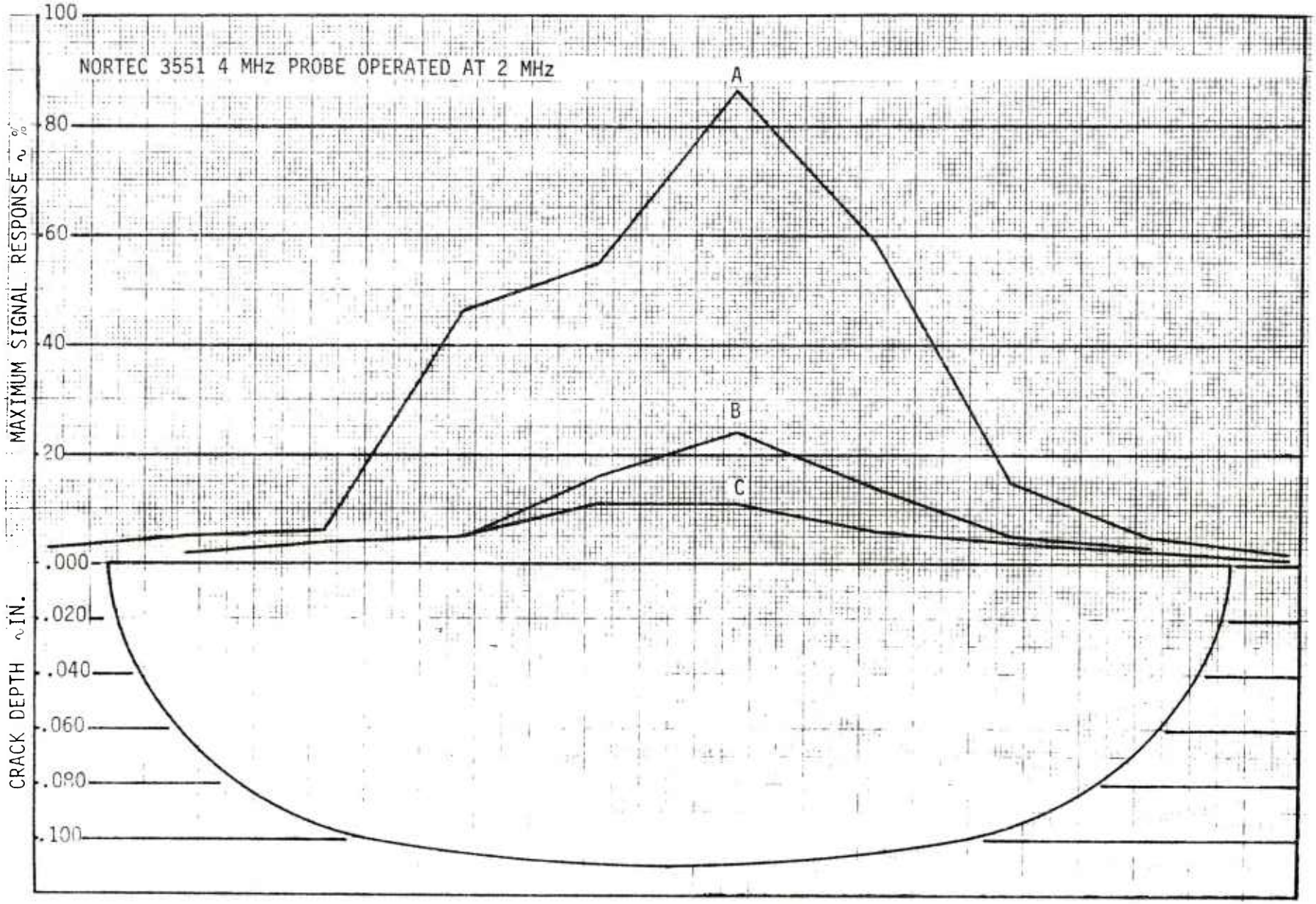

Figure 36. Profile of A, B, and C at 0.110-in. depth

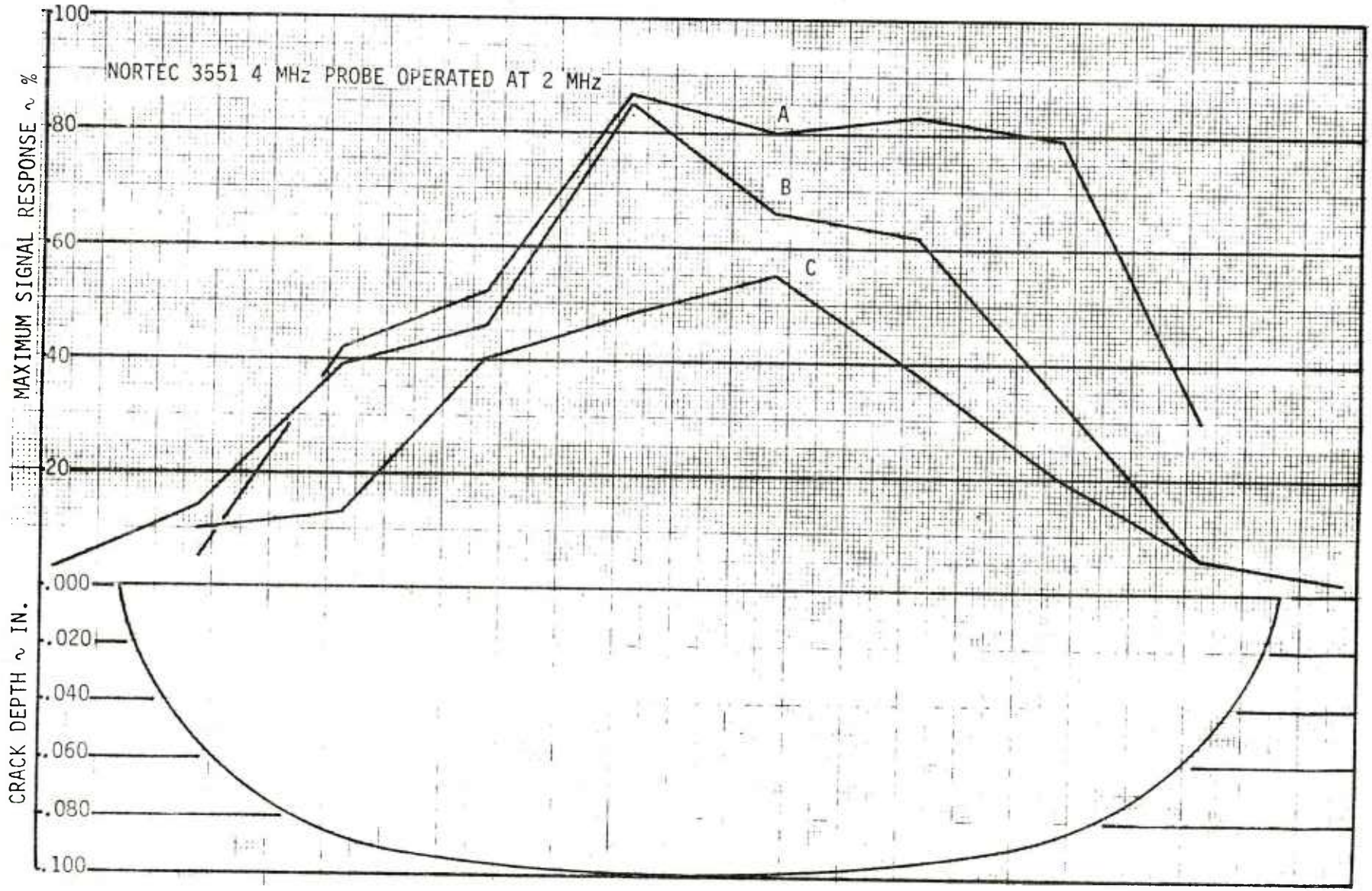

Figure 37. Profile of A, B, and C at 0.100-in. depth

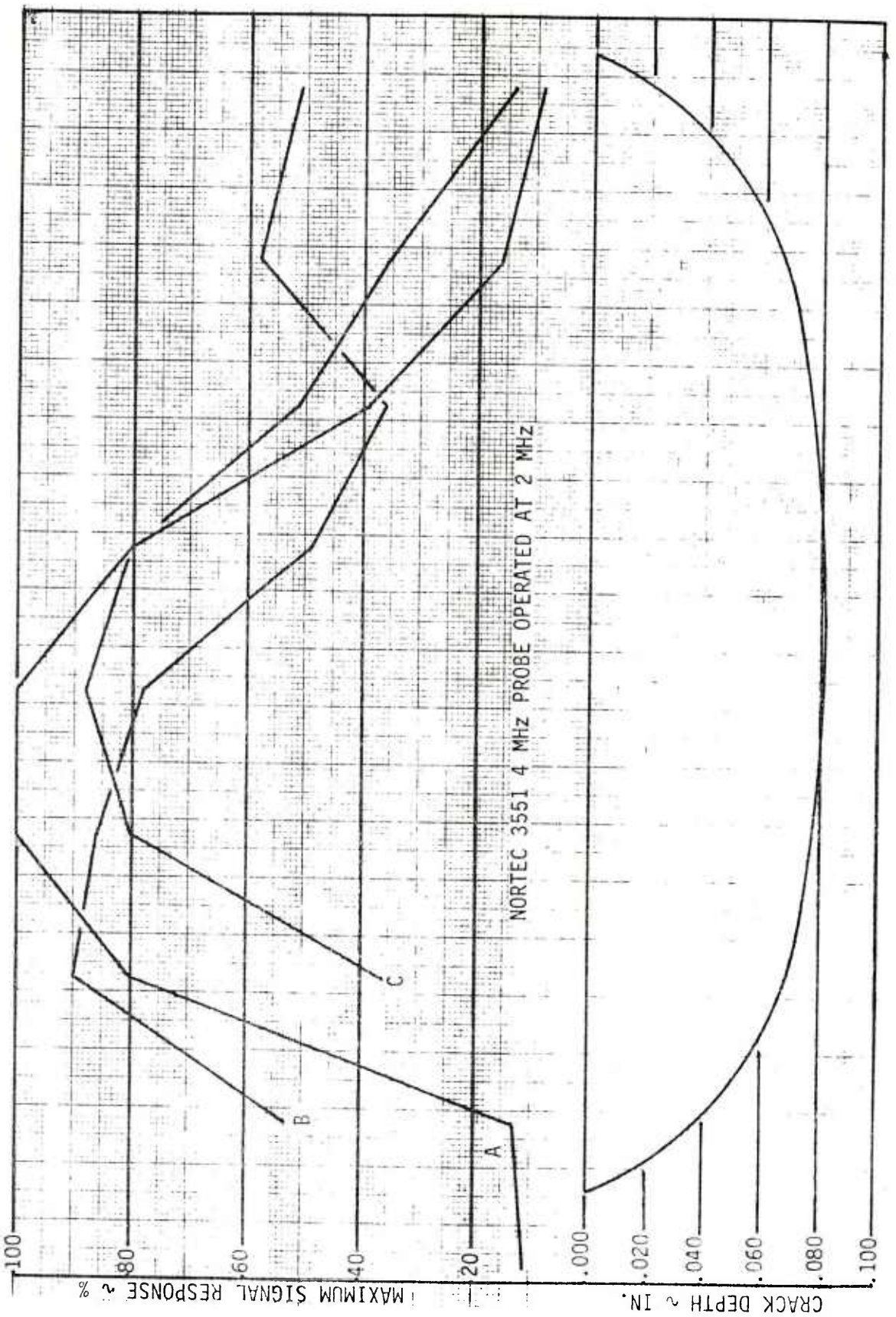

Figure 38. Profile of A, B, and C at 0.082-in. depth

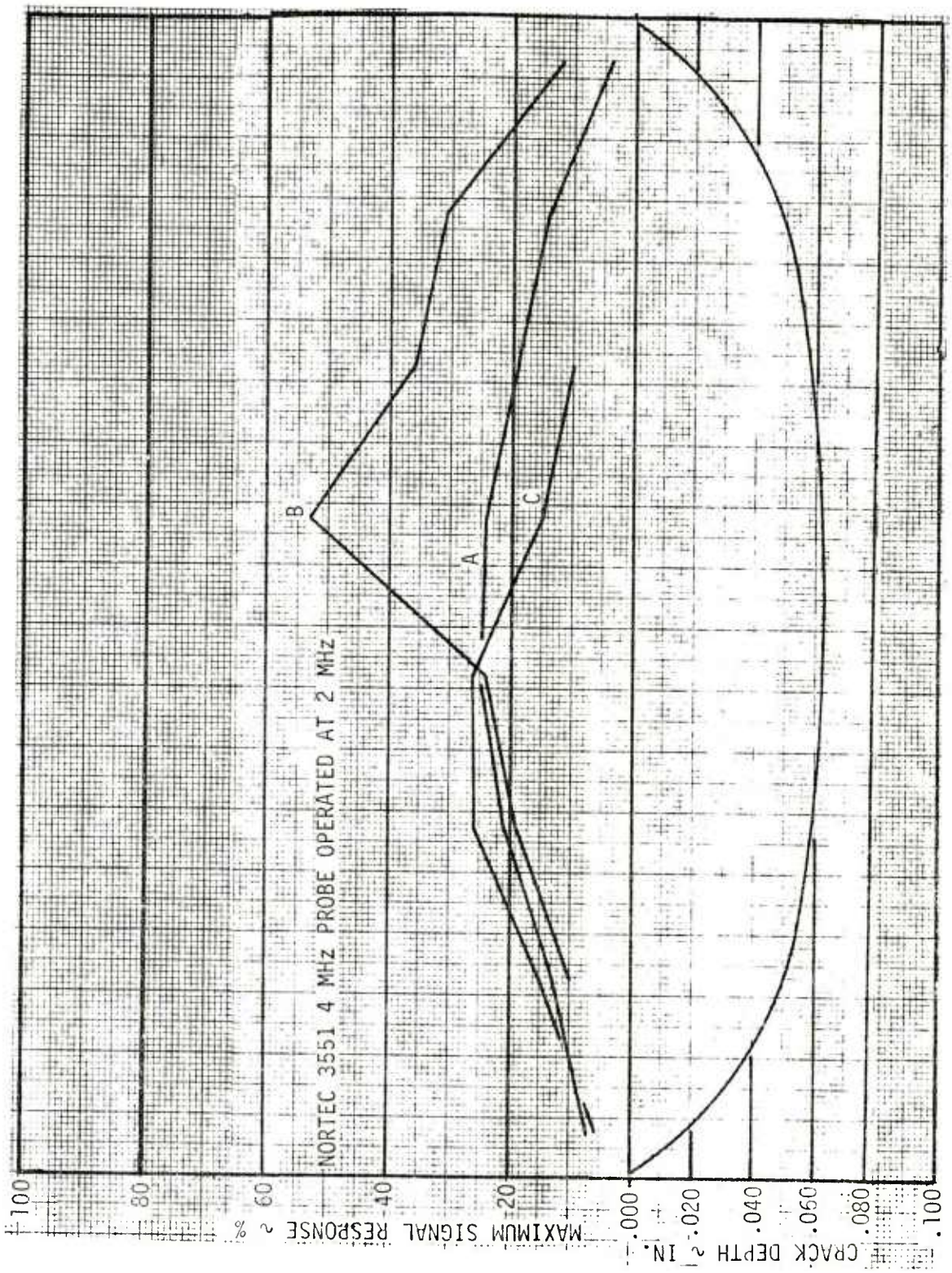

Figure 39. Profile of A, B, and C at 0.063-in. depth

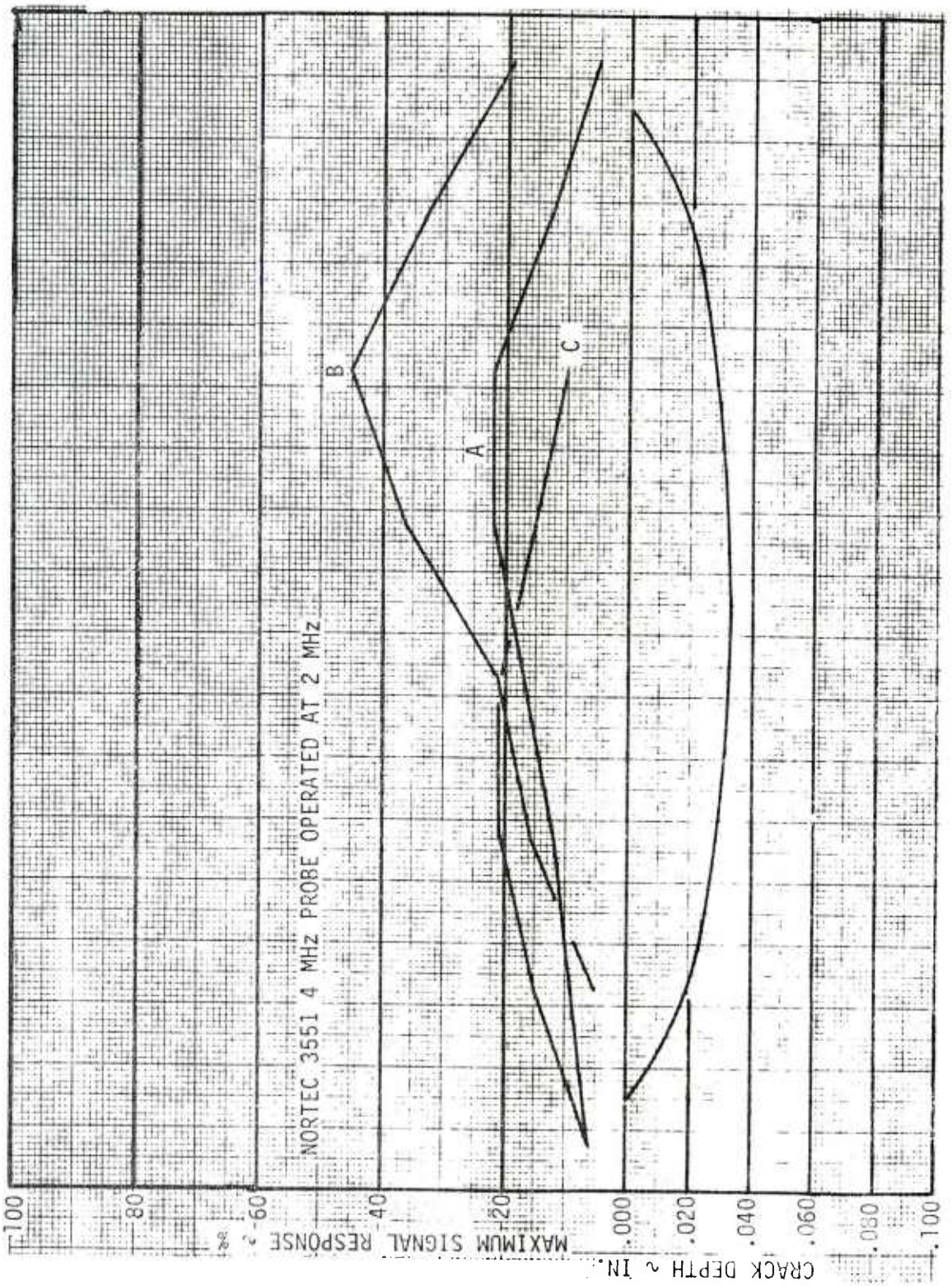

Figure 40. Profile of A, B, and C at 0.033-in. depth

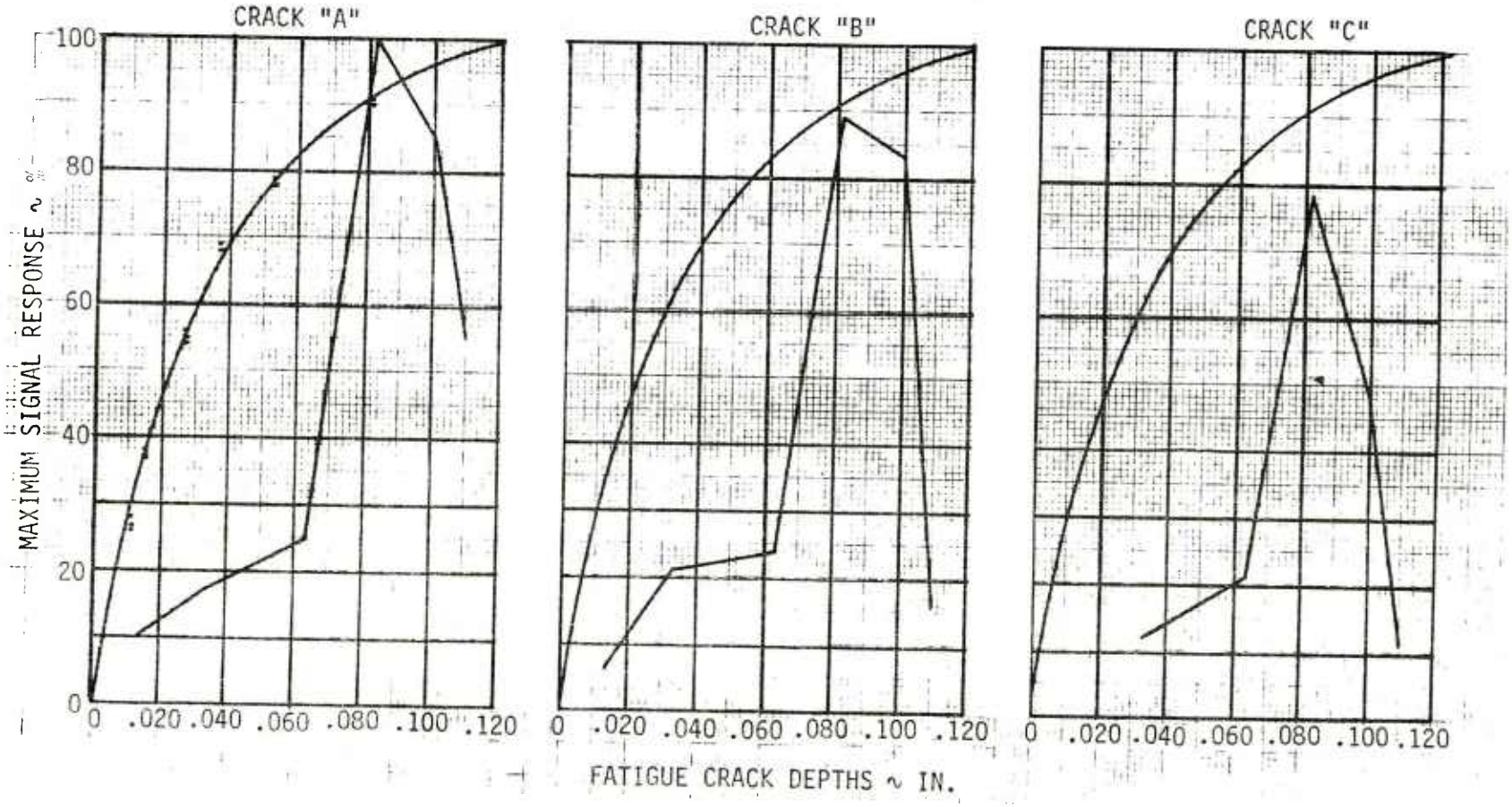

Figure 41. Eddy current response, original centerlines of A, B, and C

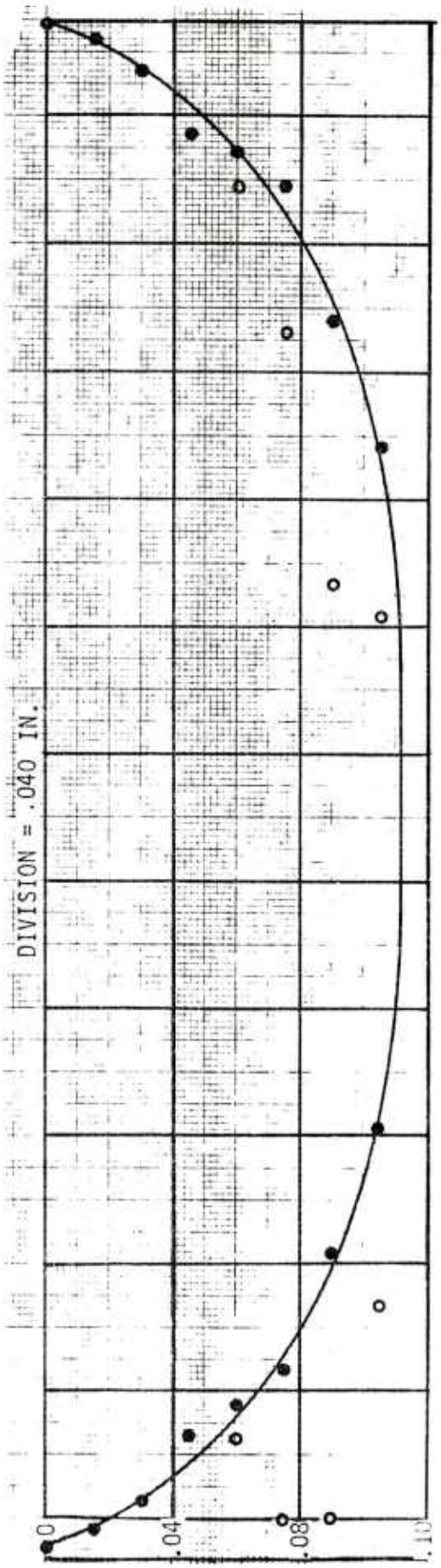

Figure 42. Dimensional profile of F

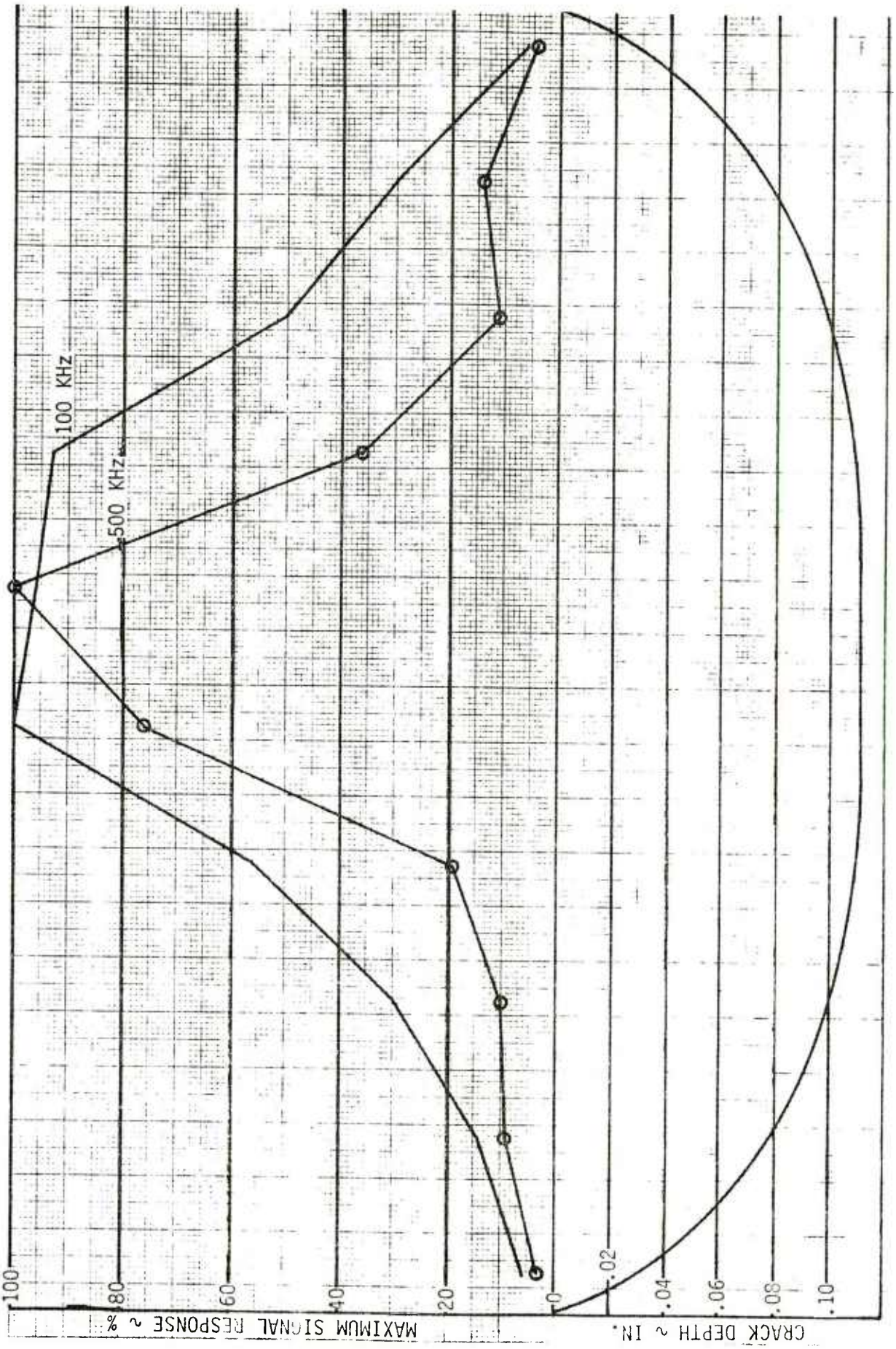

Figure 43. Profile of F at 0.112-in. depth

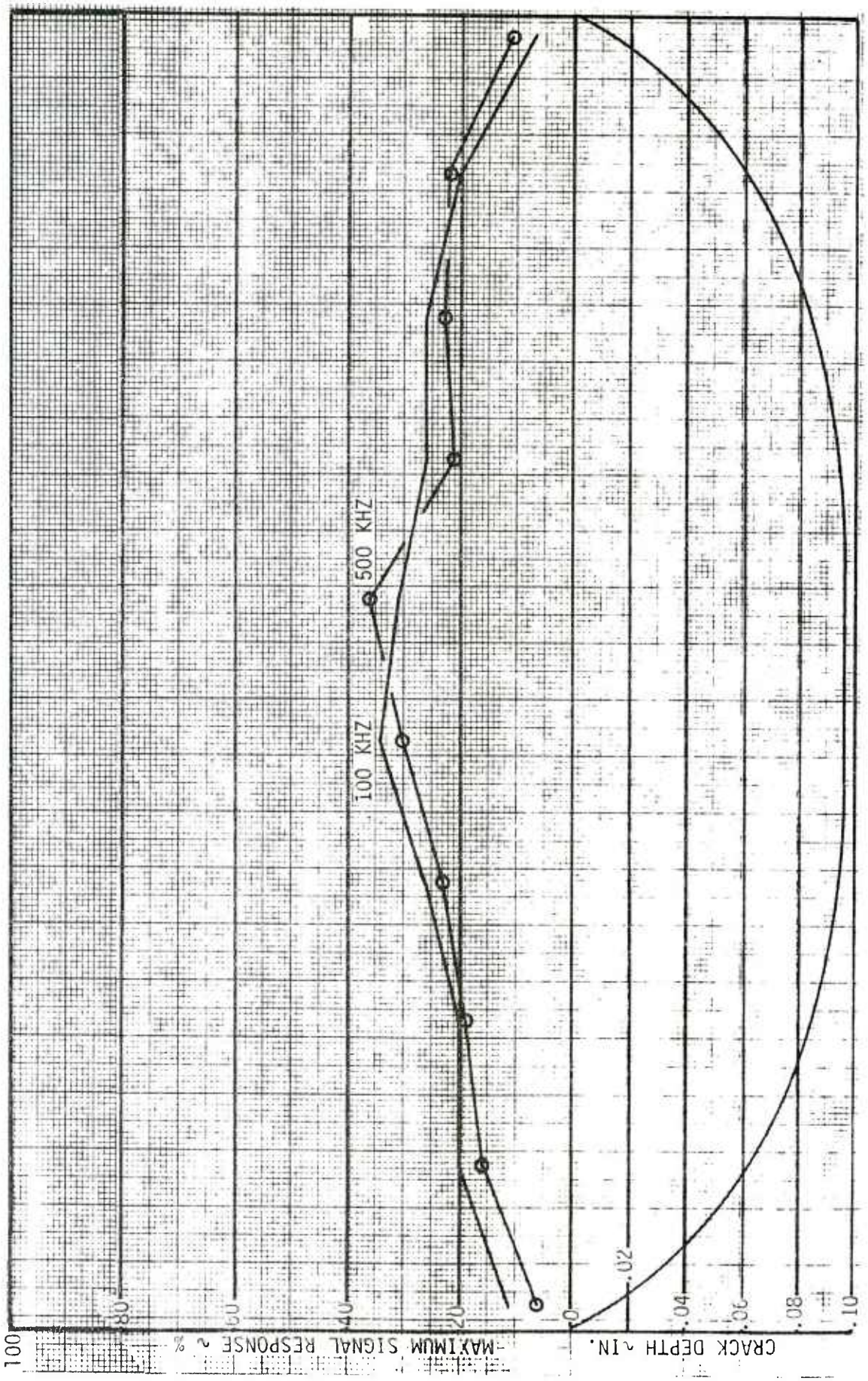

Figure 44. Profile of F at 0.097-in. depth

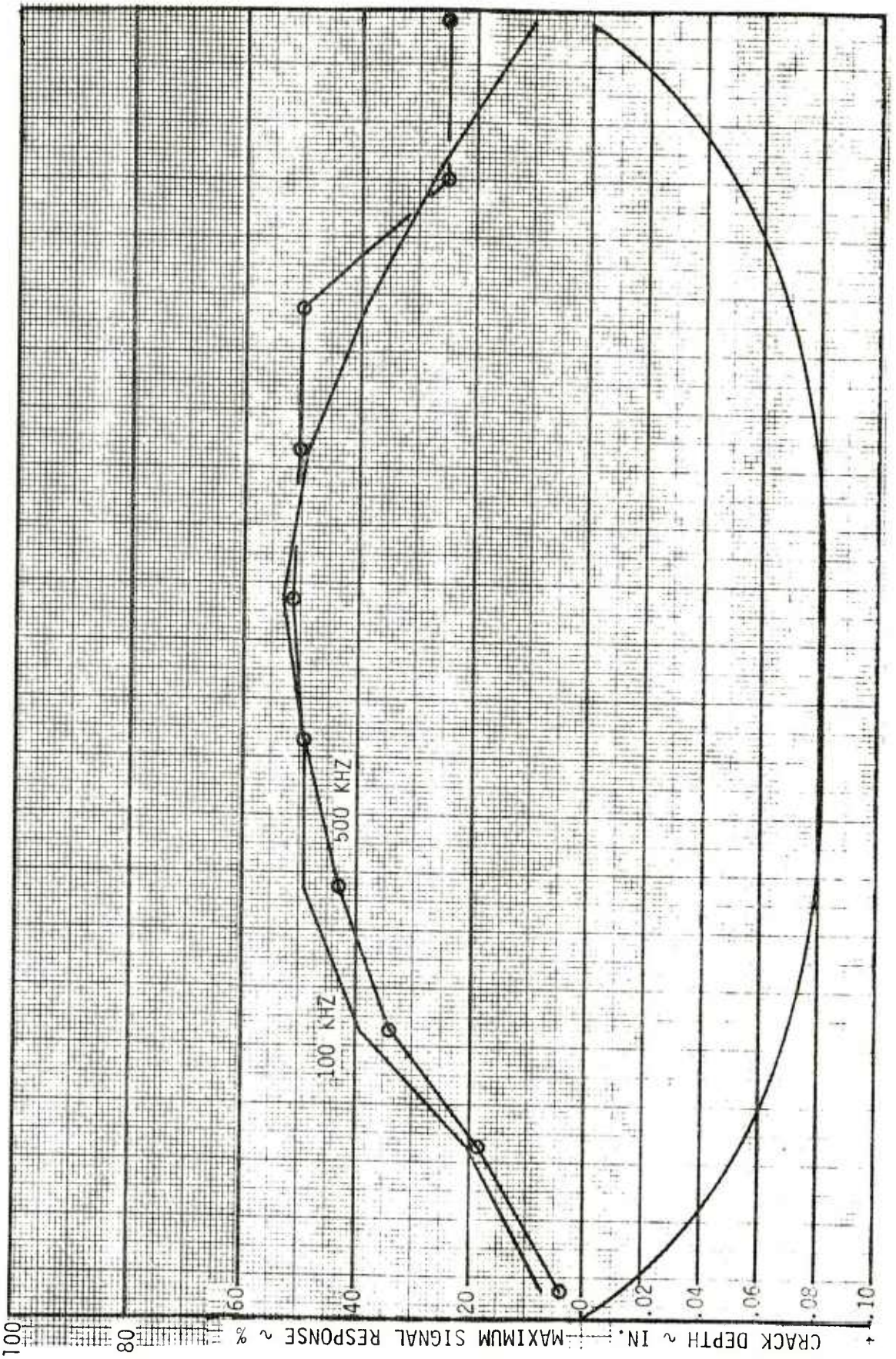

Figure 45. Profile of F at 0.082-in. depth

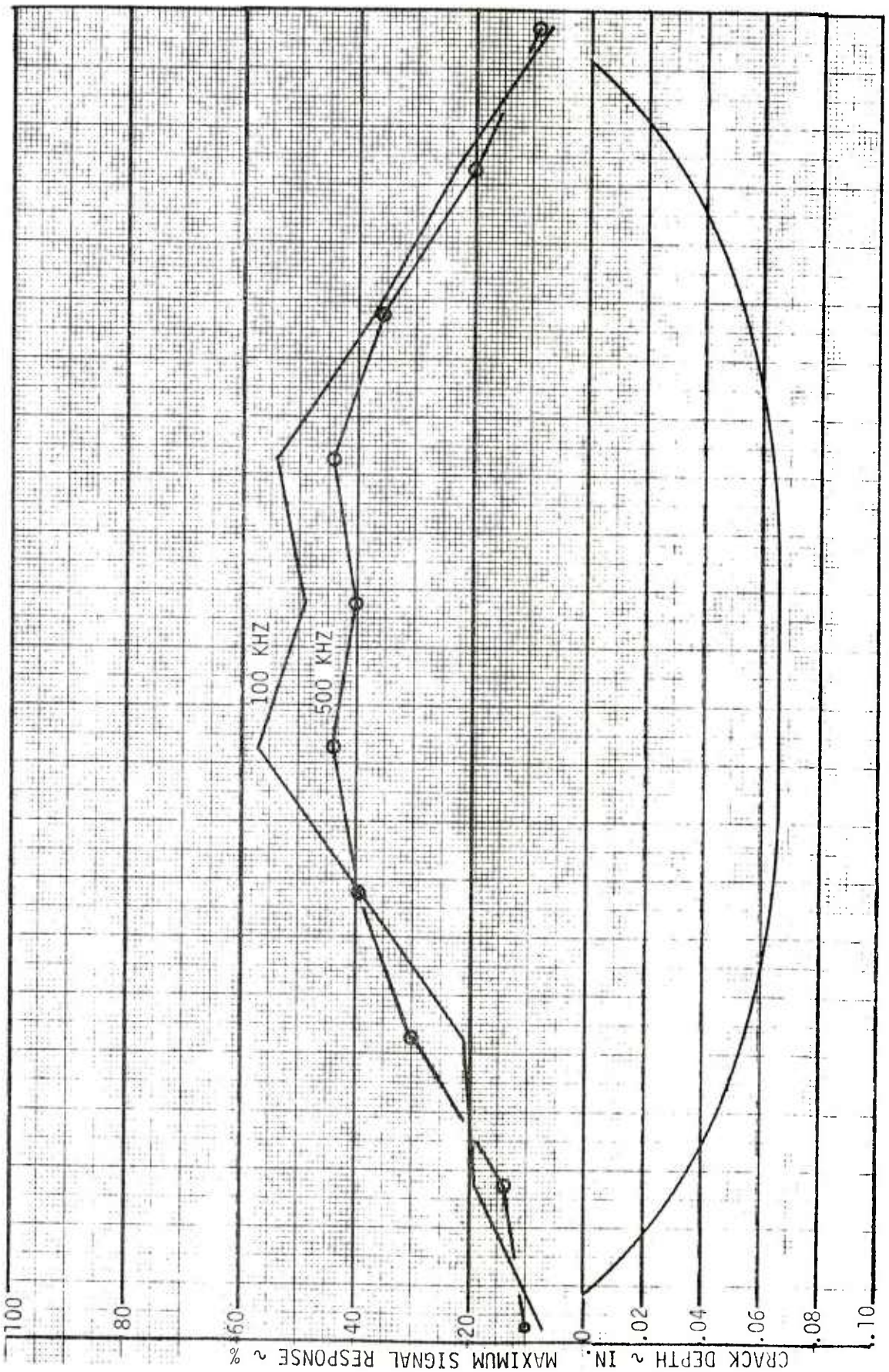

Figure 46. Profile of F at 0.067-in. depth

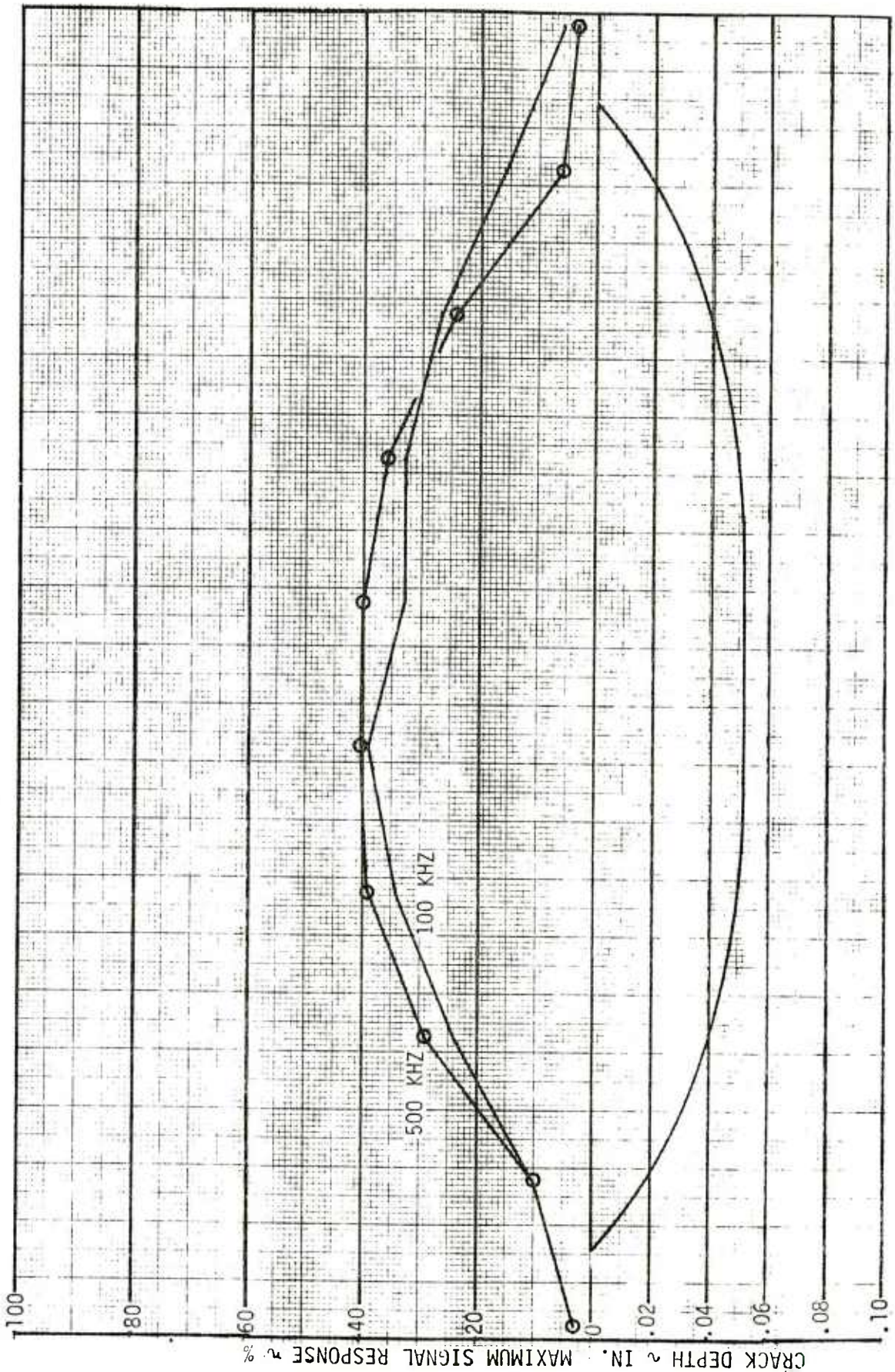

Figure 47. Profile of F at 0.052-in. depth

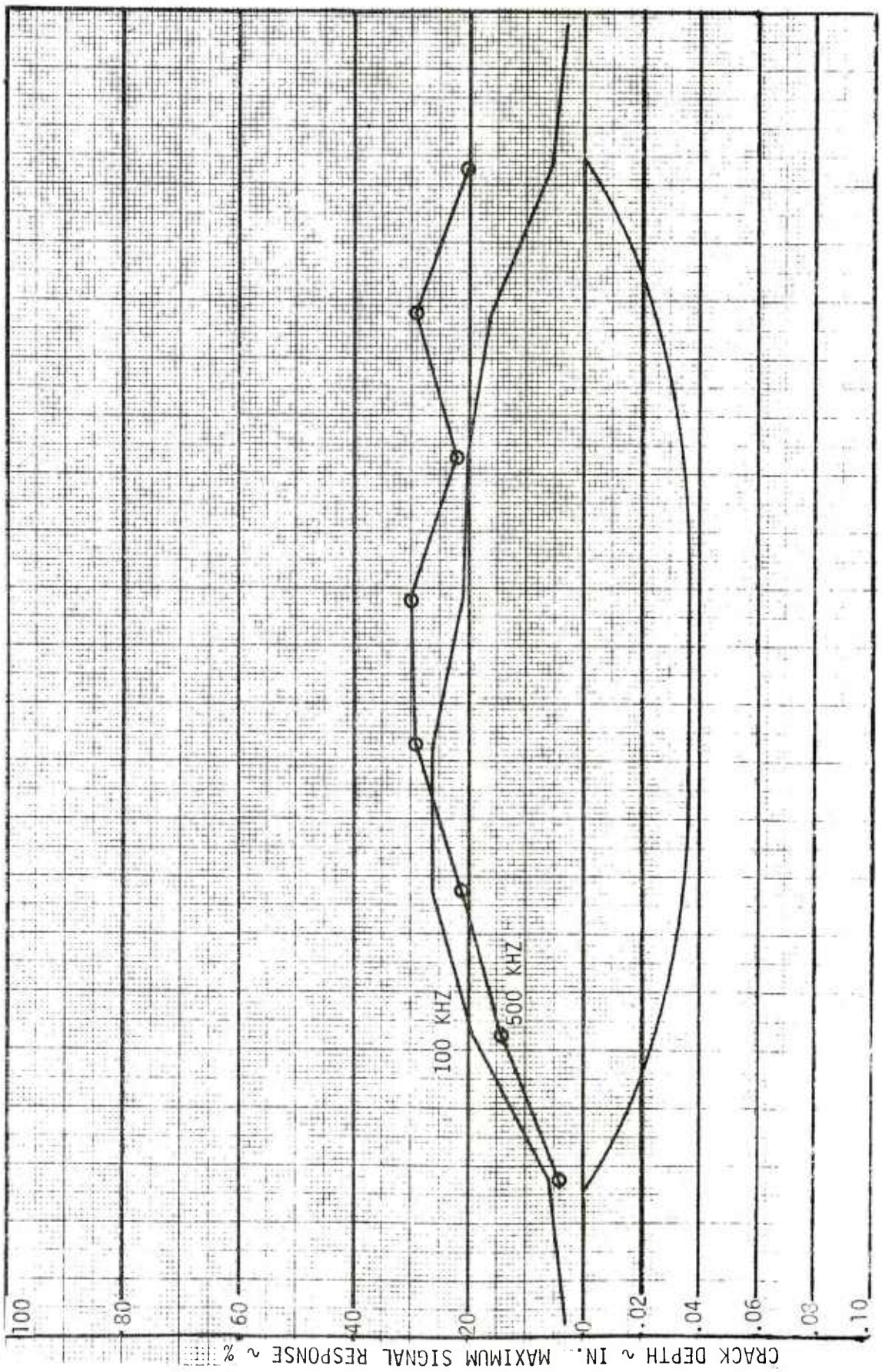

Figure 48. Profile of F at 0.037-in. depth

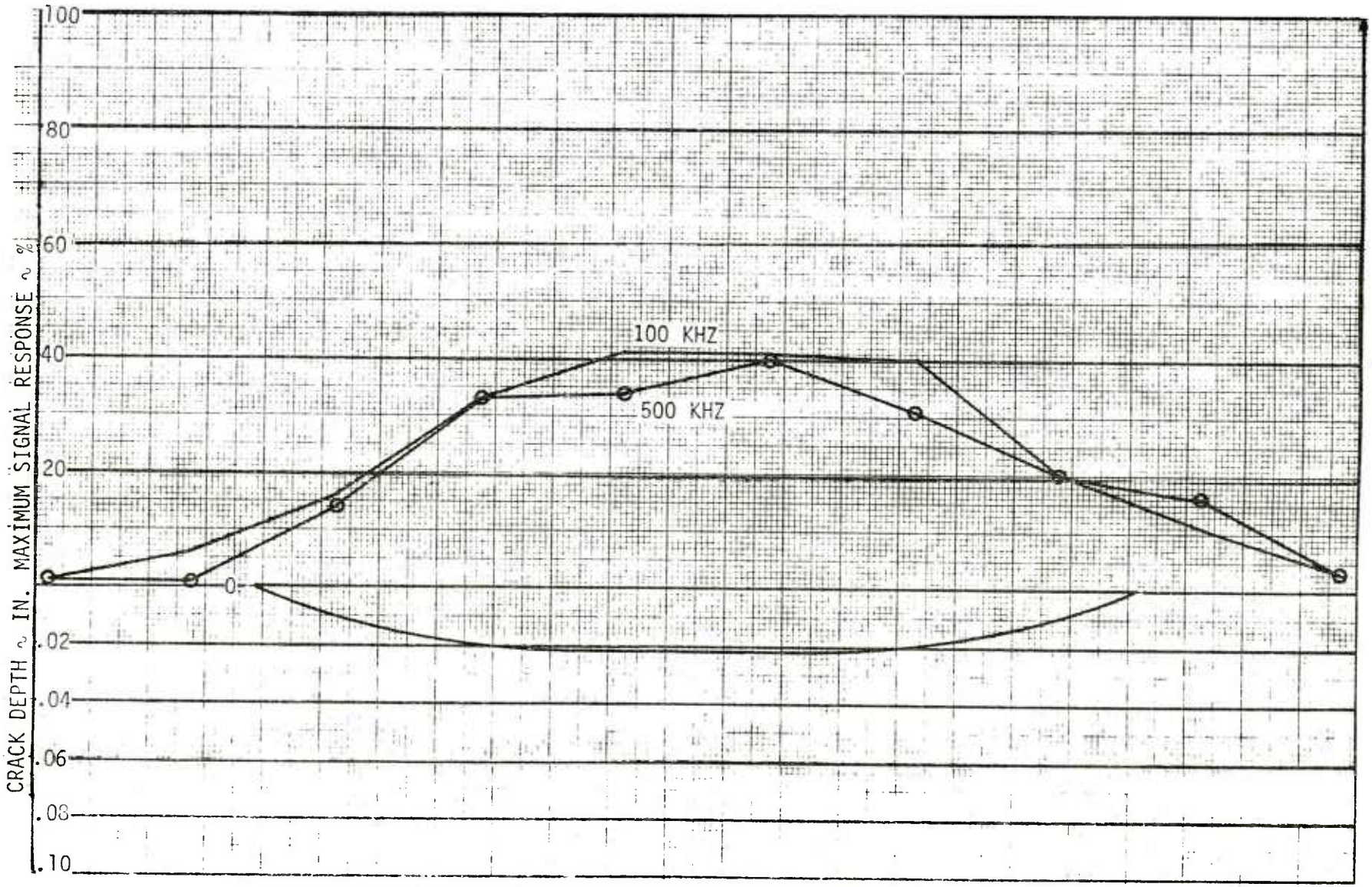

Figure 49. Profile of F at 0.022-in. depth

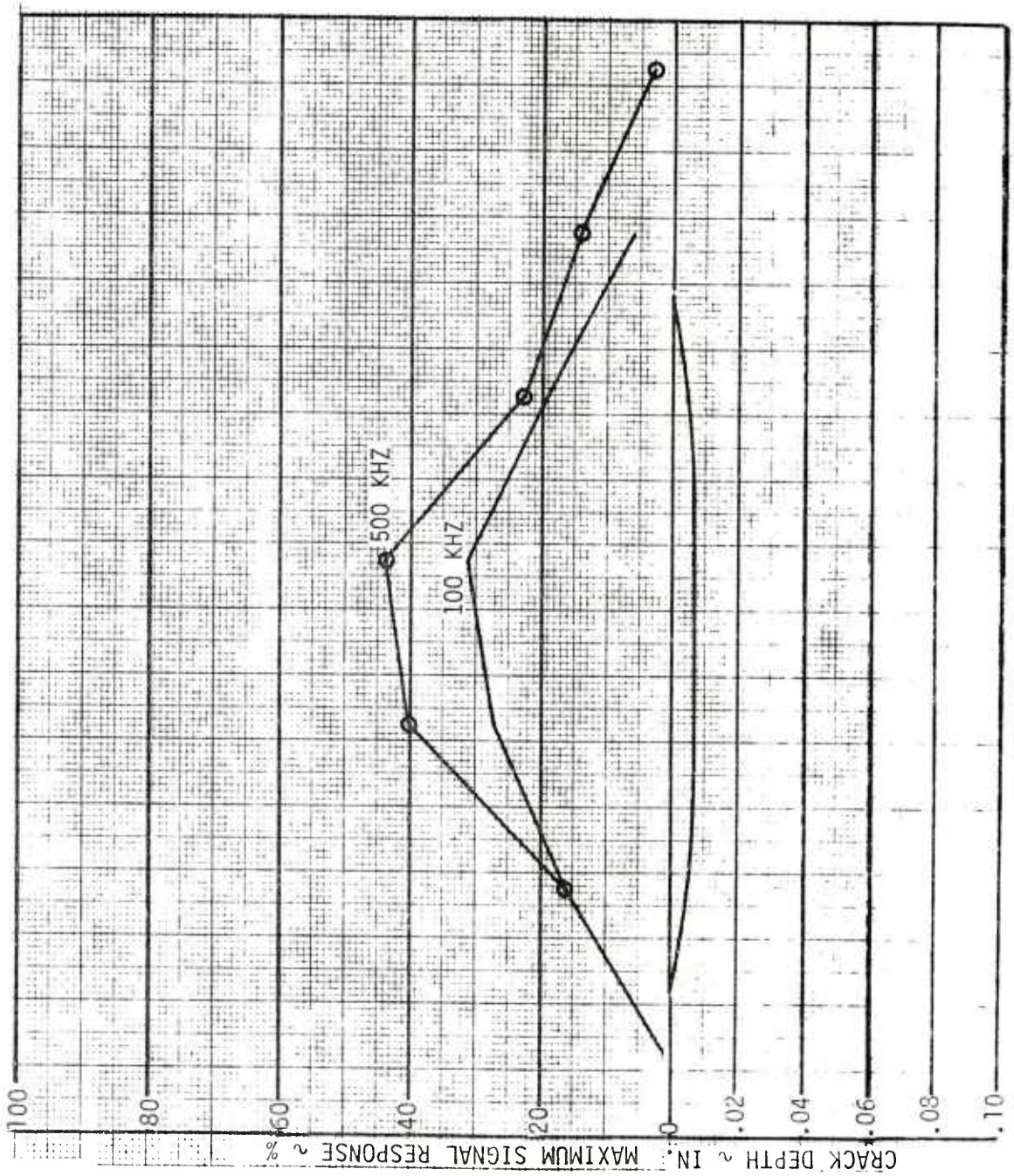

Figure 50. Profile of F at 0.007-in. depth

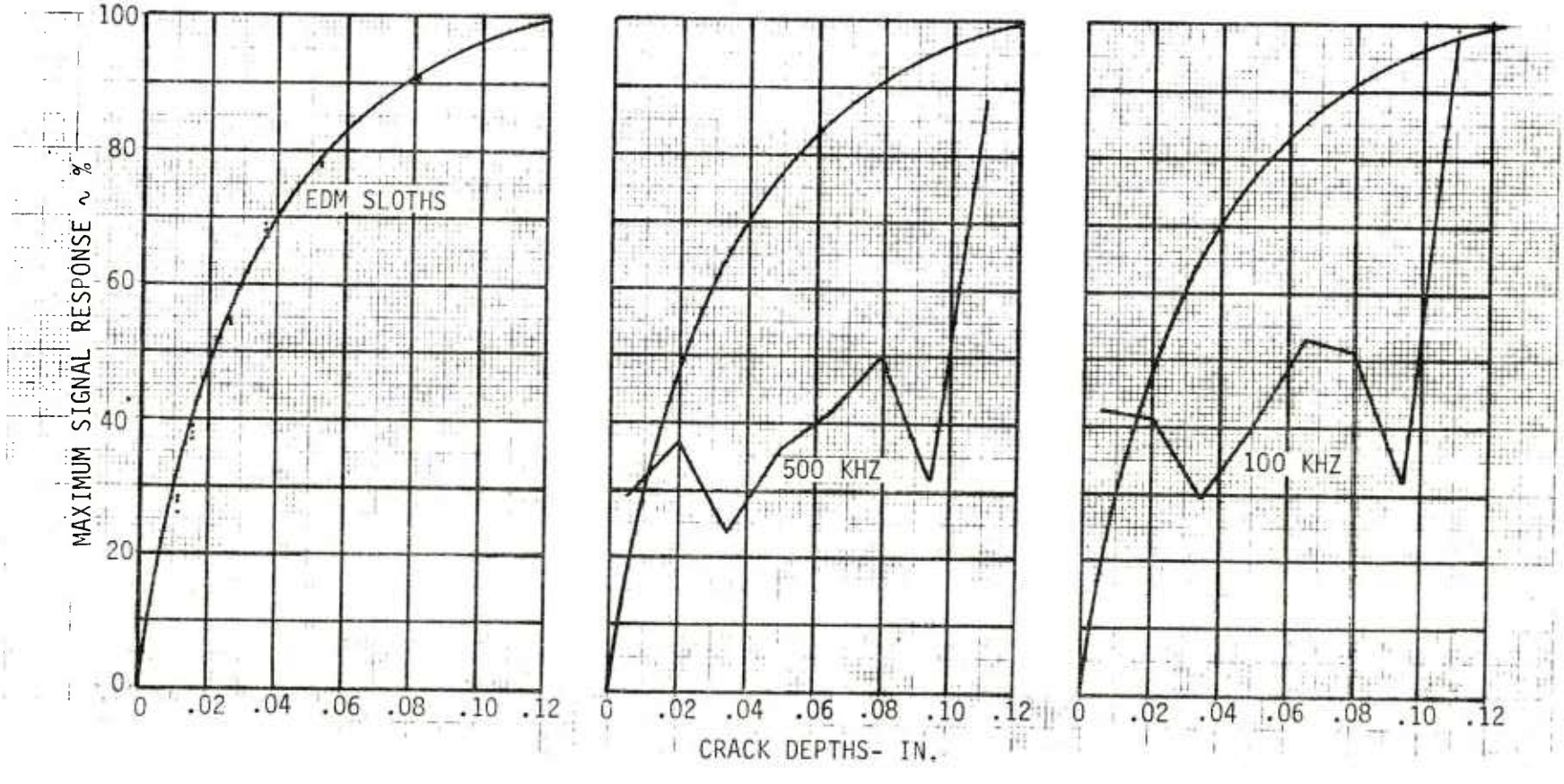

Figure 51. Eddy current response, original centerline of F

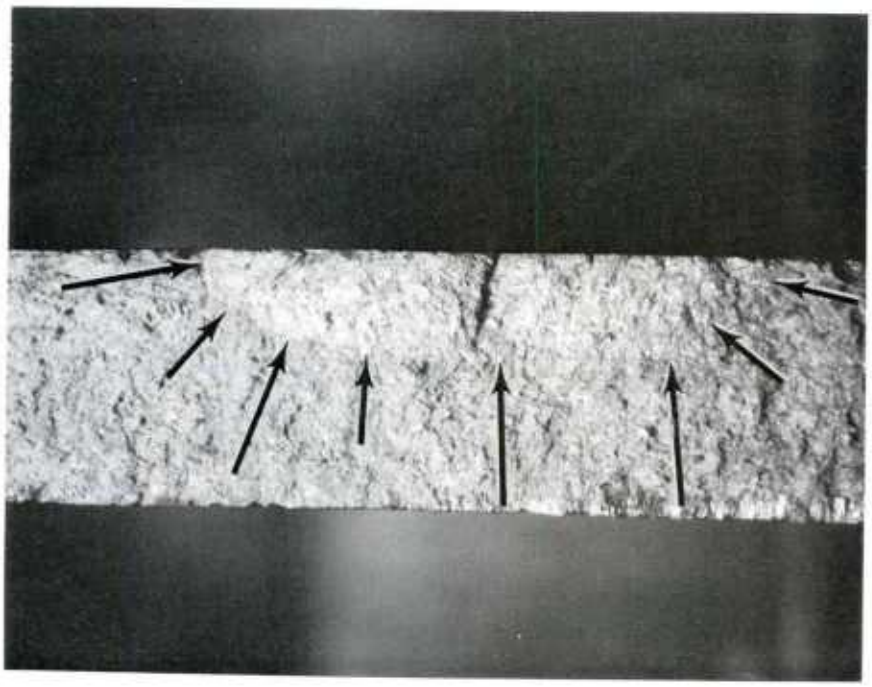

Figure 52. Fracture through fatigue crack

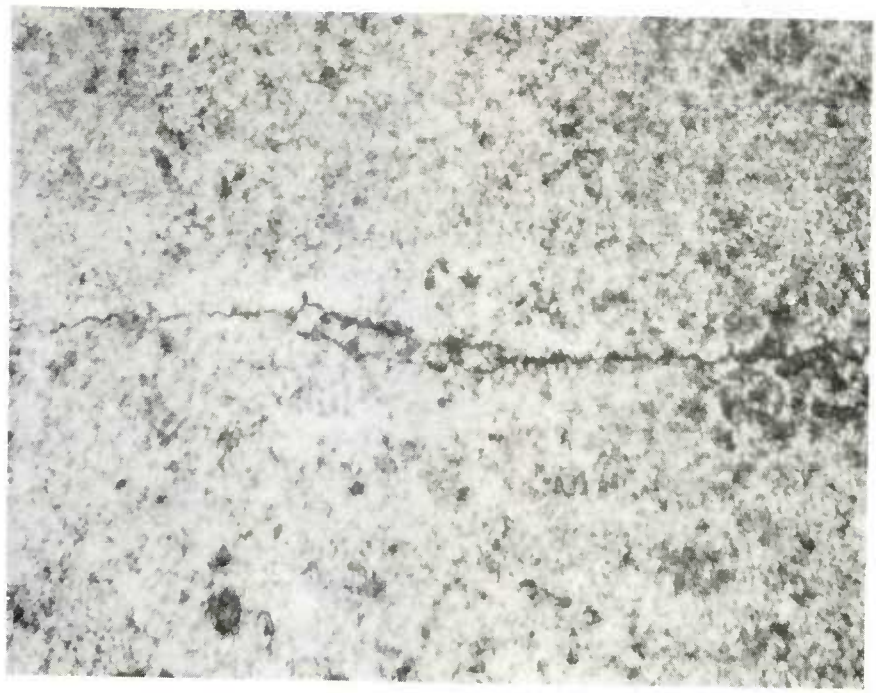

FATIGUE CRACK

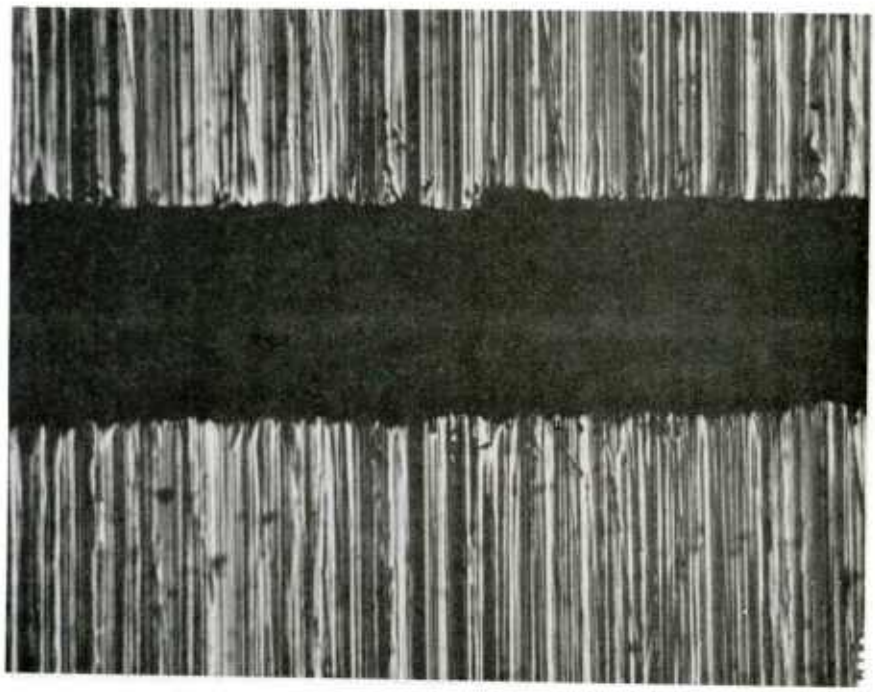

EDM SLOT

Figure 53. EDM slot versus fatigue crack 300X

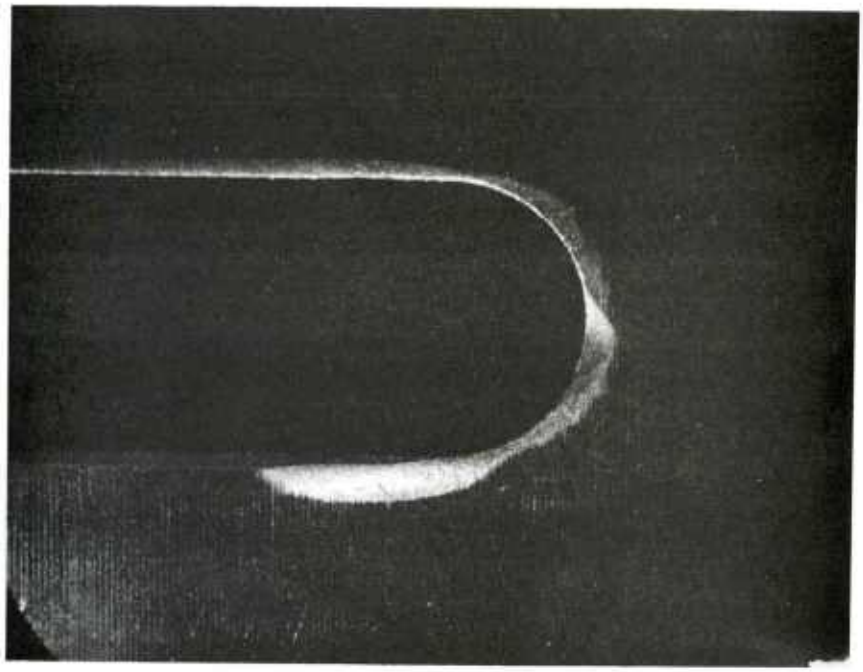

Figure 54. Slot irregularities, deburring

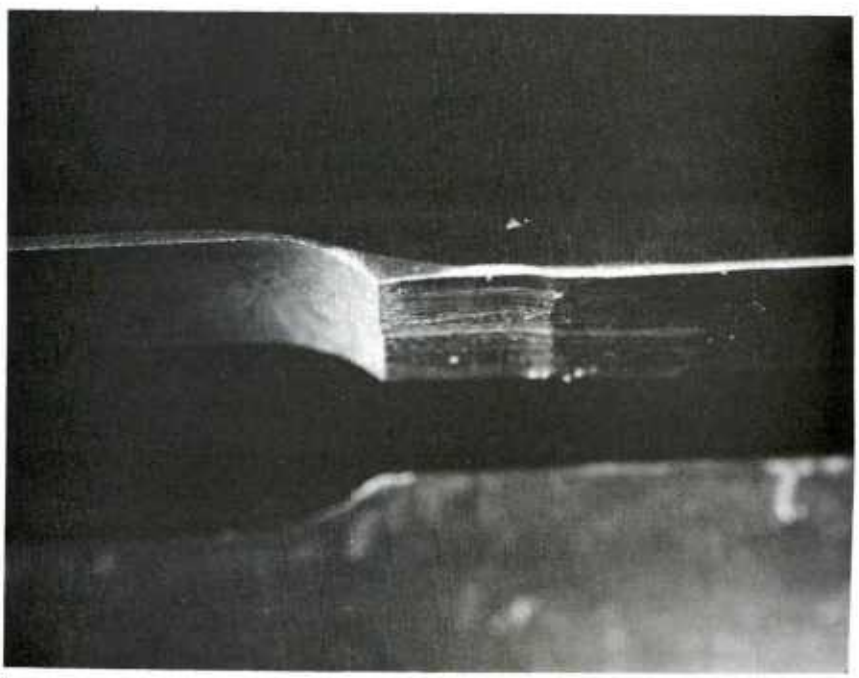

Figure 55. Slot irregularities, deburring and machining

DISTRIBUTION LIST

Metals and Ceramics Information Center
505 King Avenue
ATTN: Harold Mindlin, Director
James Lynch, Assistant Director
Columbus, OH 43201

Commander
Defense Technical Information Center
ATTN: Accessions Division (12)
Cameron Station
Alexandria, VA 22314

Commander
U.S. Army Foreign Science
and Technology Center
ATTN: DRXST-SD3
220 Seventh Street, N.E.
Charlottesville, VA 22901

Office of the Deputy Chief of Staff
for Research, Development, and Acquisition
ATTN: DAMA-ARZ-E
DAMA-CSS
Washington, DC 20310

Commander
Army Research Office
ATTN: George Mayer
J. J. Murray
P.O. Box 12211
Research Triangle Park, NC 27709

Commander
U.S. Army Materiel Development and
Readiness Command
ATTN: DRCQA-E
DRCQA-P
DRCDE-D
DRCDMD-FT
DRCLDC
DRCMT
DRCMM-M
5001 Eisenhower Avenue
Alexandria, VA 22333

Commander
U.S. Army Electronics Research
and Development Command
ATTN: DRSEL-PA-E, Stan Alster
J. Quinn
Fort Monmouth, NJ 07703

Commander
U.S. Army Missile Command
ATTN: DRSMI-TB (2)
DRSMI-TK, J. Alley
DRSMI-M
DRSMI-ET, Robert O. Black
DRSMI-QS, George L. Stewart, Jr.
DRSMI-EAT, R. Talley
DRSMI-QP
Redstone Arsenal, AL 35809

Commander
U.S. Army Materiel Systems
Analysis Activity
ATTN: DRXSY-MP
Aberdeen Proving Ground, MD 21005

Director
Ballistic Research Laboratory
U.S. Army Armament Resesarch
and Development Command
ATTN: DRDAR-TSB-S
Aberdeen Proving Ground, MD 21005

Commander
U.S. Army Troop Support and
Aviation Materiel Readiness Command
ATTN: DRSTS-PLE, J. Corwin (2)
DRSTS-Q
DRSTS-M
4300 Goodfellow Boulevard
St. Louis, MO 63120

Commander
U.S. Army Natick Research
and Development Command
ATTN: DRDNA-EM
Natick, MA 01760

Commander
U.S. Army Mobility Equipment Research
and Development Command
ATTN: DRDME-D
DRDME-E
DRDME-G
DRDME-H
DRDME-M
DRDME-T
DRDME-TQ
DRDME-V
DRDME-ZE
DRDME-N
Fort Belvoir, VA 22060

Commander
U.S. Army Tank-Automotive Materiel
Readiness Command
ATTN: DRSTA-Q (2)
Warren, MI 48090

Commander
U.S. Army Armament Materiel
Readiness Command
ATTN: DRSAR-QA (2)
DRSAR-SC
DRSAR-RDP
DRSAR-EN
DRSAR-QAE
DRSAR-LEP-L
Rock Island, IL 61299

Commander
Rock Island Arsenal
ATTN: SARRI-EN, W. M. Kisner
SARRI-ENM, W. D. McHenry
SARRI-QA
Rock Island, IL 61299

Commander
U.S. Army Armament Research
and Development Command
ATTN: DRDAR-LC, E. Kelly
DRDAR-LCA, E. G. Sharkoff
DRDAR-LCE, R. F. Walker
DRDAR-QAS, B. Aronowitz (5)
DRDAR-QAS-T, G. Zamloot (10)
DRDAR-SCM, J. D. Corrie
DRDAR-TSP, B. Stephans
DRDAR-TSS (5)
DRDAR-LCA, Harry E. Pebly, Jr.
DRCPM-CAWS, J. Pritchard (2)
DRDAR-QAR (2)
Dover, NJ 07801

Commander
Chemical Systems Laboratory
U.S. Army Armament Research
and Development Command
ATTN: DRDAR-CLD, W. E. Montanary
DRDAR-CLB-PA
DRDAR-CLJ-L
APG, Edgewood Area, MD 21010

Commander
U.S. Army Armament Research
and Development Command
Product Assurance Directorate
ATTN: DRDAR-QAC-E, W. J. Maurits
Aberdeen Proving Ground, MD 21010

Chief
Benet Weapons Laboratory, LCWSL
U.S. Army Armament Research
and Development Command
ATTN: DRDAR-LCB, T. Moraczewski
DRDAR-LCB-TL
SARWV-PPI, L. Jette
Watervliet, NY 12189

Commander
U.S. Army Aviation Research
and Development Command
ATTN: DRDAV-EXT
DRDAV-QR
DRDAV-QP
DRDAV-QE
St. Louis, MO 63120

Commander
U.S. Army Tank-Automotive Research
and Development Command
ATTN: DRDTA-UL, Technical Library
DRDTA-RCKM, S. Goodman
DRDTA-RCKT, J. Fix
DRDTA-RTAS, S. Catalano
DRDTA-TTM, W. Moncrief
DRDTA-ZS, O. Renius
DRDTA-JA, C. Kedzior
Warren, MI 48090

Director
Industrial Base Engineering Activity
ATTN: DRXIB-MT, D. Brim (2)
Rock Island, IL 61299

Commander
Harry Diamond Laboratories
ATTN: DELHD-EDE, B. F. Willis
2800 Powder Mill Road
Adlephi, MD 20783

Commander
U.S. Army Test and Evaluation Command
ATTN: DRSTE-TD
DRSTE-ME
Aberdeen Proving Ground, MD 21005

Commander
U.S. Army White Sands Missile Range
ATTN: STEWS-AD-L
STEWS-ID
STEWS-TD-PM
White Sands Missile Range, New Mexico 88002

Commander
U.S. Army Yuma Proving Ground
ATTN: Technical Library
Yuma, AZ 85364

Commander
U.S. Army Tropic Test Center
ATTN: STETC-TD, Drawer 942
Fort Clayton, Canal Zone

Commander
Aberdeen Proving Ground
ATTN: STEAP-MT
STEAP-MT-M, J. A. Feroli
STEAP-MT-G, R. L. Huddleston
Aberdeen, MD 21005

Commander
U.S. Army Cold Region Test Center
ATTN: STECR-OP-PM
APO Seattle 98733

Commander
U.S. Army Dugway Proving Ground
ATTN: STEDP-MT
Dugway, UT 84022

Commander
U.S. Army Electronic Proving Ground
ATTN: STEEP-MT
Fort Huachuca, AZ 35613

Commander
Jefferson Proving Ground
ATTN: STEJP-TD-I
Madison, IN 47250

Commander
U.S. Army Aircraft Development
Test Activity
ATTN: STEBG-TD
Fort Rucker, AL 36362

President
U.S. Army Armor and Engineer Board
ATTN: ATZKOAE-TA
Fort Knox, KY 40121

President
U.S. Army Field Artillery Board
ATTN: ATZR-BDOP
Fort Sill, OK 73503

Commander
Anniston Army Depot
ATTN: SDSAN-QA
Anniston, AL 36202

Commander
Corpus Christi Army Depot
ATTN: SDSCC-MEE, Mr. Haggerty, Mail Stop 55
Corpus Christi, TX 78419

Commander
Letterkenny Army Depot
ATTN: SDSLE-QA
Chambersburg, PA 17201

Commander
Lexington-Bluegrass Army Depot
ATTN: SDSLX-QA
Lexington, KY 40507

Commander
New Cumberland Army Depot
ATTN: SDSNC-QA
New Cumberland, PA 17070

Commander
U.S. Army Depot Activity
ATTN: SDSTE-PU-Q (2)
Pueblo, CO 81001

Commander
Red River Army Depot
ATTN: SDSRR-QA
Texarkana, TX 75501

Commander
Sacramento Army Depot
ATTN: SDSSA-QA
Sacramento, CA 95813

Commander
Savanna Army Depot Activity
ATTN: SDSSV-S
Savanna, IL 61074

Commander
Seneca Army Depot
ATTN: SDSSE-R
Romulus, NY 14541

Commander
Sharpe Army Depot
ATTN: SDSSH-QE
Lathrop, CA 95330

Commander
Sierra Army Depot
ATTN: SDSSI-DQA
Herlong, CA 96113

Commander
Tooele Army Depot
ATTN: SDSTE-QA
Tooele, UT 84074

Director
DARCOM Ammunition Center
ATTN: SARAC-DE
Savanna, IL 61074

Naval Research Laboratory
ATTN: Code 5830, J. M. Krafft
Code 2620, Library
Washington, DC 20375

Air Force Materials Laboratory
Wright-Patterson Air Force Base
ATTN: AFML-LTM, W. Wheeler
AFML-LLP, R. Rowand
Wright-Patterson Air Force Base, OH 45433

Director
U.S. Army Materials and
Mechanics Research Center
ATTN: DRXMR-PL (2)
DRXMR-X
DRXMR-PD
DRXMR-WD
DRXMR-M
DRXMR-ST
DRXMR-L
DRXMR-T
DRXMR-E
DRXMR-PR
Watertown, MA 02172

Martin Marietta Corp.
Orlando Aerospace Div.
ATTN: B. D. Woody (5)
W. R. Randle (2)
Orlando, FL 32855